A UNIFIED MODULATION SCHEME FOR THREE-PHASE INVERTER-FED INDUCTION MOTOR DRIVES

MADUSUDANAN THIRUGNANASAMBANDAMOORTHY

INFORMATION TO USERS

This manuscript has been reproduced from the microfilm master. UMI films the text directly from the original or copy submitted. Thus, some thesis and dissertation copies are in typewriter face, while others may be from any type of computer printer.

The quality of this reproduction is dependent upon the quality of the copy submitted. Broken or indistinct print, colored or poor quality illustrations and photographs, print bleedthrough, substandard margins, and improper alignment can adversely affect reproduction.

In the unlikely event that the author did not send UMI a complete manuscript and there are missing pages, these will be noted. Also, if unauthorized copyright material had to be removed, a note will indicate the deletion.

Oversize materials (e.g., maps, drawings, charts) are reproduced by sectioning the original, beginning at the upper left-hand corner and continuing from left to right in equal sections with small overlaps.

Photographs included in the original manuscript have been reproduced xerographically in this copy. Higher quality 6" x 9" black and white photographic prints are available for any photographs or illustrations appearing in this copy for an additional charge. Contact UMI directly to order.

ProQuest Information and Learning
300 North Zeeb Road, Ann Arbor, MI 48106-1346 USA
800-521-0600

A Unified Modulation Scheme for Three-phase Inverter-fed Induction Motor drives

by

© Madusudanan Thirugnanasambandamoorthy, B.Tech.

A thesis submitted to the School of Graduate Studies

in partial fulfillment of the

requirements for the degree of

Master of Engineering

Faculty of Engineering and Applied Science

Memorial University of Newfoundland

February 2001

St. John's Newfoundland Canada

Abstract

Variable speed AC motor drives are widely used for industrial applications and a majority of the industrial drives employ induction motors. In most of the drives, variable speed is achieved by V/f control strategy, where the air-gap flux in the motor can be maintained constant at all frequencies. The V/f control can be achieved by various modulation schemes in inverter-fed drives.

This thesis analyzes the advantages and limitations of the existing modulation schemes for V/f control and presents an improved modulation scheme called the unified modulation scheme (UMS). This scheme combines the advantages of two popular modulation schemes (the delta and sine-PWM modulation schemes), at the same time overcoming their disadvantages. The development, simulation results and experimental implementation of the proposed scheme are presented. Comparison between the different modulation schemes shows the advantages of the unified modulation scheme.

This thesis also presents simulation results of a SIMULINK implementation of an induction motor drive using the unified modulation scheme. These results are compared with the results of the delta-modulated inverter-fed induction motor drive. The results show that the unified modulation scheme provides improved performance in terms of lower-order harmonic attenuation and sub-harmonic elimination. Finally, a modified unified modulation scheme is presented using the conventional sine-PWM scheme, for performance enhancement.

Acknowledgements

I take this opportunity to thank all those who have made this possible.

My Mom and Dad, and my brothers Venki and Sarav for their love and inspiration. My mentor, Dr.John.E.Quaicoe for his supervision, guidance,motivation and support. My Profs, Dr. Venkatesan and Dr.Jeyasurya for their valuable advice.

I also thank Memorial University of Newfoundland and the School of Graduate Studies for giving me this opportunity and financial assistance, and the Dean and the Faculty of Engineering and Applied Science for their continued support.

I am grateful to the Lab Techs, Mr.Don Guy,Mr.Dennis Johnson and Mr.Richard Newman for their help and advice with the experimental work, and the members of CCAE, Mr.Philip van Ulden, Mr.Tom Pike and Ms. Valerie Mercer for their help with computing facilities. Special thanks to Tom for introducing me to the PIC16C77.

Last but not the least, my friends and colleagues at the Faculty of Engineering and Applied Science, Memorial University, and GE Industrial Systems, Peterborough, for their help, warmth and affection.

Contents

List of Tables

List of Figures

List of Symbols

a	Turns ratio between the stator and rotor windings
E	Induced stator voltage
f	Input or supply frequency
f_c	Carrier signal frequency (RWDM)
f_h	Harmonic frequency
f_r	Reference signal frequency
f_{rb}	Break frequency
f_s	Switching or sampling frequency
f_{sl}	Slip frequency
I_r	Rotor current
I_s	Stator current
I_{sk}	k-th harmonic per-phase stator current
k	Harmonic order
K	Unified modulation constant
k_w	Winding factor
k_T	Torque equation constant
M	Amplitude modulation index (SPWM)
N_1	Number of series turns per phase in stator winding
N_s	Motor synchronous speed in rpm

p	Ratio of carrier frequency to modulating signal frequency
P_m	Rated power output of the motor
P_n	Nominal rated power of Induction motor
P_h	Harmonic copper losses
R'_r	Rotor resistance referred to the stator circuit
R'_{rk}	k-th harmonic rotor resistance referred to the stator circuit
R_s	Stator resistance
R_{sk}	k-th harmonic per-phase stator resistance
s	Rotor slip
s_k	k-th harmonic slip
S_c	Slope of carrier signal $v_c(t)$; integrator gain (RWDM)
S_r	Slope of reference signal $v_r(t)$ (RWDM)
T	Mechanical torque developed by the motor
T_{em}	Electro-magnetic torque produced by the motor
T_L	Load counter-torque on the motor
T_S	Time period of switching signal
$v_c(t)$	Carrier signal (SPWM)
$v_r(t)$	Reference signal (SPWM)
$v'_r(t)$	Reference signal of modified UM scheme
V_k	k-th harmonic voltage amplitude

V_{l-l}	Line-to-line voltage rating of Induction motor
V_t	Stator terminal voltage
V_r	Injected rotor voltage
V_r'	Injected rotor voltage referred to the stator
V_{dc}	Input dc supply to inverter
V_{o1}	Fundamental voltage amplitude at the inverter output
V_o	Magnitude of terminal voltage boost required for V/f control at low frequency
X_s	Stator reactance
X_r'	Rotor reactance referred to the stator circuit
ΔV	Hysteresis bandwidth (RWDM)
η	Duty ratio
ϕ_{ag}	Air-gap flux
ω_{ms}	Motor synchronous speed in rad/s
ω_m	Motor operating speed in rad/s
ω_r	Angular frequency of the reference signal (RWDM) in rad/s
ω_{sl}	Slip speed

Chapter 1

Introduction

AC machines are known as the work-horses of the industry. Nearly eighty-five percent of the industrial motors in use today are induction motors. The induction motors have numerous advantages when compared to DC motors such as higher efficiency, ruggedness, lower maintenance, better reliability, lower cost, weight, volume and inertia. The presence of commutators and brushes make DC motors unsuitable for explosive and dirty environments[1].

Most of the earlier primary applications involving induction motors have been constant speed applications. This is because variable speed drives demand precise and continuous control of speed with good stability and transient performance. The induction motors are inflexible in speed when operated from a constant frequency AC supply. But the tremendous growth in power semiconductor technology has changed this scenario and enabled the widespread use of induction motors for variable speed drives. Also the advances in power circuit integration, packaging concepts and integration of power circuit with the control have greatly aided the above process.

Before the main focus of the thesis could be discussed, it would be appropriate to provide a clear picture of the induction motor speed control strategies, their characteristics and capabilities and the ways to implement variable voltage, variable frequency AC supply. It then becomes easier to point out those aspects which the thesis aims to improve. The following section describes the basic principles of speed control methods.

1.1 Speed control methods in induction motors

Speed control strategies in induction motors can be discussed under two broad topics namely

1. Vector control schemes

2. Scalar control schemes

1.1.1 Vector control schemes

The steady state performance achievable in inverter-fed AC motor drives is as good as the one compared to separately excited DC motor. However, the dynamic performance, which is a measure of how fast the motor can respond to the change in the command speed or torque, is not so good in the case of inverter-fed AC motor drives. Recently, the vector control strategies have made a great change in the dynamic performance of AC motor drives. Vector control has made it possible to control an AC motor in a manner similar to that of the separately excited DC motor, and achieve

the same quality of dynamic performance[2].

The reason for the superior dynamic performance in separately excited DC motor is due to the magnetic decoupling between the armature and field circuits. The m.m.f. produced by the field current and the m.m.f. produced by the armature current are spatially in quadrature and hence there is no magnetic coupling between the two circuits. This decoupling continues to exist, because of the repetitive switching action of the commutator on the rotor coils as the rotor rotates, irrespective of the speed or the angular position of the rotor. This makes it possible to effect fast changes in the armature circuit without being hampered by the large inductance of the field circuit. Since the armature current can change rapidly, the machine can develop torque and accelerate or decelerate very quickly when speed changes are required.

Similar to DC motors, the torque in an AC motor is produced as a result of the interaction of a current and a flux. But for singly-fed induction motors, since the power is fed on the stator side only, the current responsible for the torque and the current responsible for producing the flux are not easily separable.

The fundamental principle of vector control is to separate the component of the motor current responsible for producing the torque and the component responsible for producing the flux in such a way that they are magnetically decoupled. The two decoupled currents can then be controlled independently, as it is done in separately excited DC motors. Several schemes based on the above concept have been described

in the literature[2, 3, 4, 5, 6].

The vector control strategies are used in motor drives that require good dynamic performance, such as reversible sheet rolling mills in the metallurgy industry and other machine tool drives. Such drives are called high-performance drives and they are more recent, highly accurate, complex and expensive.

1.1.2 Scalar control schemes

The scalar control schemes are known as medium performance drives as they have very good steady state performance and reasonable dynamic performance. Most of the industrial applications need medium performance drives where accuracy and dynamic performance considerations are not so stringent. Hence this thesis focuses on scalar control schemes for speed control of induction motors. The various methods of scalar control employed in inverter-fed induction motor drives are listed below

1. Variable terminal voltage control
2. Rotor resistance control
3. Injecting voltage in the rotor circuit
4. Variable frequency control

The first and the last methods are applicable to both squirrel cage and wound rotor induction motors, whereas the second and third methods are applicable only to the wound rotor induction motor.

1.1.2.1 Variable terminal voltage control

Speed control is achieved by varying the terminal voltage until the torque required by the load is developed at the desired speed. The terminal voltage of the motor can be allowed to vary only till its rated voltage. Hence this method allows speed control only up to the rated speed[7, 8, 9]. The torque developed is proportional to the square of the terminal voltage, as shown in equation 1.1 [1]

$$T = \frac{3}{\omega_{ms}} \{ \frac{V_t^2 R_r'/s}{(R_s + \frac{R_r'}{s})^2 + (X_s + X_r')^2} \} \tag{1.1}$$

where T is the mechanical torque developed

V_t is the terminal voltage at the stator

ω_{ms} is the synchronous speed

R_s is the stator resistance

X_s is the stator reactance

R_r' is the rotor resistance referred to the stator circuit

X_r' is the rotor reactance referred to the stator circuit

s is the rotor slip

The rotor current is directly proportional to the terminal voltage. Thus the torque to current ratio decreases with the terminal voltage. Low-speed operation is only possible if the load torque decreases with speed eg: fan-type load. A set of torque-slip curves for a fan-type load is shown in Fig. 1.1. The variable voltage at the terminals is

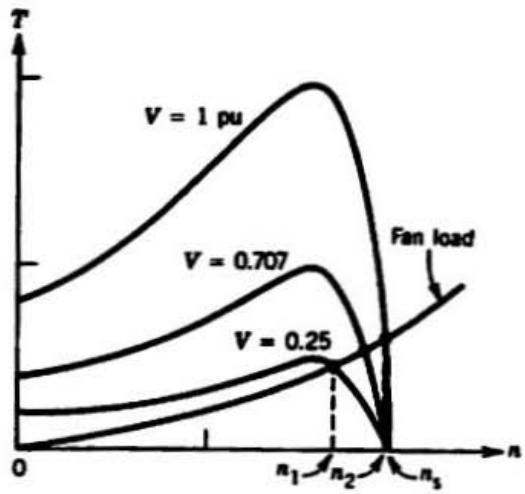

Figure 1.1: Speed control of a fan-type load by stator voltage control of an induction motor[10]

usually obtained using thyristor based AC voltage controllers. Stator voltage control is simpler and cheaper to install. It is widely used in fan and pump drives, fractional horsepower drives, and ac-powered cranes and hoists where there is a demand for large torque at high slip only for intermittent portions of the duty-cycle[1, 11]. The limitations of such drives include poor operating efficiency and motor de-rating at low speeds to avoid overheating due to excessive current and reduced ventilation.

1.1.2.2 Rotor resistance control

The wound rotor induction motors are normally designed to obtain a compromise between the normal running performance and the starting performance. The rotor winding is designed to have a low resistance so that the running efficiency is high and

the full-load slip is low. The starting performance can be improved by connecting an external resistance in series with the rotor winding. The increase in rotor resistance does not affect the value of maximum torque but increases the slip at maximum torque. This also substantially reduces the starting current. As the rotor starts accelerating, the external resistance can be slowly decreased[1, 11].

For a given load torque, the motor speed is reduced as the rotor resistance is increased. Thus speed control below the rated speed can be achieved. But the rotor resistance speed control is an inefficient method. Although it offers a constant torque operation with a high torque-to-current ratio, the rotor copper losses increase with a decrease in speed and most of it is dissipated in the external resistance. However, it has the advantages such as low cost, good power factor, and high torque-to-current ratio for a wide speed range. Rotor resistance control finds applications in low cost drives requiring a high torque-to-current ratio such as low-power excavators, crane hoists etc [12, 13].

Figure 1.2 shows the static rotor resistance control where the rotor circuit resistance is smoothly varied using the principle of a chopper. The slip frequency rotor voltages are rectified using a 3-phase diode bridge and applied across an external resistance R. The self-commutated semiconductor switch S, connected in parallel with R, has a period T and remains on for a time t_{on} for each period. Thus, the effective value of the external resistance varies from R to 0 as t_{on} varies from 0 to T. The

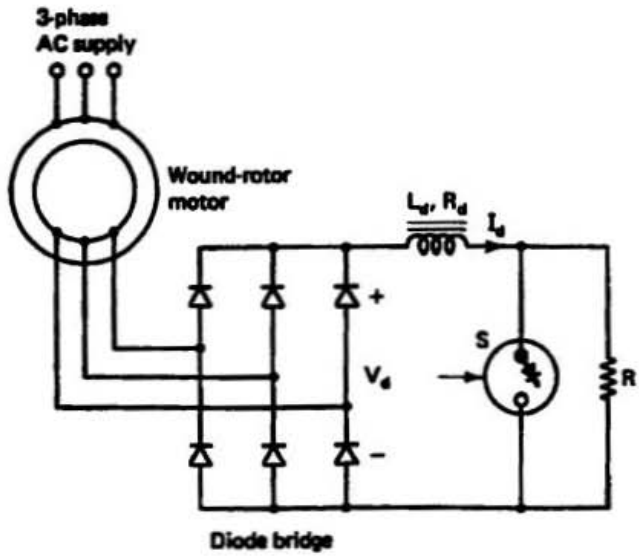

Figure 1.2: Static rotor resistance control of a wound-rotor induction motor[1]

speed-torque curves for various values of the duty-ratio ($\eta = t_{on}/T$) are given in Fig. 1.3

1.1.2.3 Injection of voltage in the rotor circuit

The equivalent circuit of the wound rotor induction motor with an injected voltage $V_r \angle \phi_r$ can be represented as shown in Fig. 1.4

In the absence of injected voltage, the rotor current I_r is zero when the rotor speed equals the synchronous speed. In the presence of injected voltage, when V_r is in phase with the induced voltage E at the stator, the condition at which the rotor current will be zero is given by the slip speed equation

$$s = \frac{aV_r}{E} \tag{1.2}$$

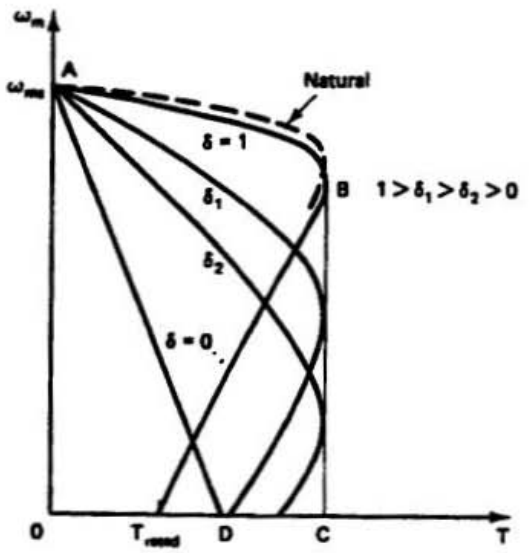

Figure 1.3: Speed-torque curves for static rotor resistance control of a wound-rotor induction motor[1]

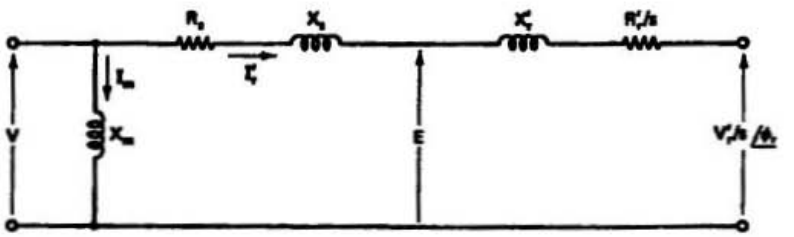

Figure 1.4: Induction motor equivalent circuit with rotor-injected voltage[1]

where a is the turns ratio between the stator and rotor windings. The motor speed is given by the equation[1]

$$\omega_m = (1 - \frac{aV_r}{E})\omega_{ms} \tag{1.3}$$

where ω_m denotes the motor speed, and ω_{ms} the synchronous speed. The speed of the induction motor can be controlled from synchronous to standstill by varying V_r from 0 to (E/a). Also if the polarity of V_r is reversed, the slip becomes negative and super-synchronous speed can be achieved.Thus by adjusting the voltage injected into the rotor circuit, speed control can be achieved[1, 14, 15, 16, 17]. The torque-speed characteristics for speed control by injection of rotor voltage are given in Fig. 1.5

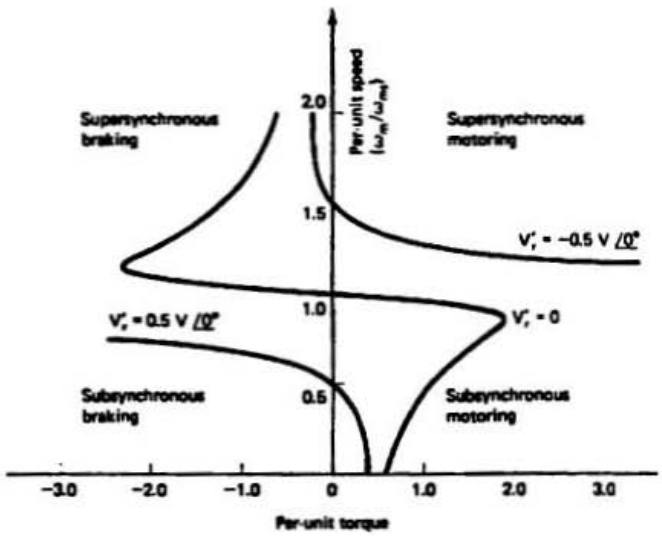

Figure 1.5: Speed control by injection of voltage in the rotor circuit[1]

1.1.2.4 Variable frequency control

The synchronous speed of the motor is directly proportional to the supply frequency. Thus by changing the supply frequency, the synchronous speed and the motor speed can be controlled above and below the rated speed.

1.2 Need for constant Volts/Hertz control

The rotating air-gap flux wave Φ induces a counter e.m.f. E_1 in the stator winding. This counter e.m.f. is less than the applied stator terminal voltage V_1 by the stator leakage impedance drop. Thus the magnitude of the induced e.m.f. E_1 is proportional to the magnitude of the terminal voltage V_1 and is given by the following equation[18]

$$E_1 = 4.44 k_w f N_1 \Phi \tag{1.4}$$

where k_w is the winding factor, f is the supply frequency and N_1 is the number of series turns per phase of stator winding . From equation 1.4 it can be inferred that the air-gap flux Φ is proportional to E_1/f. If the stator drop is neglected, the air-gap flux can be considered proportional to V_1/f. Induction motors are usually designed to operate at the knee-point of the magnetization curve to make full use of the magnetic material. Thus for effective utilization, the air-gap flux must be kept constant at all frequencies. Any reduction in the supply frequency, without a corresponding reduction in the terminal voltage, will increase the air-gap flux and saturate the motor. This leads to an increase in magnetization current, distortion

in the line current and voltage, increased core losses and stator copper loss, and a high-pitched acoustic noise (magnetic hissing).

At lower frequencies of operation, the stator drop cannot be neglected since it is comparable to the induced e.m.f. E_1. In order to maintain the air-gap flux constant for a given torque, a voltage boost is required.

Having explained the various speed control strategies applicable to induction motors, the next section discusses the induction motor characteristics and its capabilities.

1.3 Induction motor characteristics and capabilities

The characteristics and capabilities of the induction motor can be discussed by identifying three distinct regions in the operation of the motor as shown in Fig. 1.6 namely

1. Constant-Torque region
2. Constant-Power region
3. High-speed motoring region

1.3.1 Constant-Torque region

The region of speed below the rated speed is referred to as the constant torque region. The electromagnetic torque T_{em} produced by the motor is given by the equation[11]

$$T_{em} = k_T \Phi_{ag}^2 f_{sl} \tag{1.5}$$

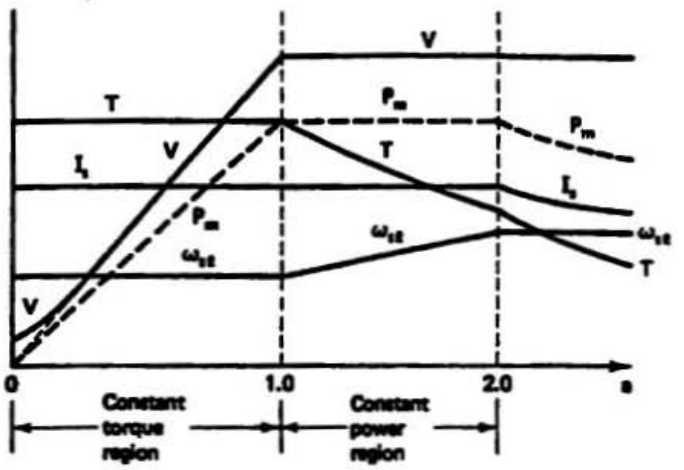

Figure 1.6: Induction motor characteristics[1]

where k_T denotes the proportionality constant and f_{sl} denotes the slip frequency. The slip frequency f_{sl} equals sf,where s is the slip and f the supply frequency. In the constant-torque region, f_{sl} remains constant at its rated value and the air-gap flux ϕ_{ag} is kept constant by maintaining a constant volts/hertz ratio. Thus as per equation 1.5 the machine delivers the constant rated torque. The characteristics in Fig. 1.6 show various motor parameters such as terminal voltage V, motor torque T, output power P_m, stator current I_m and slip speed ω_{sl} versus per unit frequency a. Also the figure shows the voltage boost required at low frequency operation.

1.3.2 Constant-power region

If the stator frequency is increased beyond the rated value, the motor speed increases beyond the rated speed. But in most of the applications, the terminal voltage is

not increased beyond the rated value. Thus keeping the supply voltage constant and increasing the supply frequency causes a decrease in the air-gap flux. The electromagnetic torque in equation 1.5 becomes proportional to $1/f^2$. But the constant power operation demands that the electromagentic torque vary inversely with frequency. By suitable control of the rotor frequency, in a controlled-slip drive, the motor torque can be made to vary inversely with f as required. This constant-power mode of operation corresponds to the field weakening operation of the DC motor.

1.3.3 High-speed motoring region

This mode requires that the motor be operated at speeds higher than those achieved in the constant-power region. In this region, the supply voltage is maintained at the rated voltage and the slip frequency is maintained at its maximum value as the stator frequency is increased. The output torque therefore varies inversely as speed squared. This is shown in Fig. 1.6.

1.4 Implementation of variable frequency AC supply

The need for constant V/f control has been outlined in the previous sections. In order to implement the required V/f control, a variable frequency - variable voltage AC supply is necessary. The generation of variable frequency AC power can be achieved by rotating frequency converters and static frequency converters.

The rotating frequency converter usually consists of a synchronous machine driven

at variable speed in order to generate a variable frequency power. Maintaining the field current constant, enables the synchronous machine to deliver a constant volts/hertz output. Also at low speeds, the field current can be increased so that the volts/hertz can be boosted for low frequency operation.

Static frequency converters offer improved performance and reliability over rotating frequency converters. Static frequency converters employ static solid-state switching devices such as power transistors, gate turn-off thyristors (GTO), insulated gate bipolar transistors (IGBT) and MOS-controlled thyristors (MCT).

The static frequency converters can be classified as follows

1. DC link converter

2. Cycloconverter

1.4.1 DC link converter

The block diagram of the DC link converter is shown in Fig. 1.7. The fixed voltage

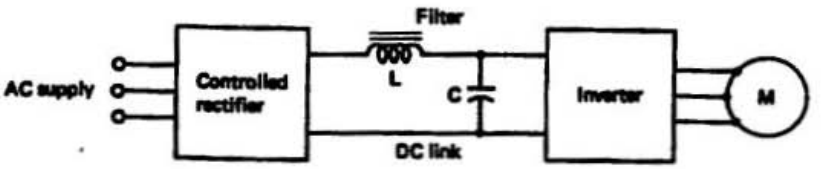

Figure 1.7: Block diagram of DC link converter [18]

fixed frequency AC supply is rectified using a standard rectifier and the resulting DC power is fed into the static inverter. The static inverter uses semiconductor switching

devices to convert the DC input into an AC output. The switches of the inverter are switched sequentially such that the output is as close to a perfect AC waveform as possible. The output frequency of the inverter is determined by the rate at which the inverter switches are triggered into conduction. The inverter control circuit usually consists of a group of logic circuitry which generate and distribute firing pulses in the correct sequence to the various switches. The output of the inverter, both the voltage and its frequency, can be controlled using the control circuit of the inverter. But the output voltage waveform is not sinusoidal and may contain various dominant harmonics. External filter circuits are not often employed due to the difficulty in obtaining effective operation over a wide range of frequencies. Harmonic effects must be taken into consideration while choosing a motor for inverter driven applications.

The non-sinusoidal output of the inverter is directly fed to the induction motor. This does not pose serious limitations except a slight reduction in the rating and efficiency of the motor. The V/f output of the inverter can be controlled by various control techniques which can be used to implement the inverter control circuitry. These techniques will be outlined in chapter 2.

The DC link converter involves double power conversion to achieve variable voltage, variable frequency AC supply. The efficiency of the converter can be anywhere from 85% to 95% in practice.

1.4.2 Cycloconverters

In this type of static frequency converters, AC voltage at supply frequency is directly converted to AC voltage at load frequency without intermediate rectification. The output frequency is usually about one-third the supply frequency and hence the drive is suitable only for low-speed operation. Thyristors are used to selectively connect the load to the supply and the low-frequency output is fabricated from segments of the supply voltage waveform. This is shown in Fig. 1.8.

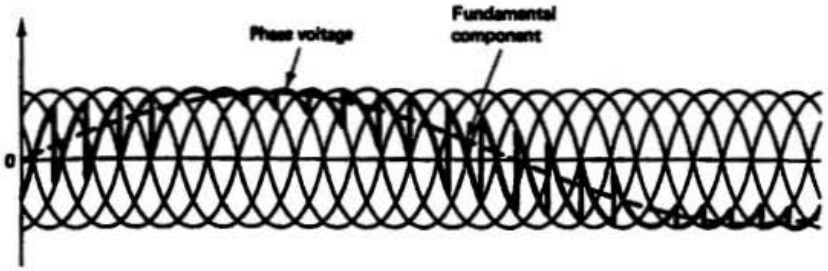

Figure 1.8: Input and output waveforms of phase-controlled cycloconverter [18]

As stated above, the output frequency of the cycloconverter is less than the supply frequency. As the output frequency approaches the supply frequency, the harmonic distortion in the output voltage increases, since the output voltage waveform is now being composed of fewer segments of the supply voltage. This results in increased losses in the cycloconverter and the AC motor, and the overall efficiency of the system is reduced.

1.5 Objectives and outline of the thesis

The previous sections explained the various speed control strategies, the induction motor characteristics, and the implementation techniques for a variable voltage variable frequency AC supply. Most of the industrial drives employing induction motors operate in the constant-torque region. Hence efficient V/f control becomes critical. In order to realize the constant volts/hertz control, DC link converters are widely used.

This thesis aims to develop an improved V/f control strategy after a thorough review of the available control strategies used in the inverter control of the DC link inverter. Thus the principal focus of the thesis is to develop an improved inverter control strategy for the DC link converter which aims to provide an efficient and feasible V/f control characteristic in the constant-torque region.

Chapter 2 focuses on the review of available V/f control strategies such as sinusoidal PWM and delta modulation schemes, discussing their advantages and limitations. It also looks at the limitations of these control strategies for variable frequency induction motor drives, thereby setting the stage for the development of the improved modulation technique.

Chapter 3 outlines the development of the improved modulation scheme called the unified modulation scheme and discusses the characteristic features of the new scheme. A comparison of the characteristics of the new scheme with that of the

existing schemes is also carried out. Also, this chapter briefly discusses the effects of harmonics on motor drives.

Chapter 4 deals with the experimental verification of the proposed modulation scheme using PIC micro-controller. The experimental results are also discussed.

Chapter 5 focuses on the application of the unified modulation scheme for an induction motor drive. The simulation results obtained using SIMULINK models are compared with the results of an induction motor drive implemented using the delta modulation technique. Machine de-rating calculations due to harmonics are also carried out.

Chapter 6 outlines the development of a modified unified modulation scheme based on the unified modulation scheme and the conventional sine PWM scheme. The characteristics of this modified unified modulation scheme are discussed along with its application for a variable frequency induction motor drive.

Finally chapter 7 summarizes the entire thesis focusing on the contribution of the research work and the scope for future research.

Chapter 2

Review of existing modulation schemes

The dc link converter, as described earlier, is a two-stage conversion device in which fixed voltage, fixed frequency AC power is converted into variable voltage, variable frequency AC power. DC link converters are widely used to realize V/f control characteristics required for speed control in induction motor drives. The second stage of the DC link converter involves the inverter which is responsible for generating a variable voltage, variable frequency output. This chapter will discuss in detail the various inverter control techniques used in attaining the required volts/hertz control. This chapter also provides the opportunity to discuss the characteristic features of each of these techniques, thereby bringing out the necessity for an improved control scheme.

2.1 Inverter control techniques

The function of the inverter is to change a DC input power into a symmetrical AC output of desirable magnitude and frequency. The inverter could be controlled to give either a fixed or variable voltage output at a fixed or variable frequency. The frequency control is achieved by controlling the frequency of the control signal usually known as the modulating signal. The variable voltage output is achieved by varying the DC input voltage and maintaining the inverter gain constant, or by maintaining a constant DC input and varying the inverter gain. The inverter gain can be defined as the ratio of the AC output voltage to the DC input voltage.

In most of the practical variable speed control applications, the DC input voltage is maintained constant and the AC output voltage is varied by varying the inverter gain. This general method of voltage control is termed pulse-width modulation (PWM). In a more refined form of PWM, the pulse width is varied throughout the half-cycle in a sinusoidal manner. Also in recent years, the use of delta modulation techniques which are simple forms of differential pulse code modulation technique have gained much popularity. The following sections elaborate on these control techniques used in inverters namely

- Sinusoidal pulse width modulation (SPWM) technique
- Delta modulation technique

2.2 Sinusoidal PWM modulation technique

The characteristic feature of the sine PWM is that the pulse width at a particular angle should be proportional to the sine of that angle. Voltage control is obtained by varying the widths of all pulses and still maintaining the sinusoidal relationship. In the case of inverter control, a high frequency triangular carrier wave $v_c(t)$ is compared with a sinusoidal reference wave $v_r(t)$ at the desired frequency as shown in Fig. 2.1. The cross over points are used to determine the inverter switching instants. The

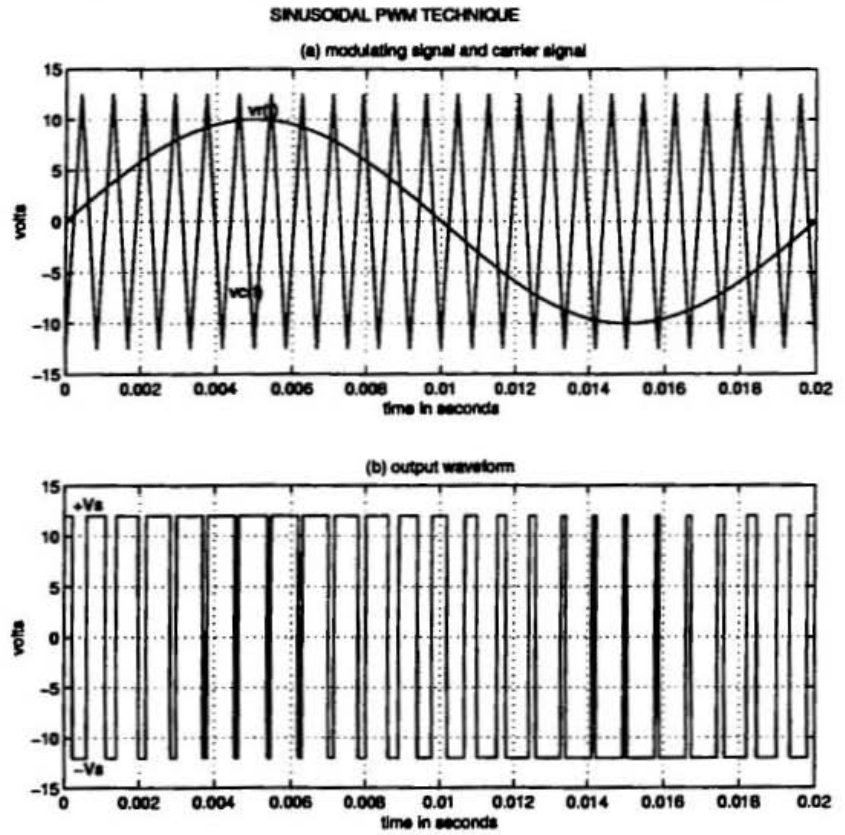

Figure 2.1: Sinusoidal pulse width modulation technique

triangular carrier has a fixed amplitude and a constant switching frequency. The ratio of the sine wave amplitude to the amplitude of the carrier is termed as modulation index M. Control of the output voltage is achieved by variation of the amplitude of the modulating signal i.e. the sine wave. This variation alters the pulse widths in the output voltage waveform but preserves the sinusoidal property.

The ratio of the carrier frequency to the modulating frequency is termed as the carrier ratio p. The distribution of undesired harmonics depends on the carrier ratio. For large carrier ratios, the sine PWM inverter delivers a high-quality output voltage waveform in which the dominant harmonics are in the higher order, clustered around the carrier frequency and its harmonics.Thus the carrier ratio is crucial in determining the order of the dominant harmonics in the output voltage of the sine-PWM inverter. The harmonic spectrum of the output waveform, obtained using Fourier series analysis, shows that the harmonics occur at the side-bands of the carrier frequency and its multiples. In general form, the harmonic order can be given by $k = np \pm m$. The harmonics are non-existent when both m and n are either even or odd. Therefore for even values of n, there is an odd side-band spectrum and for odd values of n, there is an even side-band spectrum.The harmonic magnitudes are independent of the carrier ratio p, provided p is greater than nine[11]. The magnitudes of the major harmonic components plotted as a function of the modulation index M are given in Fig. 2.2 Figure 2.2 shows the harmonic magnitude V_k expressed as a fraction of the maximum

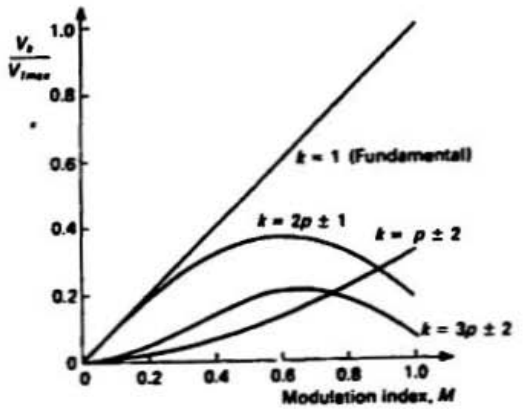

Figure 2.2: Harmonic content of the sinusoidal PWM voltage as a function of modulation index

fundamental magnitude V_{1max} plotted for values of the modulation index M between zero to unity. The linear relationship between the fundamental voltage magnitude and the modulation index can be seen from Fig. 2.2. Also it can be seen that the lowest harmonics of appreciable magnitude is of order $p-2$. The fundamental voltage amplitude V_{o1} is given by the following equation 2.1, which is also a measure of voltage utilization or inverter gain by the modulation scheme.

$$V_{o1} = MV_{dc} \; for \; 0 \leq M \leq 1 \tag{2.1}$$

where V_{dc} is the voltage magnitude of the DC supply. Improved voltage utilization can be achieved if the molduation index M is increased above unity. Such an increase in M overrides the normal sinusoidal modulation and is termed as the over-modulation.

The penalty paid is the appearance of lower order harmonics at the output voltage waveform and the relationship between the amplitude of the fundamantal and M becomes nonlinear.

Improvements to the conventional sine PWM technique have resulted in the uniform sampling technique[19] based on the sample and hold principle, where the sine modulating signal is replaced by an equivalent stepped signal. This called for a microcomputer implementation, and the power of the microcomputer was also used in harmonic elimination.

With an overview of the sine PWM scheme, we proceed to discuss the application of the sine PWM technique to induction motor drive with the V/f control strategy.

2.3 Sinusoidal PWM inverter fed induction motor drives

In the case of variable frequency induction motor drives requiring V/f control, the application of constant volts/hertz supply at the motor terminals results in a constant air-gap flux, provided the stator voltage drop is negligible. At low frequencies, this drop constitutes a large proportion of the terminal voltage. Thus, for motoring operation, there is severe under-excitation and intolerable loss of torque capability. This problem is usually tackled by implementing a terminal voltage boost at low frequencies to compensate for the stator drop. This is shown in Fig. 2.3a. The linear characteristic represents the ideal V/f curve. The non-linear characteristic shows the

voltage boost required at low frequencies. In the offset linear characteristic, a constant voltage component V_o is added to the frequency-proportional component $k\omega_1$, to define the stator voltage as[11]

$$V_1 = V_o + k\omega_1 \tag{2.2}$$

If the load requires a high starting torque, V_o can be adjusted such that a large

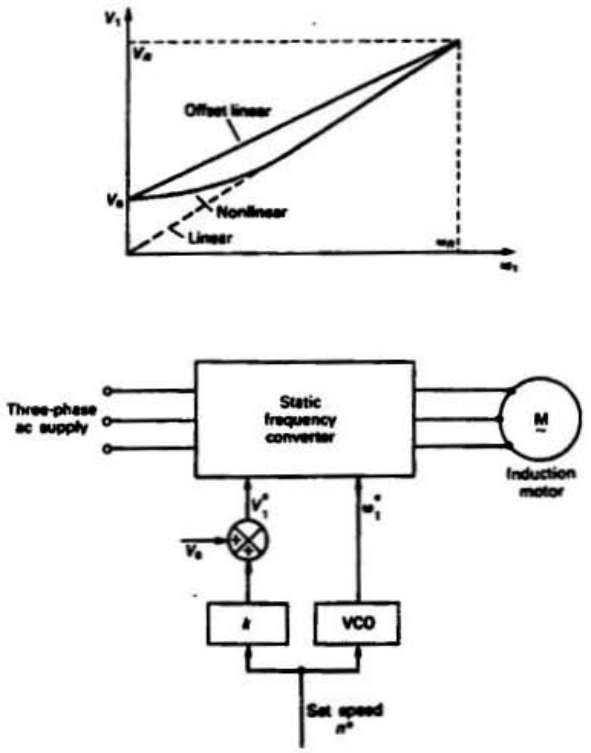

Figure 2.3: Linear,non-linear and offset V/f characteristics for induction motor drives [11]

motor current flows at starting. However, this large boost may cause overheating if

the motor operates continuously at low frequencies.

Fig. 2.3b shows the block diagram for an induction motor requiring V/f control. Most of the medium performance drives involving open-loop speed control use sine PWM voltage-source inverters. The absence of speed or flux sensing makes this a low-cost, commercially viable adjustable-speed drive. Also, the sine PWM scheme has a constant switching frequency and hence there is no frequency modulation. The amplitude modulation required to achieve variable output voltage is accomplished by varying the amplitude of the reference signal. However there are sufficient limitations to the use of sine PWM scheme for the V/f control of inverter fed induction motor drives. The sine PWM scheme lacks an inherent V/f feature. This calls for the use of additional circuitry in analog implementation. However in digital hardware implementation, the difference in complexities are not so significant. Also in sine PWM, due to constant switching frequency operation, at lower operating frequencies there will be significant attenuation of lower-order harmonics. But as the frequency of operation increases towards the break frequency of the V/f curve, the output of the modulator becomes more of a square wave thereby causing significant presence of lower-order harmonics at the output frequency spectrum. Also, a constant switching frequency for all frequencies of the reference signal signifies that the switching frequency will always not be an integral multiple of the reference frequency. This causes the generation of sub-harmonics in the frequency spectrum of the output. These

harmonics increase the copper losses, decrease the efficiency and also cause torque pulsations as will be explained in chapter 3. Computationally intensive and improvised sine PWM techniques which aim at harmonic elimination have been attempted to improve the performance [20, 21].

2.4 Delta modulation scheme

The use of delta modulation technique in static PWM inverters was first introduced by Ziogas [22]. The delta modulation scheme can be used for variable speed drives because it offers the following advantages

- Inherent V/f control
- Attenuation of lower order
- Smooth transition from the V/f mode to the constant volts mode

Delta modulators are simple forms of differential pulse modulation and can be grouped into the following categories [23]

- The linear delta modulator (LDM)
- The sigma-delta modulator ($\Sigma - \Delta M$)
- The adaptive delta modulator (ADM)
- The asynchronous delta modulator (ASDM)

We limit our focus to one particular type of asynchronous delta modulator known as the rectangular wave delta modulator (RWDM) which has been successfully implemented and analyzed [24].

The rectangular wave delta modulator has found wide acceptance in inverter applications. The block diagram of the rectangular wave delta modulator is shown in Fig. 2.4. It consists of a comparator, a hysteresis quantizer in the feed-forward path and an integrator or a low-pass filter in the feedback path. The reference signal $v_r(t)$ is compared with the feedback carrier signal $v_c(t)$, which is obtained by integrating the modulator output signal. Based on the sign and the magnitude of the resultant error signal $e(t)$, the output of the modulator has two possible levels $\pm V_s$. The time duration between two successive levels is determined by the slope of the reference signal. Assume the output of the modulator to be $+V_s$. This output is integrated by the integrator in the feedback path to produce a signal which ramps up with a slope S_c equal to the integrator gain. When the magnitude of the integrator output exceeds the reference signal by a preset value$+\Delta V$, known as the hysteresis bandwidth, the modulator output switches to $-V_s$. Now the integrator output will ramp down with the same slope till the error signal $e(t)$ reaches the preset value $-\Delta V$ (the lower hysteresis limit), when the modulator output switches to $+V_s$. The equations characterizing the rectangular wave delta modulator are given as[25]

$$e(t) = v_r(t) - v_c(t) \tag{2.3}$$

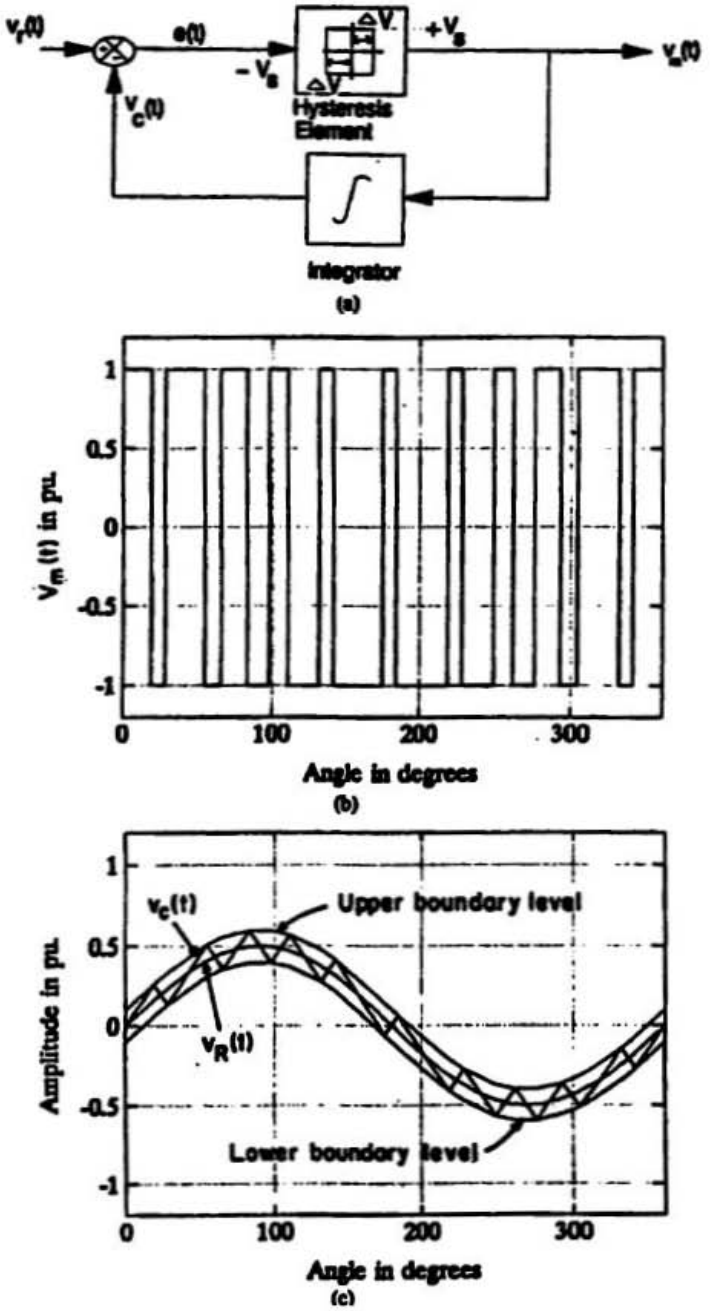

Figure 2.4: Block diagram of the rectangular wave delta modulator, the modulator output and the modulation process [25]

$$v_o(t) = V_s sgn[e(t)] \tag{2.4}$$

where $v_o(t)$ is the modulator output

V_s is the saturation level of the hysteresis comparator

$v_r(t)$ is the reference signal

$v_c(t)$ is the carrier signal

sgn is the sign function

A detailed performance analysis including the effects of the modulator parameters on the output waveform of the rectangular wave delta modulator was reported by Abdel Rahim [25]. He showed that the parameters of the modulator that affect the frequency spectrum of the modulator output are: the integrator gain S_c, the hysteresis bandwidth ΔV, the amplitude V_r and angular frequency ω_r of the reference signal. He further reported that the amplitude of the modulator output depends on the modulation index and the integrator gain. The order of dominant harmonics at the output depends on the hysteresis bandwidth and the integrator gain, both of which have a direct bearing on the switching frequency.

As enumerated earlier, one of the attractive features of the delta modulation technique is its inherent V/f feature i.e. the output voltage changes in a certain constant proportion with the input signal frequency, which lends itself suitably for inverter-fed variable frequency control of induction motor drives, as will be explained later in this chapter and in chapter 5.

It is also important to discuss the limitations of the delta modulation technique. First among them is known as the idle channel condition, which occurs when the reference signal is DC. This condition usually does not arise in inverter applications, although the phenomenon may occur at low frequencies (0.5 - 1 Hz). The second limitation is known as the slope overload condition, where the rate of change of the reference signal is faster than that of the carrier signal. When the slope of the reference signal increases and slowly approaches that of the carrier signal, the output of the modulator starts to become more of a square waveform. Square wave mode of operation results when the slope of the reference signal is greater than that of the carrier signal over the whole cycle. Thus to avoid the slope overload condition, the maximum slope of the reference signal must be less than or equal to that of the carrier signal. For motor drives, this phenomenon is likely to occur at high speed operation.

In the case of the delta modulated inverter, frequency modulation occurs in conjunction with duty-cycle modulation. This adds complexity in small signal modeling of delta modulated inverters. Also, the output waveform is not synchronized to the modulating waveform and hence is not periodic. This asynchronous operation introduces a periodic asymmetry at the output. Thus the spectrum of the delta modulator cannot be analyzed using Fourier series because of the non-periodic nature of the output. Bird et al. [26] have used the technique of Fourier series expansion in two variables to analyze asynchronous PWM systems. This method is valid as

far as the asynchronous signal is either due to frequency modulation or duty-ratio modulation. So far in the literature, the analysis of the delta modulation scheme has been simplified by considering the output to be periodic over several cycles of the modulating signal. It was further simplified by Rahman et al. [27] by considering the output to be periodic. This, however, produces accurate results only in a small number of special cases. In an attempt to minimize the asynchronous nature of the output signal, Green et al. [28] developed a scheme in which the carrier signal was forced to zero at the zero-crossings of the modulating signal. The approach resulted in a quarter-wave symmetry of the output signal. However, in some cases, the pulse width of the PWM signal near the zero-crossings were so small that it infringed on the minimum pulse-width requirement for the inverter switches. Christiansen et al. [29] attempted a synchronized delta-modulation technique by adding synchronizing pulses to the error signal of the feedback loop of the delta modulator in order to fix the switching frequency. This technique suffers setbacks such as period doubling, loss of synchronism following slope transition and loss of commutation cycles during slope transition.

The order of dominant harmonics in the output waveform depends on the frequency of the carrier signal. The frequency of the carrier signal f_c is given by the expression [28]

$$f_c = \frac{S_c}{2h}(1 - m^2), \tag{2.5}$$

where $m = S_r/S_c$ and $h = 2\Delta V$. S_r is the slope of the reference signal. From the equation 2.5 it can be seen that modulation of the frequency of the carrier signal occurs, as mentioned earlier. Hence the order of the dominant harmonics at the output spectrum is not an exact integer multiples of the reference frequency. This causes the generation of sub-harmonics in the output frequency spectrum. Also the order of the dominant harmonics changes with the change of the reference frequency. There is substantial attenuation of lower order harmonics at frequencies well below the break frequency (the frequency at which the slope of the reference signal equals that of the carrier signal). But as the reference frequency approaches the break frequency, the shape of the output waveform approaches a square wave and becomes a complete square wave at the break frequency. Thus for frequencies close to the break frequency, there exist significant lower order harmonics at the output.

In conclusion, the delta modulation scheme presents an inherent V/f characteristic which is much needed for V/f speed control. However, as a result of the frequency modulation, the order of dominant lower order harmonics is unpredictable. As well, the frequency and duty-cycle modulation produce asymmetrical output signals.

2.5 Delta-modulated inverter fed induction motor drive

The delta modulation scheme, with its inherent V/f characteristics is especially suited for V/f control of induction motor drives. But surprisingly, to the best of author's

knowledge, an actual implementation of such a drive has not been found in the literature. The delta-modulated inverter fed induction motor drive has been modeled using the SIMULINK software package available in MATLAB. The discussion about the modeling and the simulation results obtained are scheduled for Chapter 5. This section outlines the advantages and limitations of the delta modulation scheme when applied to inverter fed induction motor drives. The inherent V/f feature of the delta modulation scheme serves as a great advantage in the case of variable frequency induction motor drives employing V/f control. The scheme also boasts attenuation of lower-order harmonics and a smooth transition from the V/f mode to the constant volts mode, which are highly welcome in the case of induction motor drives. The major limitations are the accommodation of voltage boost required at low frequencies, the lower-order harmonics at operating frequencies close to the break frequency, and generation of sub-harmonics.

2.6 Motivation for the development of an improved modulation scheme

Among the existing modulation schemes, the sine PWM scheme lacks an inherent V/f control characteristic but possesses a constant switching frequency. The concept of constant switching frequency helps in predicting the order of the dominant lower harmonics at the output. Implementing the required V/f control feature using sine PWM requires the use of additional circuitry.

On the other hand, the delta modulation scheme possesses an inherent V/f control characteristic, but due to the frequency modulation, the varying switching frequency results in sub-harmonics and unpredictable frequency spectrum of the output signal.

This thesis attempts to develop a modulation scheme that combines the fixed switching frequency characteristics of the sine PWM and the inherent V/f characteristics of the delta modulation scheme. The goal is to develop a unified modulation scheme that eliminates the disadvantages of the two modulation schemes.

2.7 Summary

This chapter discussed the fundamental concepts of the two modulation schemes for static inverters, namely the delta modulation technique and the sine-PWM technique. The advantages and limitations of both sine PWM and delta modulation schemes, when applied to inverter fed induction motor drives requiring V/f control, were outlined.

It is shown that the development of a unified modulation scheme that combines the advantages of the two modulation schemes would greatly simplify the circuitry and improve the performance of V/f control of induction motor drives.

Chapter 3

The unified modulation scheme

Based on the discussion in the previous chapter, there exist two V/f control schemes each with their own advantages and disadvantages. The possibility of a single modulation scheme that can combine the advantages of both the schemes and at the same time eliminate their disadvantages served as a strong motivation. Thus the idea for an improved modulation scheme to achieve the needed V/f characteristic is derived from both the sine PWM and delta modulation schemes. This chapter deals with the development of this improved modulation scheme called the unified modulation scheme. The characteristic features of the unified modulation scheme and the improvements it offers, over the existing schemes, are discussed.

3.1 Development of the unified modulation scheme

The unified modulation scheme is a product of the combination of the delta and sine PWM schemes. The advantages of the delta modulation scheme, namely its inherent V/f feature and lower-order harmonic attenuation, and that of the sine PWM scheme

namely the absence of frequency modulation are to be the characteristic features of this improved scheme.

The duty-ratio modulation in the case of the delta modulation scheme as derived by Abdel Rahim, et al[30] is based on an important assumption that the modulator switching frequency can be assumed to be high so as to approximate a small portion of the reference or modulating signal by a straight line during one switching cycle of the modulator.

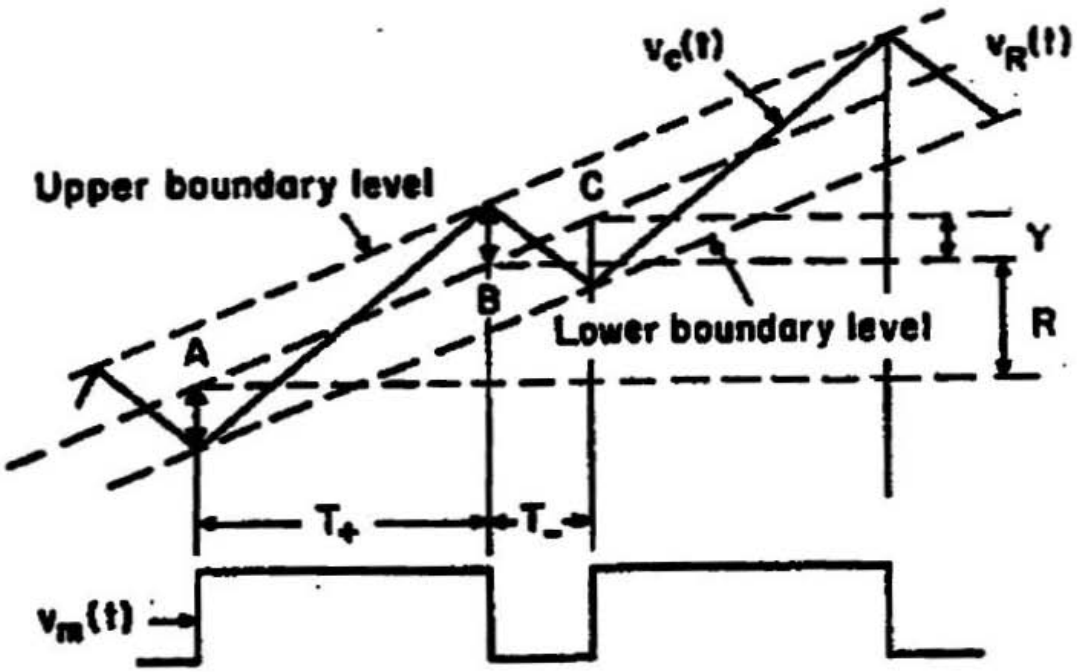

Figure 3.1: Graphical illustration of RWDM waveforms for obtaining an expression for duty-ratio modulation[25]

Fig. 3.1 shows a small portion of the reference signal $v_r(t)$ and the carrier signal

$v_c(t)$ along with the modulator output pulses, $v_m(t)$.

During the positive output pulse between AB, the slope of the modulating wave S_r is given by

$$S_r|_{AB} = \frac{R}{T_+}. \tag{3.1}$$

and the slope of the carrier wave S_c is given by

$$S_c|_{AB} = \frac{R + 2\Delta V}{T_+} \tag{3.2}$$

$$= S_r|_{AB} + \frac{2\Delta V}{T_+}. \tag{3.3}$$

Using equations 3.1 and 3.2, the expression for T_+ can be obtained as

$$T_+ = \frac{2\Delta V}{S_c - S_r}. \tag{3.4}$$

If $h = 2\Delta V$ and $m = S_r/S_c$, equation 3.4 can be expressed as

$$T_+ = \frac{h}{S_c(1-m)}. \tag{3.5}$$

During the negative output pulse BC, the slope of the modulating wave S_r is given by

$$S_r|_{BC} = \frac{Y}{T_-}, \tag{3.6}$$

and the slope of the carrier wave S_c is given by

$$S_c|_{BC} = \frac{2\Delta V - Y}{T_-} \tag{3.7}$$

$$= \frac{2\Delta V}{T_-} - S_r|_{AB}. \tag{3.8}$$

Using equations 3.6 and 3.7, the expression for T_- can be obtained as

$$T_- = \frac{2\Delta V}{S_c + S_r}. \tag{3.9}$$

In terms of h and m, equation 3.9 can be expressed as

$$T_- = \frac{h}{S_c(1+m)}. \tag{3.10}$$

The expression for one-cycle period of the modulator output pulse, T can be obtained from equations 3.5 and 3.10 as

$$T = T_+ + T_- = \frac{h}{S_c}(\frac{2}{1-m^2}). \tag{3.11}$$

Now, using equations 3.5 and 3.11, the duty-ratio η can be given by

$$\eta = \frac{T_+}{T} \tag{3.12}$$

$$= \frac{1+m}{2}. \tag{3.13}$$

Substituting for $m = S_r/S_c$, the duty-ratio modulation can be expressed as

$$\eta = \frac{1}{2}(1 + \frac{S_r}{S_c}). \tag{3.14}$$

With the reference signal defined as $v_r = V_r \sin(\omega_r t)$, its slope is given by $S_r = V_r\omega_r \cos(\omega_r t)$.

Substituting for S_r in equation 3.14, gives

$$\eta = \frac{1}{2} + (\frac{V_r}{2S_c})\omega_r \cos(\omega_r t). \tag{3.15}$$

Simplifying equation 3.15, the duty-ratio variation in the case of the delta modulation scheme can be generalized to the form

$$\eta = 0.5 + K f_r \cos(\omega_r t). \tag{3.16}$$

where $K = (V_r \pi)/S_c$ is designated the unified modulation constant. K has units of seconds, and its value decides the slope of the V/f characteristic, which is a constant for a particular V/f curve.

In order to achieve a similar duty-ratio modulation and an inherent V/f feature as the conventional delta modulator, equation 3.16 is used as the modulating signal or the reference signal, instead of the conventional reference signal $v_r = V_r \sin(\omega_r t)$. Since the duty-ratio modulation is a function of the reference frequency f_r, any required V/f characteristics can be achieved. Furthermore, the output pulses are obtained by sampling the modulating signal at a sampling frequency that is always an integral multiple of the modulating signal frequency. This approach ensures that the switching frequency is fixed for a particular reference frequency. The resulting conversion of the amplitude of the reference signal to corresponding pulse widths can be achieved as shown in Fig. 3.2.

3.2 Characteristic features of the unified modulation scheme

The unified modulation scheme uses a modulating signal of the form given in equation 3.16. The switching frequency must be an integral multiple of the frequency of the

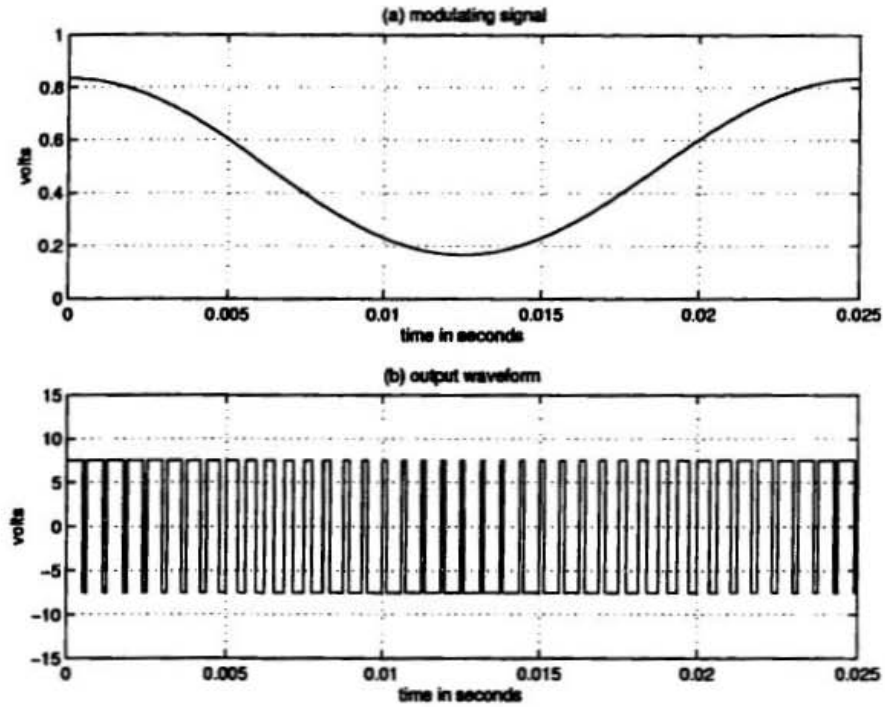

Figure 3.2: Unified modulation scheme waveforms for $f_r = 40Hz$, $f_s = 40f_r$ and $V_{dc} = 12V$

modulating signal. The characteristic features of the unified modulation scheme can be studied with the help of a design example of the modulator.

Design specifications

$V_{dc} = 12V$ (DC supply voltage)

$f_{rb} = 60Hz$ (Break frequency)

$f_s = 40f_r$ (Sampling or Switching frequency)

$K = 8.333 \exp -3s$ (Unified modulation constant)

The V/f characteristics pertaining to the above design specifications is shown in Fig. 3.3 In order to simulate the unified modulation scheme with the above design speci-

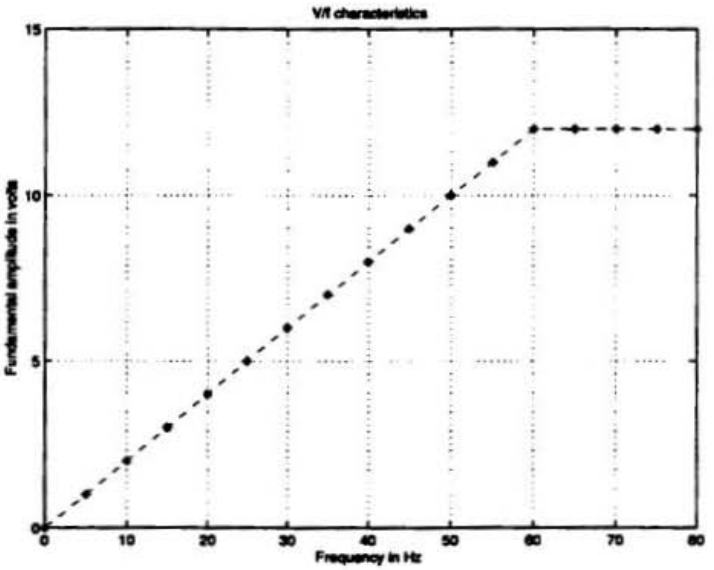

Figure 3.3: V/f characteristics with $K = 8.333 \exp -3s$ and $f_{rb} = 60Hz$

fications, a MATLAB program was written and the output of the unified modulator

was analyzed using Fast Fourier transform (FFT) algorithm. The modulating signal, the output of the unified modulator and the frequency spectrum of the output for operating frequencies $f_r = 40Hz$ and $f_r = 60Hz$ are shown in Fig. 3.4 and Fig. 3.5 respectively.

The frequency spectra for the two operating frequencies show that the unified modulation scheme maintains a constant V/f ratio. Also it can be seen from the frequency spectra of the output that the order of the dominant harmonics are dependent on the switching frequency which is an integral multiple of the modulating frequency. In this case the dominant harmonics occur around the 40th harmonic.

The characteristic features of the unified modulation scheme can be summarized as follows:

- The modulating signal, $\eta = 0.5 + K f_r \cos(\omega_r t)$, describes the duty-ratio modulation of the modulator output pulses.

- The switching frequency f_s is always an integral multiple of the reference frequency i.e. $f_s = p f_r$ where p is a constant. Although the switching frequency varies with the modulating signal frequency, the effect of frequency modulation is significantly reduced. Unlike the conventional delta modulator, the number of commutations per cycle of the modulating signal is dependent on p and is fixed.

- The product $K f_r \cos(\omega_r t)$ can be termed as the duty-ratio modulation index

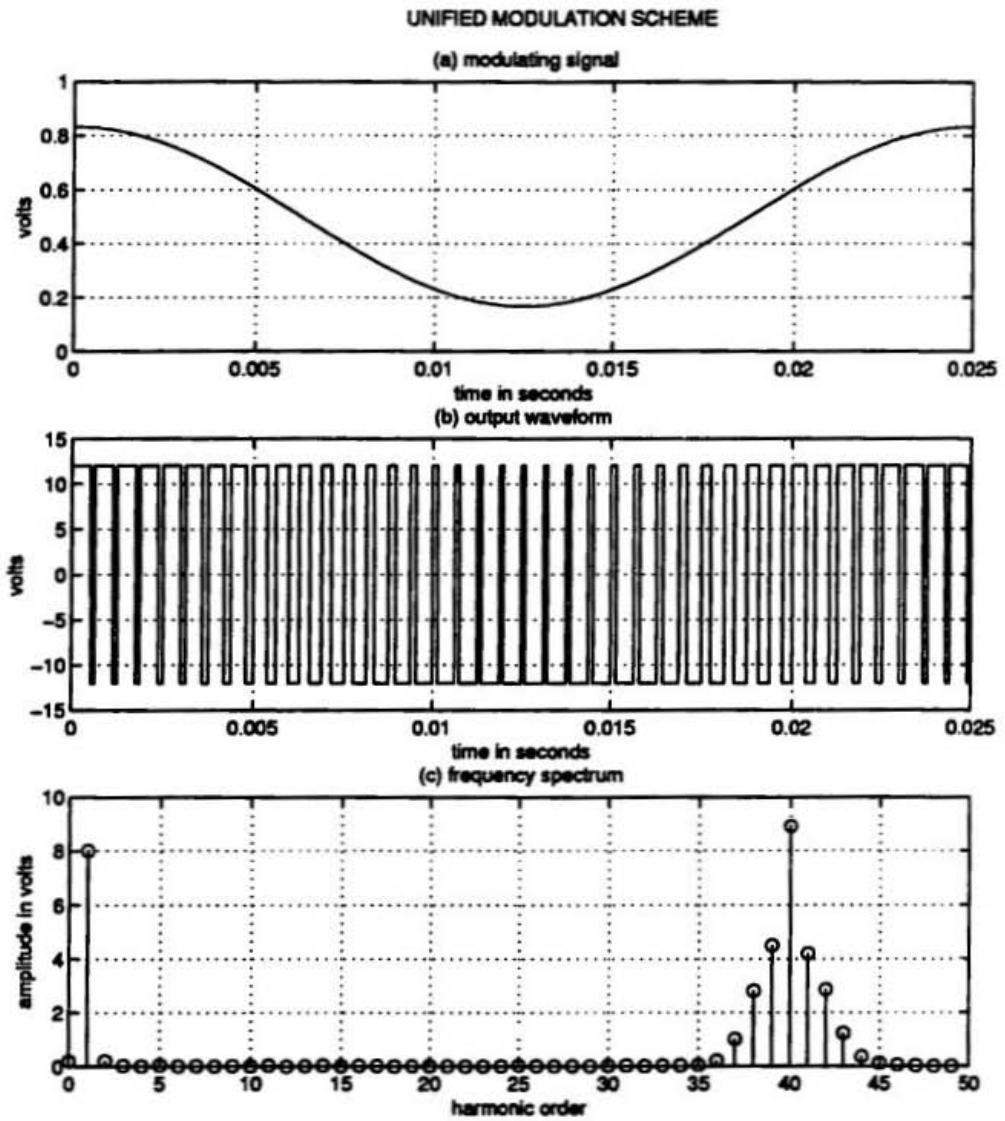

Figure 3.4: Unified modulation scheme: $f_r = 40Hz, f_{rb} = 60Hz, V_{dc} = 12V$ and $K = 8.333 \exp -3s$

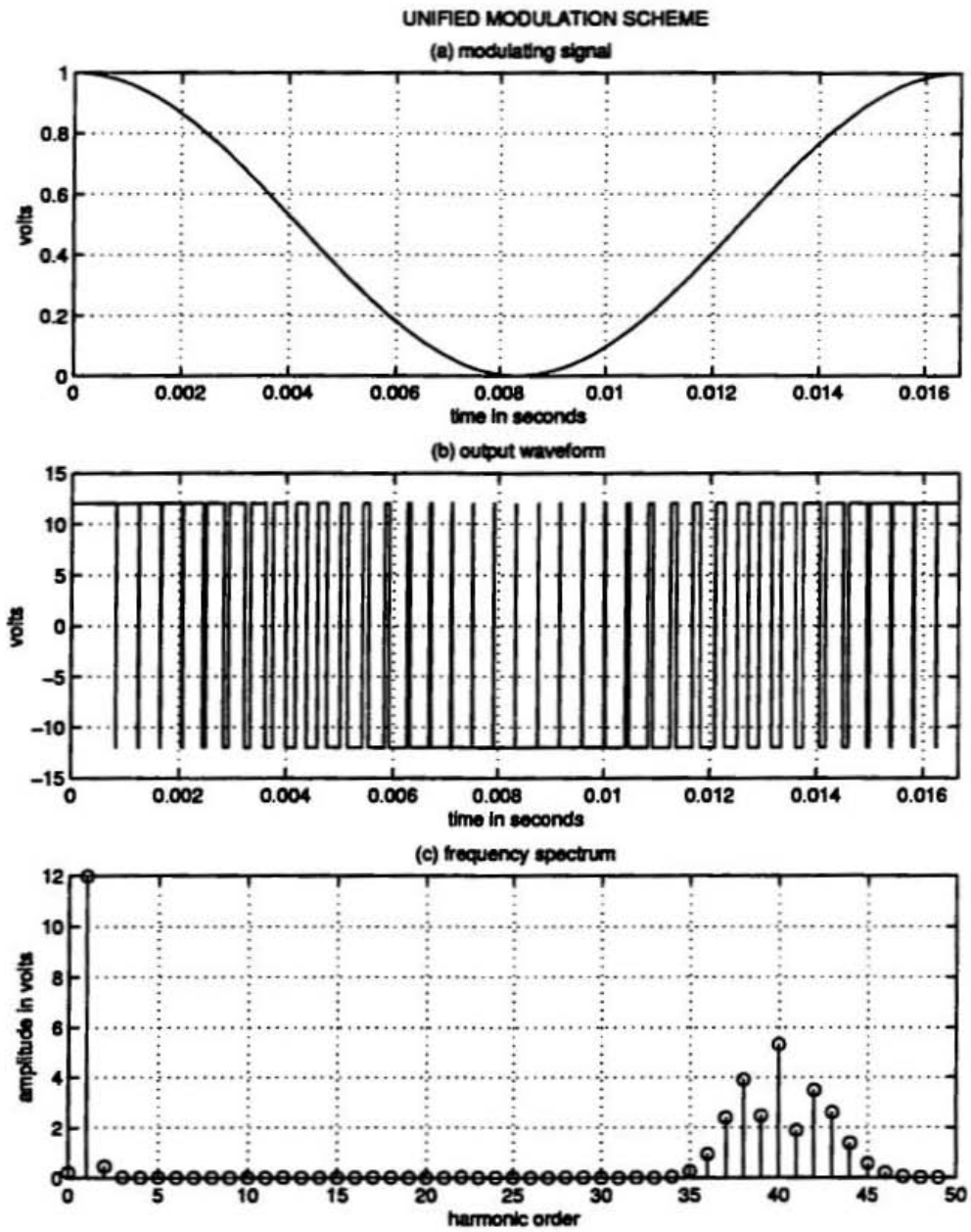

Figure 3.5: Unified modulation scheme: $f_r = 60Hz, f_{rb} = 60Hz, V_{dc} = 12V$ and $K = 8.333 \exp -3s$

M_{dr} since it controls the magnitude of the modulating signal η_{max} and hence the magnitude of the fundamental component at the output. Hence η_{max} can be termed as the unified modulation index.

$$M_{dr} = Kf_r \cos(\omega_r t) \tag{3.17}$$

$$(M_{dr})_{max} = Kf_r \tag{3.18}$$

$$\eta_{max} = 0.5 + Kf_r \tag{3.19}$$

$$Vol = \eta_{max} V_{dc} \tag{3.20}$$

Ideally the value of the duty-ratio modulation index $(M_{dr})_{max}$, can vary from 0 to 0.5. The value of the duty-ratio modulation index constant, K decides the slope of the V/f characteristic. It is chosen such that for a particular break frequency f_{rb} on that V/f characteristic, the product Kf_{rb} must be 0.5 and for all values of f_r greater than f_{rb}, the value of Kf_r must be kept at Kf_{rb} in order to maintain constant voltage . But in practical applications, the value of Kf_r ranges between $(Kf_r)_{min}$ and $(Kf_r)_{max}$. $(Kf_r)_{min}$ is chosen to be slightly greater than zero and $(Kf_r)_{max}$ is chosen to be slightly less than 0.5, depending on the type of application namely, UPS or V/f control, for which the modulation scheme is used. This is necessary in order to avoid any commutation failure and to avoid any infringement on the minimum and maximum pulse width criteria for successful inverter operation.

- The order of dominant harmonics at the output of the unified modulator is dependent on the switching frequency. Since the switching frequency is an integral multiple of the frequency of the modulating signal, the order of the dominant harmonics at the output spectrum can be given by $f_h = mf_s \pm n$ where m=1,2,3..., and n=1,2,3.... Figure 3.6 shows the normalized harmonic

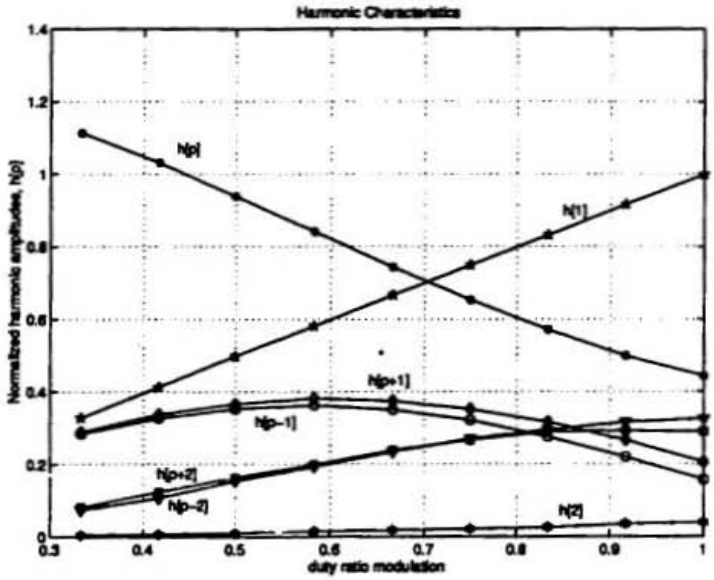

Figure 3.6: Harmonic content of the output of the unified modulation scheme as a function of the duty-ratio modulation index

amplitude $h[p]$, which is the ratio of harmonic amplitude V_k to the maximum fundamental amplitude V_{1max} plotted for normalized values of the duty-ratio modulation index M_{dr}. It can be seen that the relationship between the normalized fundamental voltage magnitude $h[1]$ and the duty-ratio modulation

index is linear.

3.3 Comparison between the modulation schemes

With the discussion on the development and the characteristic features of the unified modulation scheme, it is essential to compare the characteristics of the unified modulation scheme with that of the existing schemes so as to bring out its improvements and its disadvantages.

3.3.1 Common design specifications - A basis for comparison

In order to compare the characteristics of the unified modulation scheme with those of the delta and the sine PWM schemes, a set of common design specifications for the V/f characteristics shown in Fig. 3.3, was established. All the modulation schemes were designed based on these specifications and the designs were simulated using programs written in MATLAB [31]. The design specifications are as follows:

- The modulation scheme design must be in accordance to the V/f characteristic shown in Fig. 3.3 i.e. break frequency $f_{rb} = 60Hz$ and $V_{o1}|_{f_{rb}} = 12V$.
- In the case of the sine PWM scheme which does not possess an inherent V/f characteristic, the amplitude of the modulating signal is changed at each operating frequency, so as to vary the modulation index and achieve the required V/f characteristic.

- In the case of sine PWM , the switching frequency is maintained constant. In the delta modulation scheme, the switching frequency is relatively high at lower frequencies of the reference signal and vice versa. The switching frequency of a delta modulator is dependent on the slope of the reference signal, integrator gain and the hysteresis bandwidth, as given in equation 2.2. In the case of the unified modulation scheme, the switching frequency is chosen such that it will always be a constant integral multiple of the reference signal frequency. For V/f control from 0Hz to 60Hz, it has been found that the switching frequency of the delta modulator at about 30Hz is 750Hz. Hence the average switching frequency for the comparison of the three modulation schemes is chosen to be 1200Hz.

- For the unified modulation scheme, the switching frequency is chosen as $f_s = 25f_r$, since the switching frequency at the reference signal frequency of 30Hz is 750Hz.

3.3.2 Comparison between Unified, Delta and Sinusoidal PWM modulation schemes

The designs were simulated with the help of MATLAB programs and the output waveforms were subjected to FFT analysis in order to obtain the frequency spectrum. The simulation results obtained for the sine PWM, the delta and the unified modulation schemes at modulating frequencies $f_r = 20Hz$, $f_r = 30Hz$ and $f_r = 55Hz$

are shown in Fig. 3.7 to Fig. 3.15 respectively.

Based on the simulation results obtained for the two modulating frequencies, the following inferences can be made:

- Amplitude of the fundamental component in the frequency spectrum of the output waveform: Figures 3.7 to 3.15 show that the amplitudes of the fundamental components for the three schemes are consistent with the V/f ratio specified. It should be noted however, that the DMS and UMS do not require any special arrangement to provide the specified V/f ratio. On the other hand, as noted above, the modulation index of the SPWM had to be adjusted to provide the specified V/f ratio.

- Number of commutations per cycle of the modulating signal: Figures 3.7b to 3.15b show that for the SPWM, the number of commutations per cycle of the modulating signal is large at lower frequencies and it decreases with increasing modulating frequency. Figures 3.8b and 3.14b indicate that the DMS exhibits the same characteristics as the SPWM. However, figures 3.9b and 3.15b show that for the UMS scheme, the number of commutations per cycle of the modulating signal always remains a constant. This is because the switching frequency is always an integral multiple of the modulating frequency i.e. $f_s = 25f_r$ for this design.

- Switching losses: In the case of SPWM and DM schemes, the switching losses

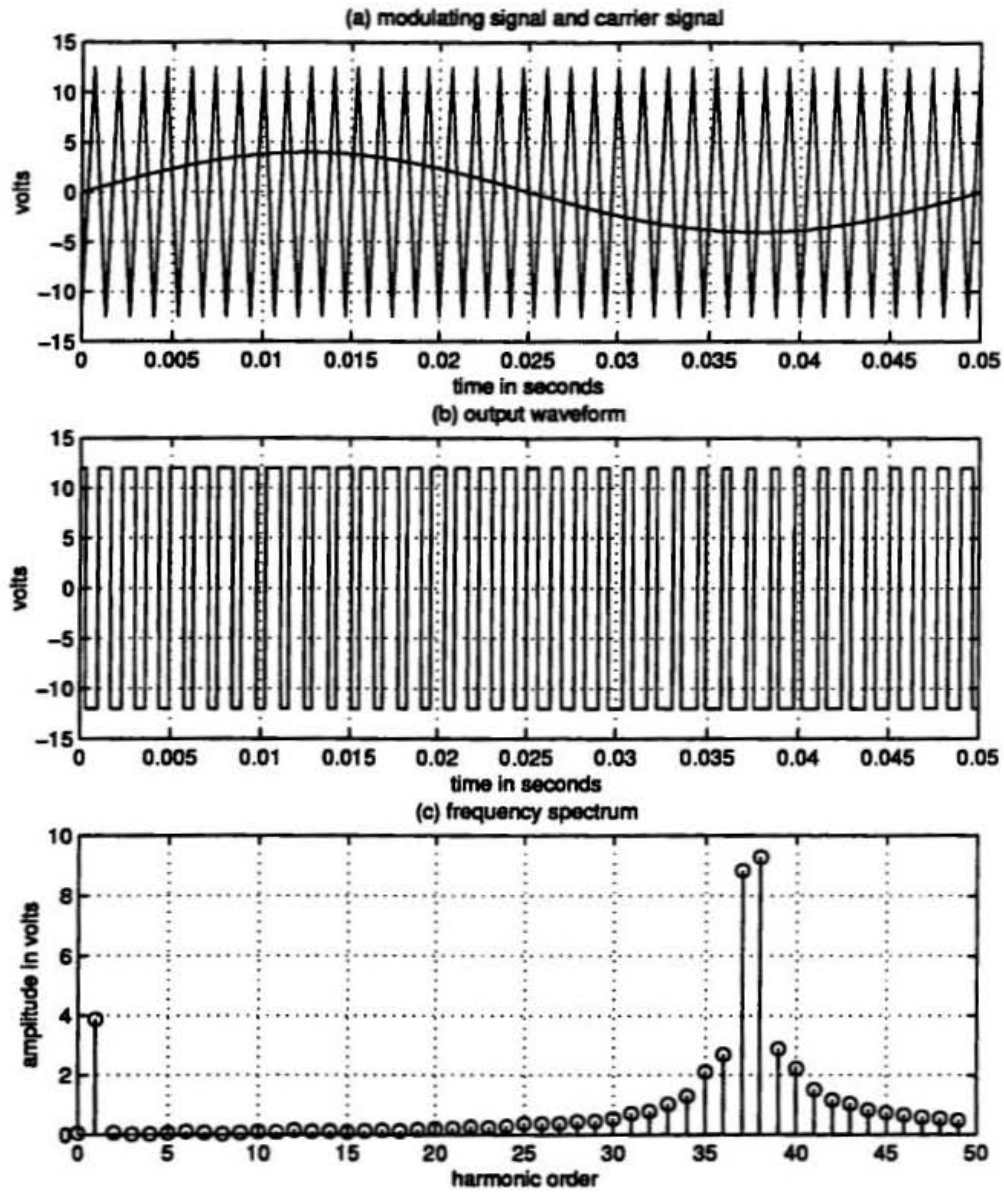

Figure 3.7: Sine PWM scheme waveforms at $f_r = 20Hz$, $f_{rb} = 60Hz$ and $V_{dc} = 12V$

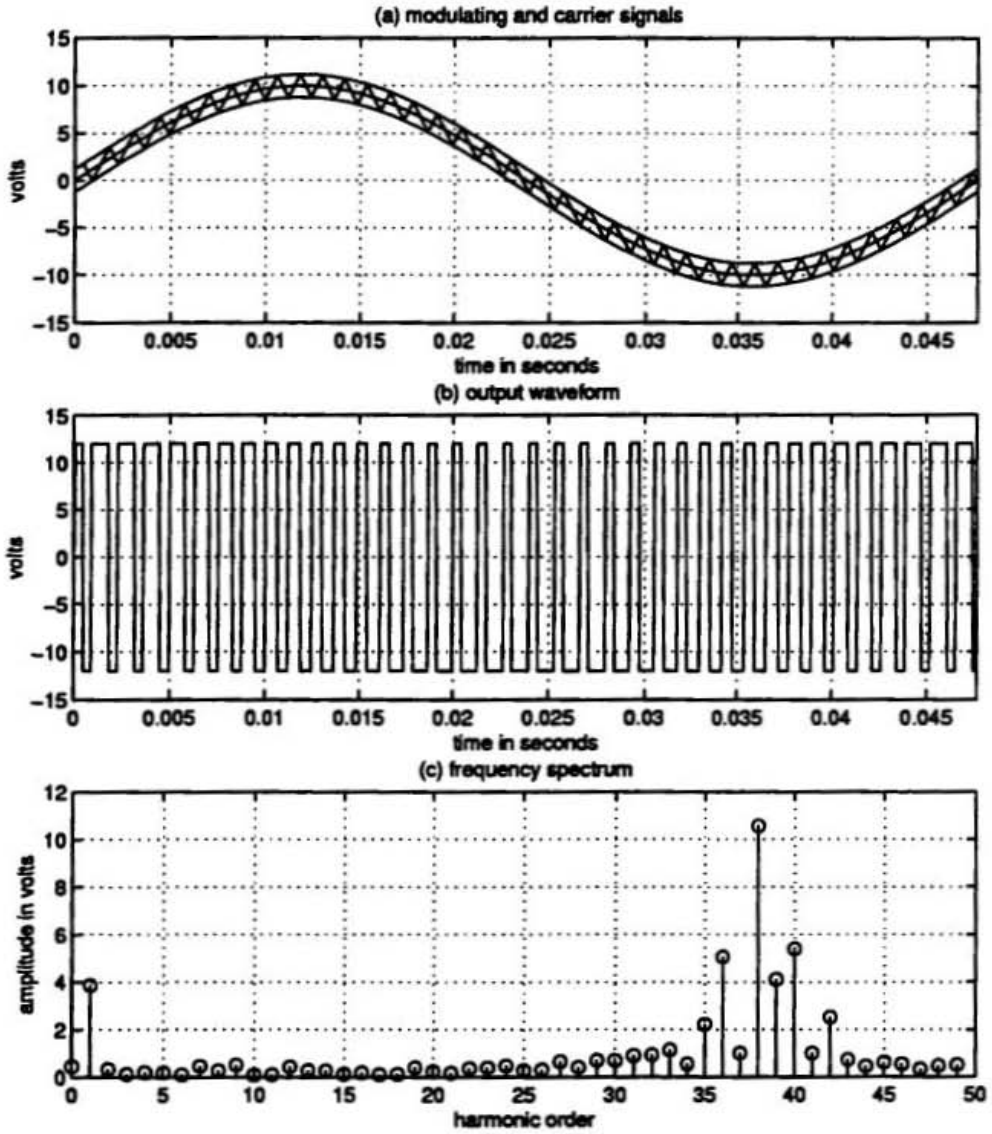

Figure 3.8: Delta modulation scheme waveforms at $f_r = 20Hz, f_{rb} = 60Hz$ and $V_{dc} = 12V$

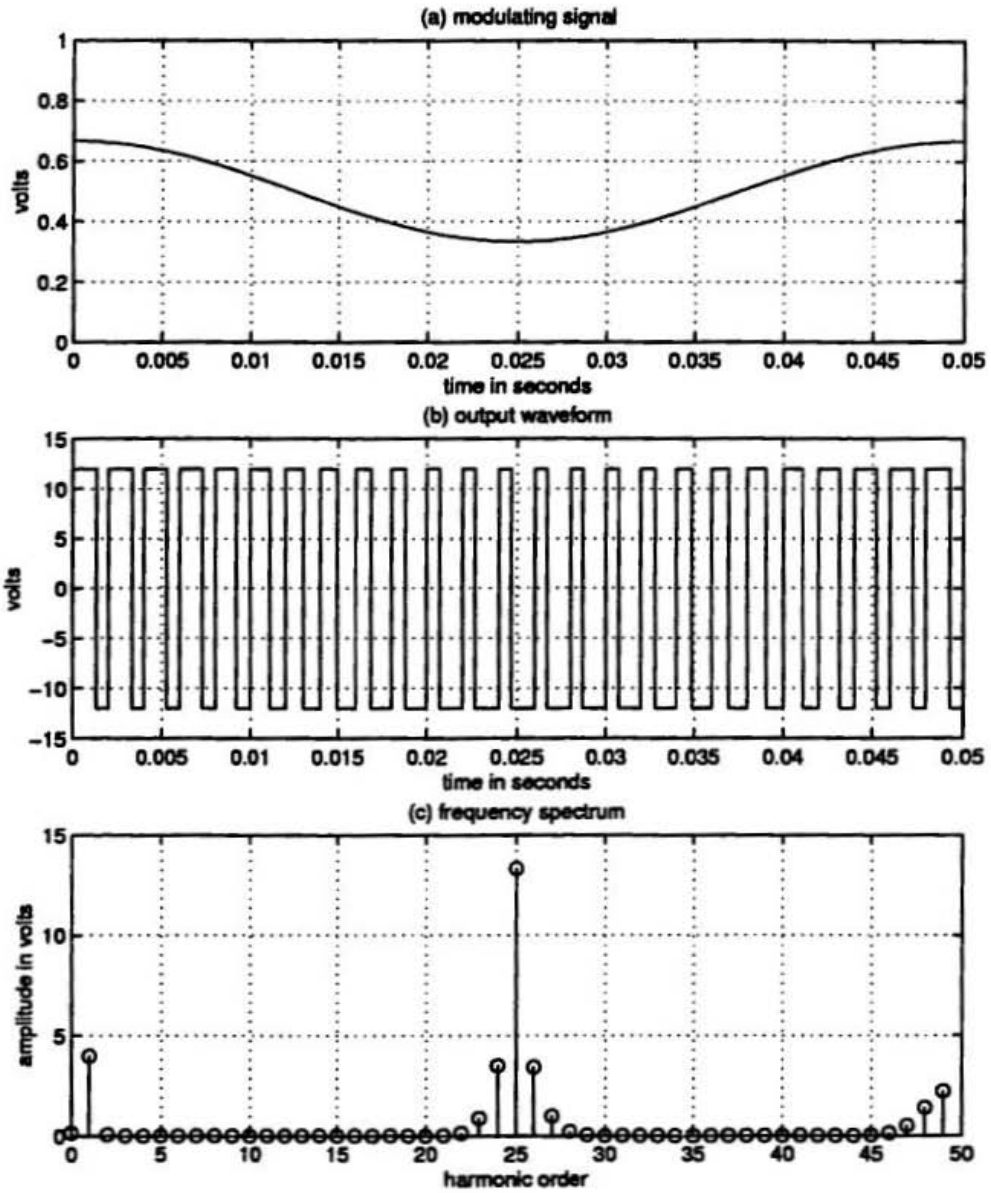

Figure 3.9: Unified modulation scheme waveforms at $f_r = 20Hz, f_{rb} = 60Hz$ and $V_{dc} = 12V$

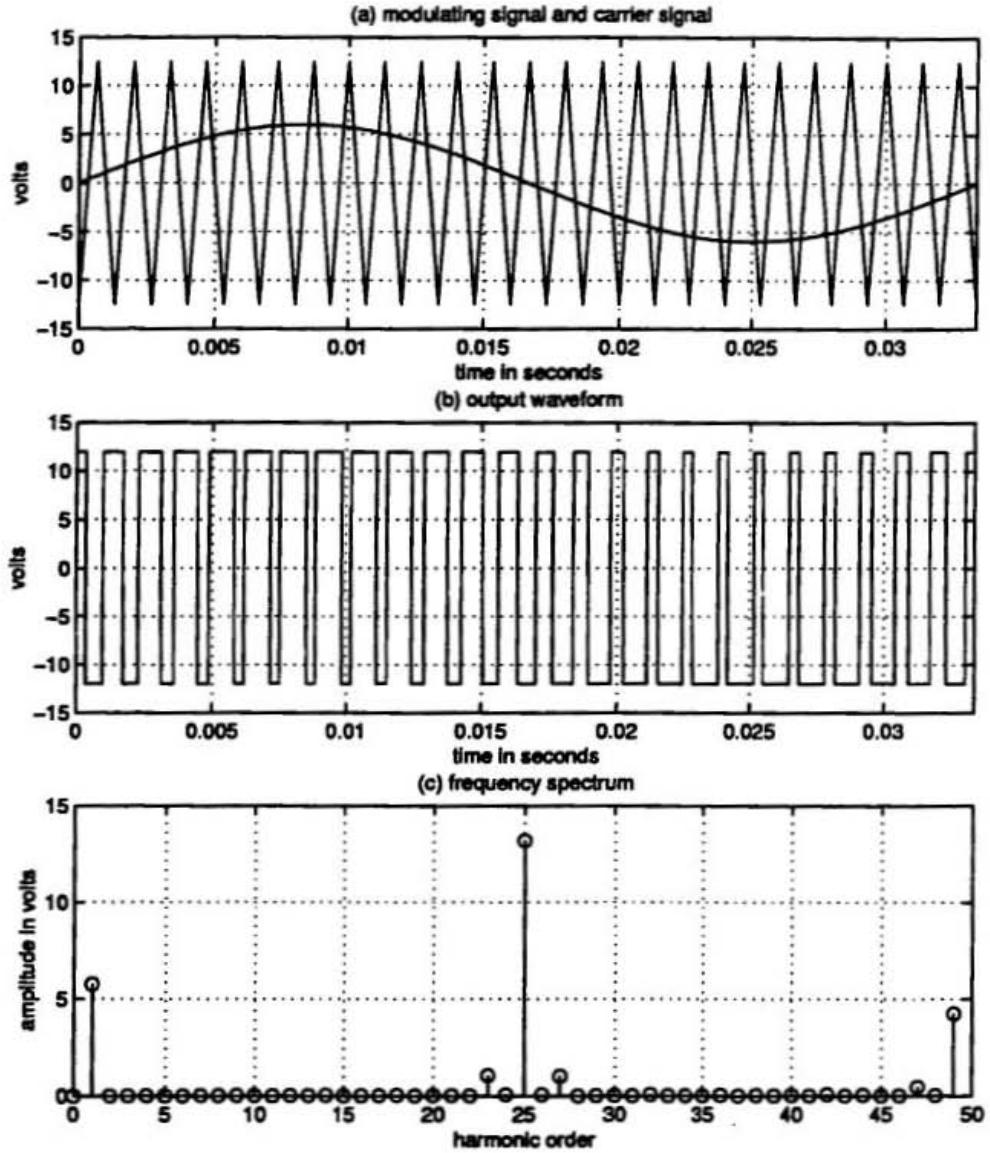

Figure 3.10: Sine PWM scheme waveforms at $f_r = 30Hz, f_{rb} = 60Hz$ and $V_{dc} = 12V$

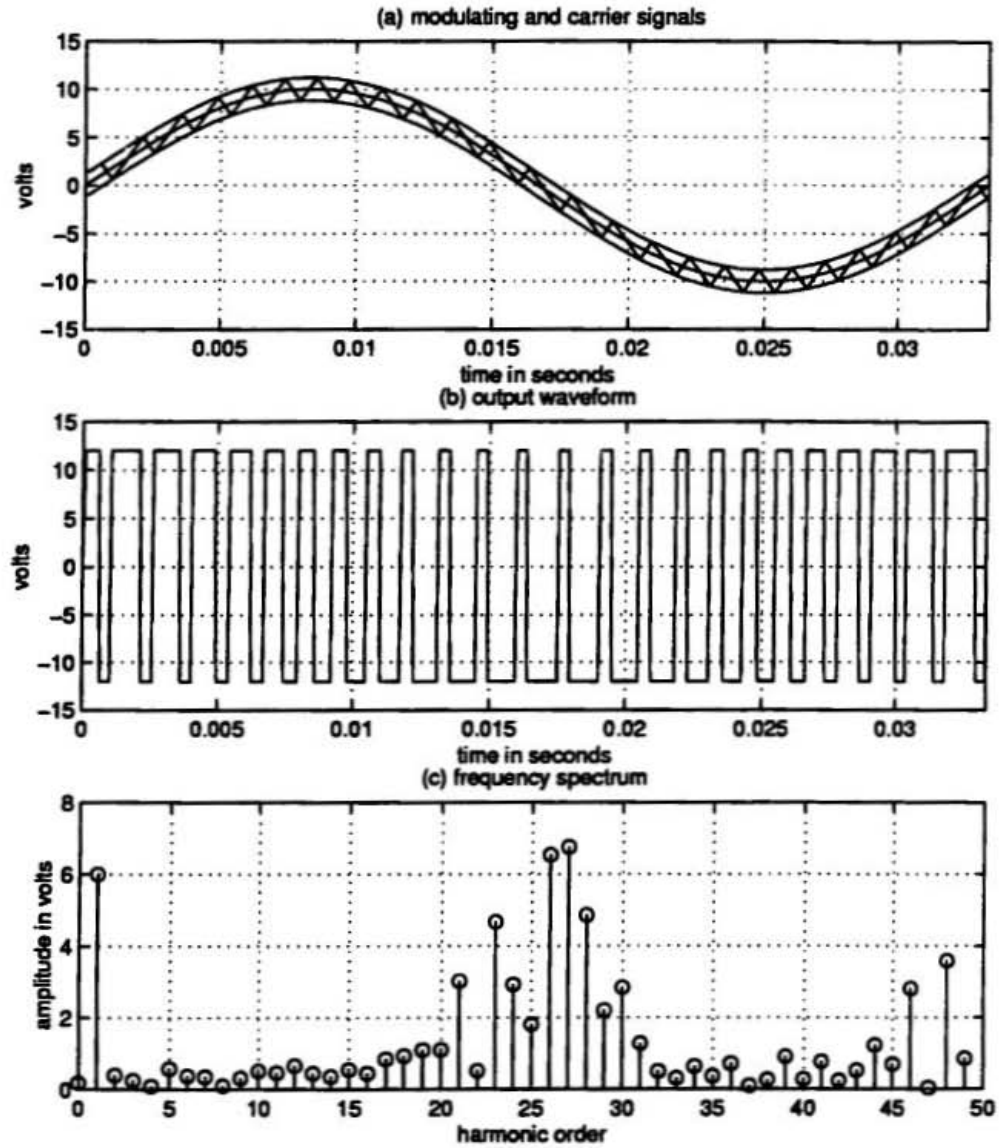

Figure 3.11: Delta modulation scheme waveforms at $f_r = 30Hz, f_{rb} = 60Hz$ and $V_{dc} = 12V$

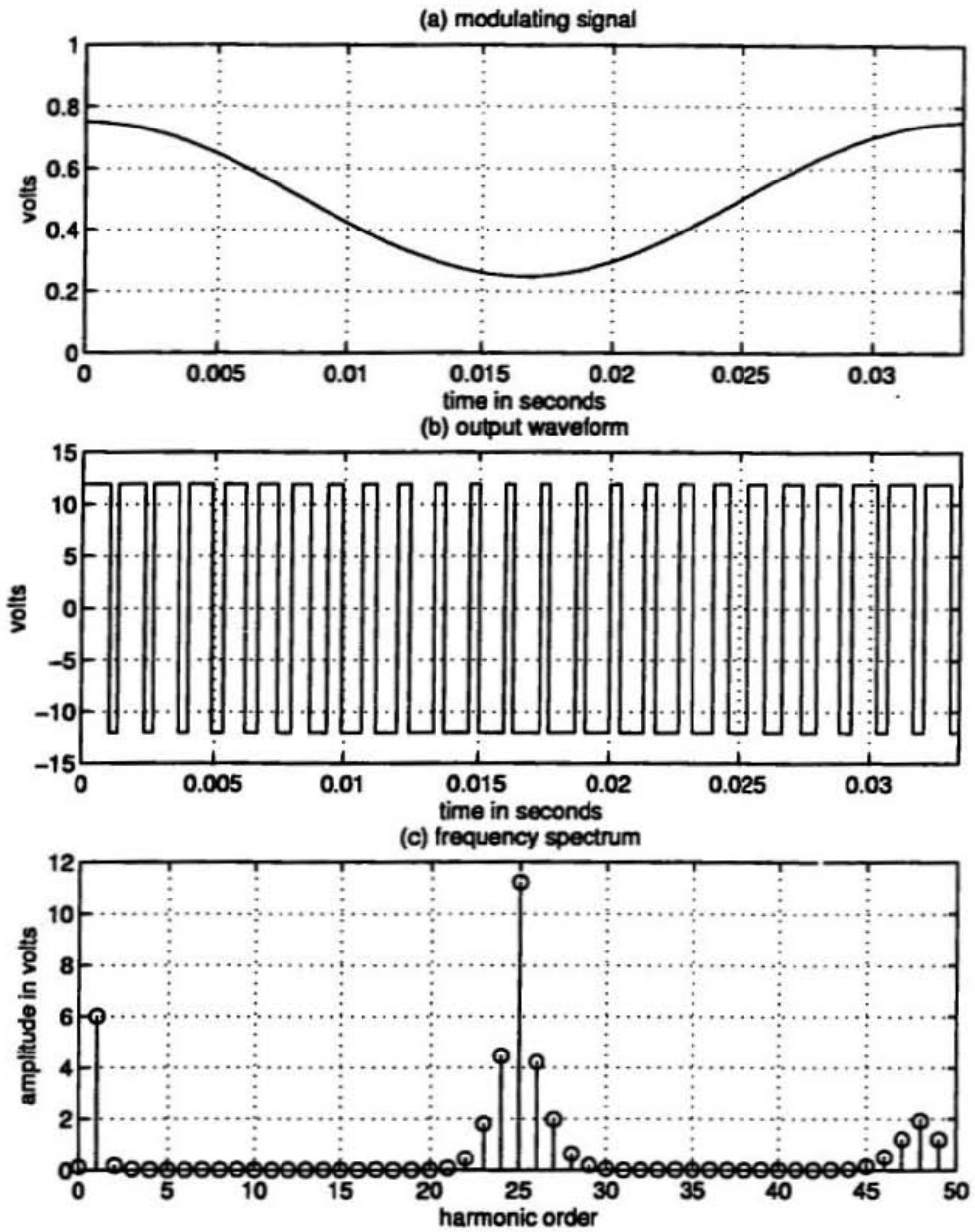

Figure 3.12: Unified modulation scheme waveforms at $f_r = 30Hz, f_{rb} = 60Hz$ and $V_{dc} = 12V$

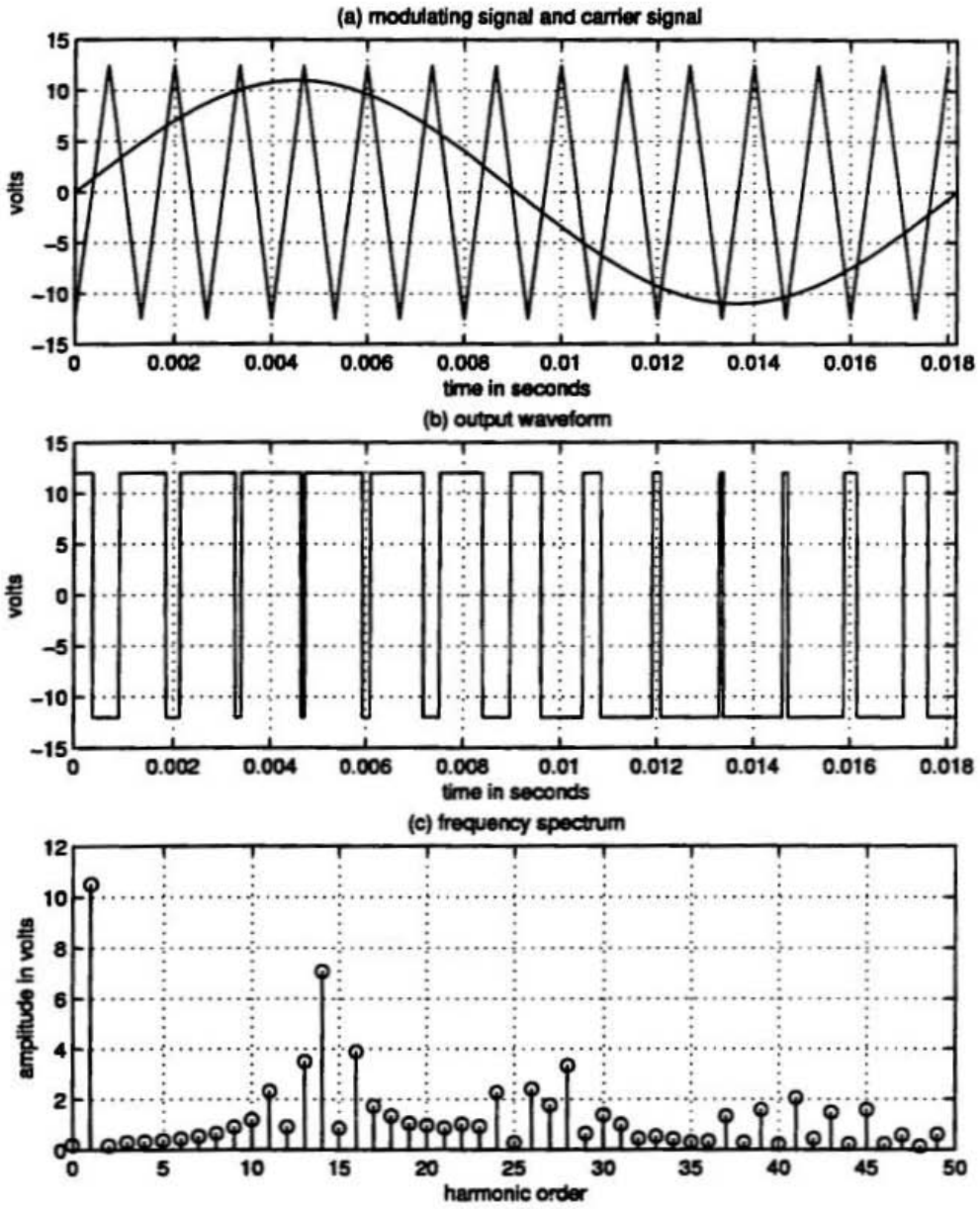

Figure 3.13: Sine PWM scheme waveforms at $f_r = 55Hz$, $f_{rb} = 60Hz$ and $V_{dc} = 12V$

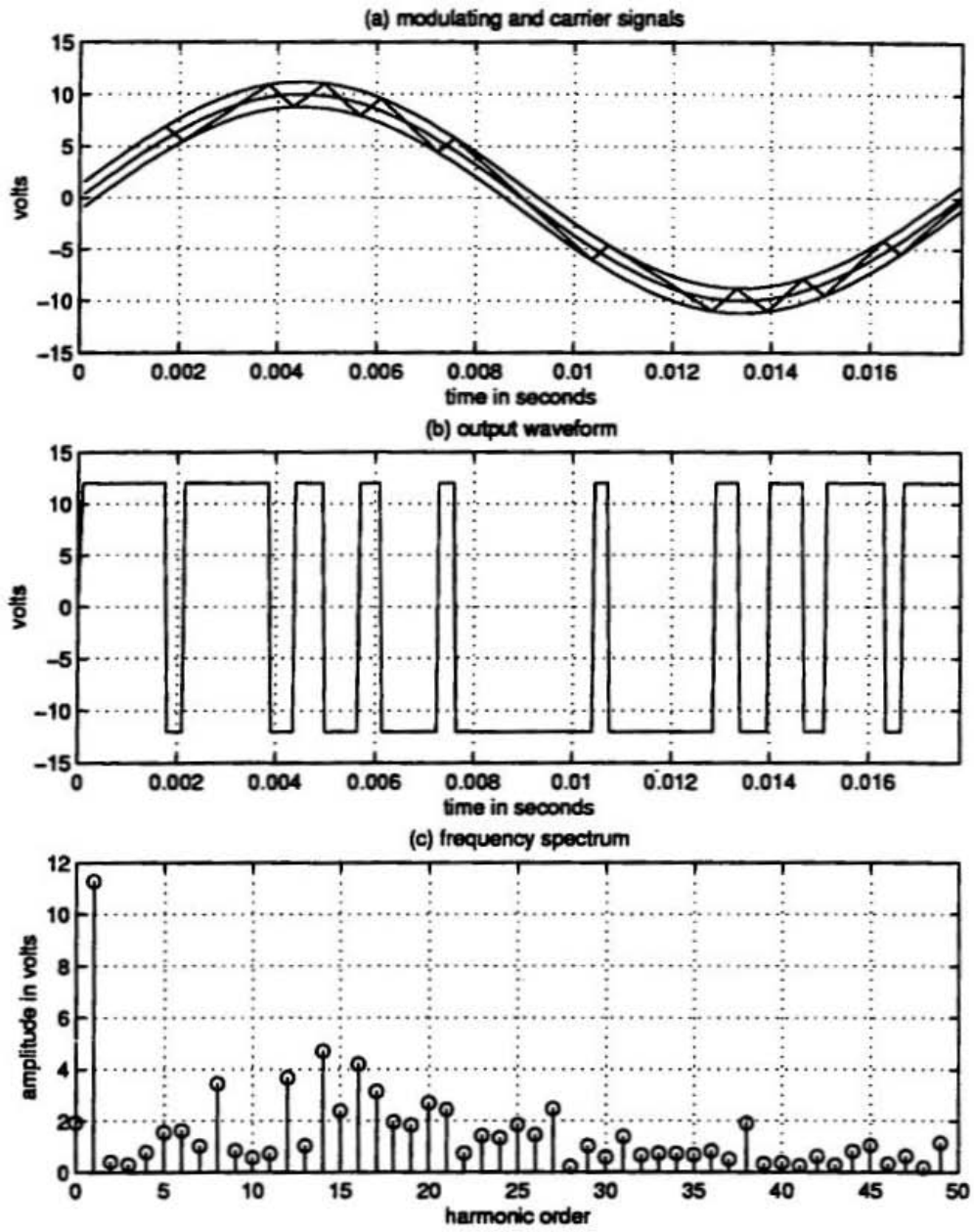

Figure 3.14: Delta modulation scheme waveforms at $f_r = 55Hz, f_{rb} = 60Hz$ and $V_{dc} = 12V$

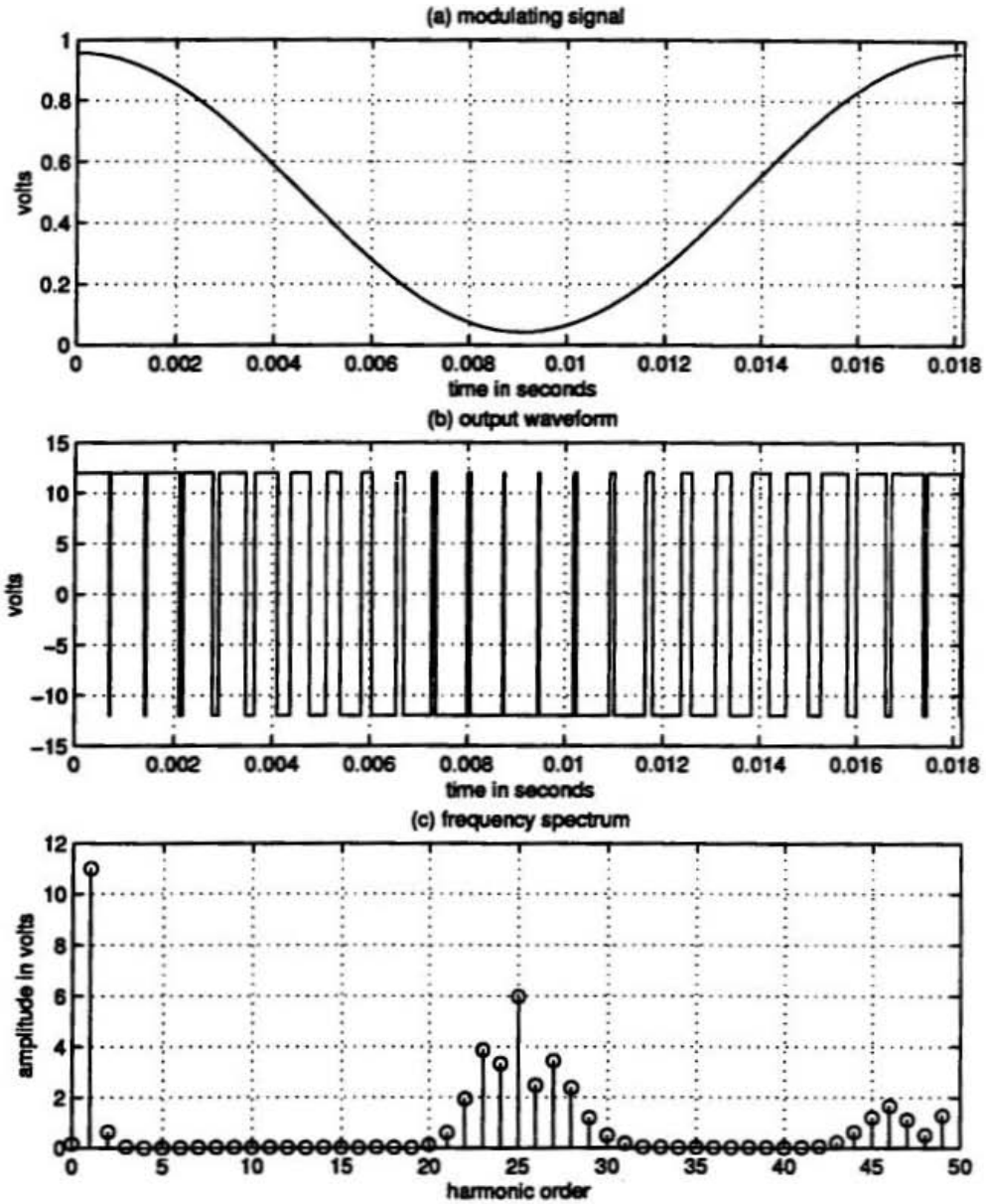

Figure 3.15: Unified modulation scheme waveforms at $f_r = 55Hz, f_{rb} = 60Hz$ and $V_{dc} = 12V$

are higher at lower operating frequencies and decrease with increasing operating frequencies. They are unpredictable and cannot be predetermined. But in the UM scheme the switching losses are uniform and can be predetermined, since the number of commutations is always a constant.

- Attenuation of lower order harmonics: There is significant attenuation of lower-order harmonics in the unified modulation scheme output (figures 3.9c, 3.12c and 3.15c). Since the switching frequency $f_s = 25f_r$, the dominant harmonics occur around the 25-th harmonic. In the case of SPWM and DM schemes, there is significant attenuation of lower-order harmonics at lower frequencies of the modulating signal. This is because the number of commutations is high at lower frequencies. But as the modulating frequency increases and moves closer to the break frequency, the number of commutations decrease and the output waveform becomes more of a square wave, resulting in significant lower order harmonics.

- Sub-harmonics: Figures 3.8c, 3.11c and 3.14c, show that the DM scheme produces random frequency spectra for varying operating frequency. This is due to frequency modulation and duty-ratio modulation occurring simultaneously in the modulation process. The result is an asynchronous output signal which in turn produces random frequency spectra and sub-harmonics. For instance, at some frequencies the DM scheme produces a dc component in the output

(Fig. 3.11c). Sub-harmonics in the SPWM and UM schemes are significantly reduced or non-existent because of the absence of frequency modulation in the modulating process.

Thus in conclusion, the unified modulation scheme has the advantages of the delta modulation scheme such as inherent V/f characteristics and lower-order harmonic attenuation, and that of the sine PWM scheme namely, the absence of frequency modulation.

3.4 Summary

This chapter discussed the need for an improved V/f control technique and outlined the development and the characteristic features of the unified modulation scheme. The characteristics of the unified modulation scheme were compared with those of sine PWM and delta modulation schemes. It has been shown that the unified modulation scheme provides an inherent V/f feature and there is no frequency modulation. It also offers improved performance in terms of lower-order harmonic attenuation and elimination of sub-harmonics. The next chapter deals with the experimental verification of the unified modulation technique.

Chapter 4

Experimental verification of the unified modulation scheme

Having established the characteristic features and the advantages of the unified modulation scheme, an experimental verification of the same is presented to ascertain the validity of the scheme. This chapter describes the issues related to the digital implementation of the unified modulation scheme using the PIC microcontroller and presents the experimental results.

4.1 Considerations for implementation

The unified modulation scheme uses the modulating signal, $\eta = 0.5 + (Kf_r)\cos(\omega_r t)$, which is sampled at regular intervals of time as determined by the switching time $T_s = 1/f_s$, where f_s is the switching frequency, which is an integral multiple of the modulating or reference frequency under all conditions. The modulating signal produces the duty-ratio modulation of the modulator output pulses. The amplitude of the samples specifies the pulse-width of the output pulses. Thus to implement the

unified modulation scheme, the modulating signal must be computed or sampled at regular intervals of time, which is decided by the switching frequency, and the samples converted into the corresponding pulse-widths. The sampling nature of the modulating process suggests a digital implementation of the unified modulation scheme. Besides the ease of implementation, the digital scheme provides flexibility in real-time applications.

4.2 Flowchart for the implementation of the unified modulation scheme

The flowchart for the implementation of the unified modulation scheme is shown in Fig. 4.1.

The system accepts the following inputs namely, the modulating signal frequency f_r, the switching constant p which defines the switching frequency as a multiple of the reference frequency i.e.$f_s = pf_r$, and the modulation index constant K, which defines the slope of the V/f characteristic. For simplicity, the value of p is chosen to be 36, i.e 36 samples in one cycle of the modulating signal, each at 10 degree intervals. As noted in Chapter 3, the value of the duty-ratio modulation index ($M_{dr} = Kf_r$) must range between $(Kf_r)_{min} = 0$ and $(Kf_r)_{max} = 0.5$. If the value of M_{dr} is greater than $(Kf_r)_{max}$, then M_{dr} is reset to $(Kf_r)_{max}$. Similarly, if it is less than $(Kf_r)_{min}$, it is reset to $(Kf_r)_{min}$. The amplitude of the modulating signal, which defines the duty-ratio modulation, is computed at regular intervals in accordance with

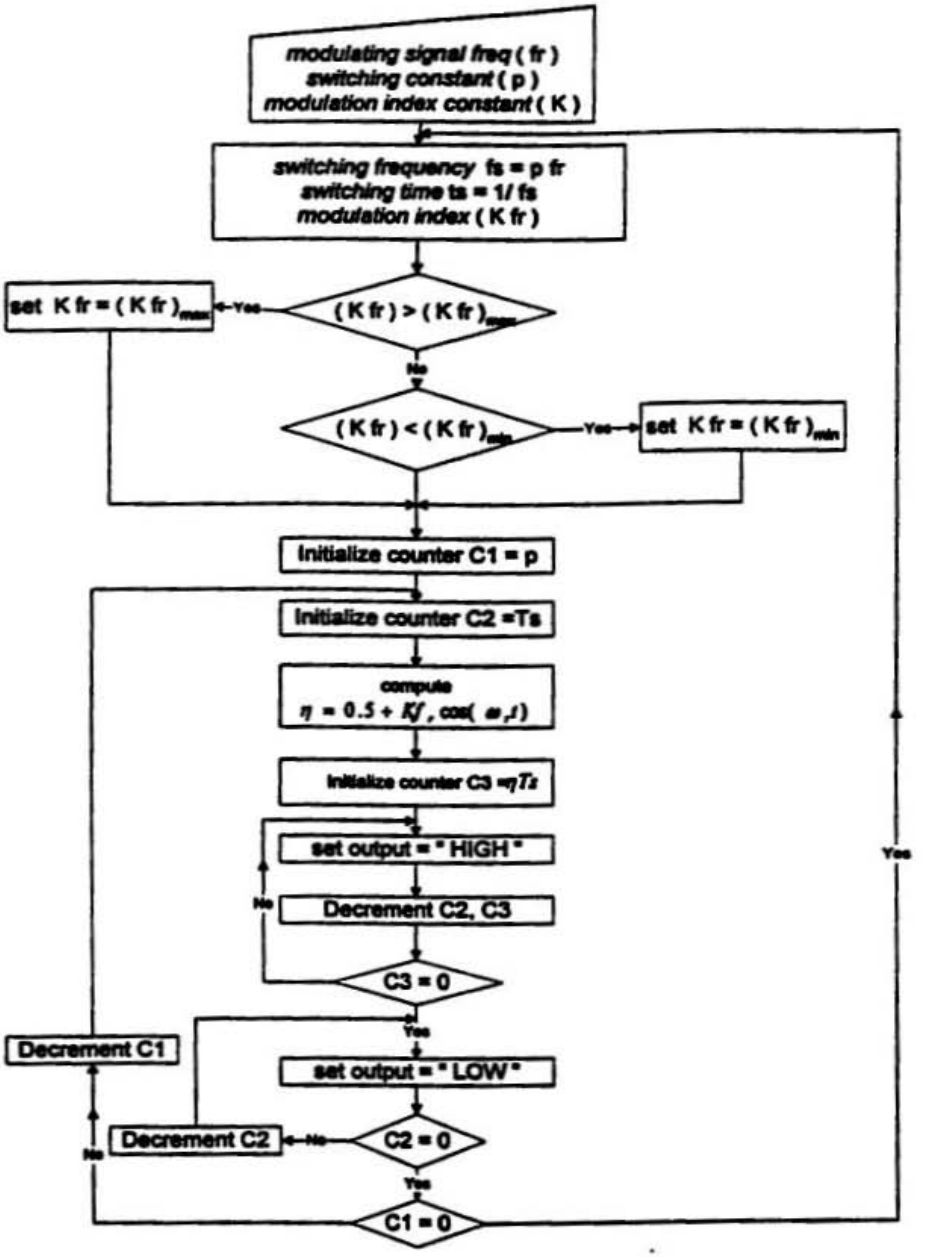

Figure 4.1: Flowchart for the implementation of unified modulation scheme

the switching frequency and this amplitude is multiplied with the switching cycle time T_s to determine the pulse-width at the output. Any change in the frequency of the modulating signal comes into effect only at the beginning of the next cycle.

4.3 The PIC16C77 Microcontroller

A microprocessor or a microcontroller can be used to implement the flowchart design. In this thesis, the PIC16C77 is used. It belongs to an inexpensive family of 8-bit CMOS microcontrollers with a huge range of possible applications, and it is highly recommended for timer functions, serial communication, capture and compare, PWM and coprocessor applications [32]. The PIC microcontroller families use MPLAB, a Windows-based Integrated Development Environment (IDE) to write, debug and optimize PIC applications, and PICSTART Plus to program the PIC microcontroller.

4.4 Specifications for experimental design

The experimental design was based on a simple and ideal V/f characteristic with the following specifications

- Magnitude of the modulator DC voltage output, $V_{dc} = 7.5V$
- Break frequency of the V/f characteristic, $f_{rb} = 60Hz$
- Switching frequency constant, $p = 36$ so that $f_s = 36f_r$. The value of p is chosen to be 36 such that it becomes easy to compute the value of $\cos(\omega_r t)$ at

the sampling intervals.

- $(Kf_r)_{min} = 0$ and $(Kf_r)_{max} = 0.5$
- Duty-ratio modulation index constant, $K = 8.333 \exp -3s$

The V/f characteristic pertaining to the above design specifications is shown in Fig. 4.2

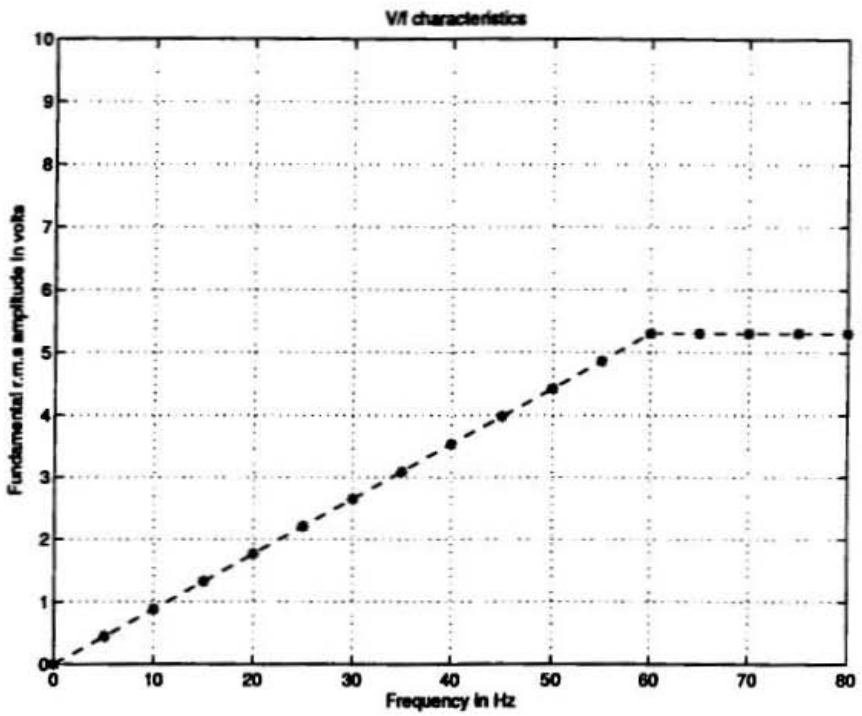

Figure 4.2: V/f characteristics for the implementation of unified modulation scheme

4.5 Experimental set-up

The design of the unified modulation scheme was based on the given set of design specifications. The design was coded using ANSI-C and the code was compiled and

simulated using MPLAB Integrated Development Environment. Since the output pulses of the PIC are unipolar in nature. The output of the PIC is fed to a comparator with a reference ground, to convert the unipolar pulses to bipolar pulses. The block diagram of the experimental set-up is shown in Fig. 4.3 and the circuit diagram of the experimental verification is shown in Fig. 4.4

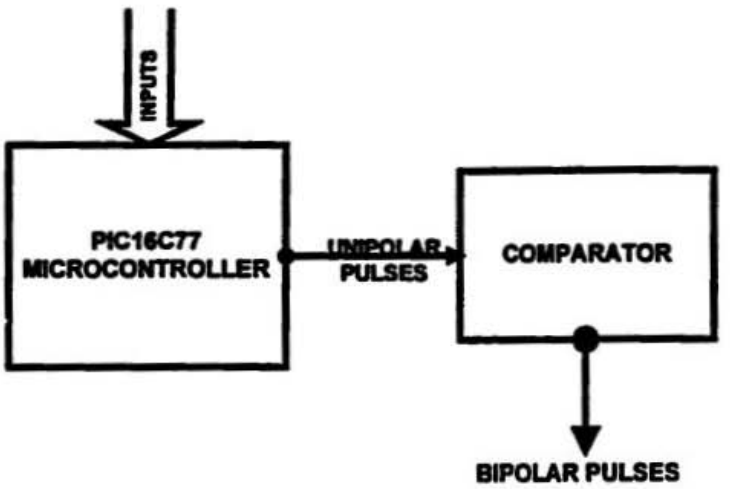

Figure 4.3: Block diagram of the experimental set-up

The comparator circuit was implemented using HA2505 which has a better slew rate than the traditional Op-amp $\mu A - 741$. The positive and negative input voltage level was $+V = 10V$ and $-V = 10V$ respectively. The positive and negative output voltage level of the comparator was $+7.5V$ and $-7.5V$ respectively. The output of

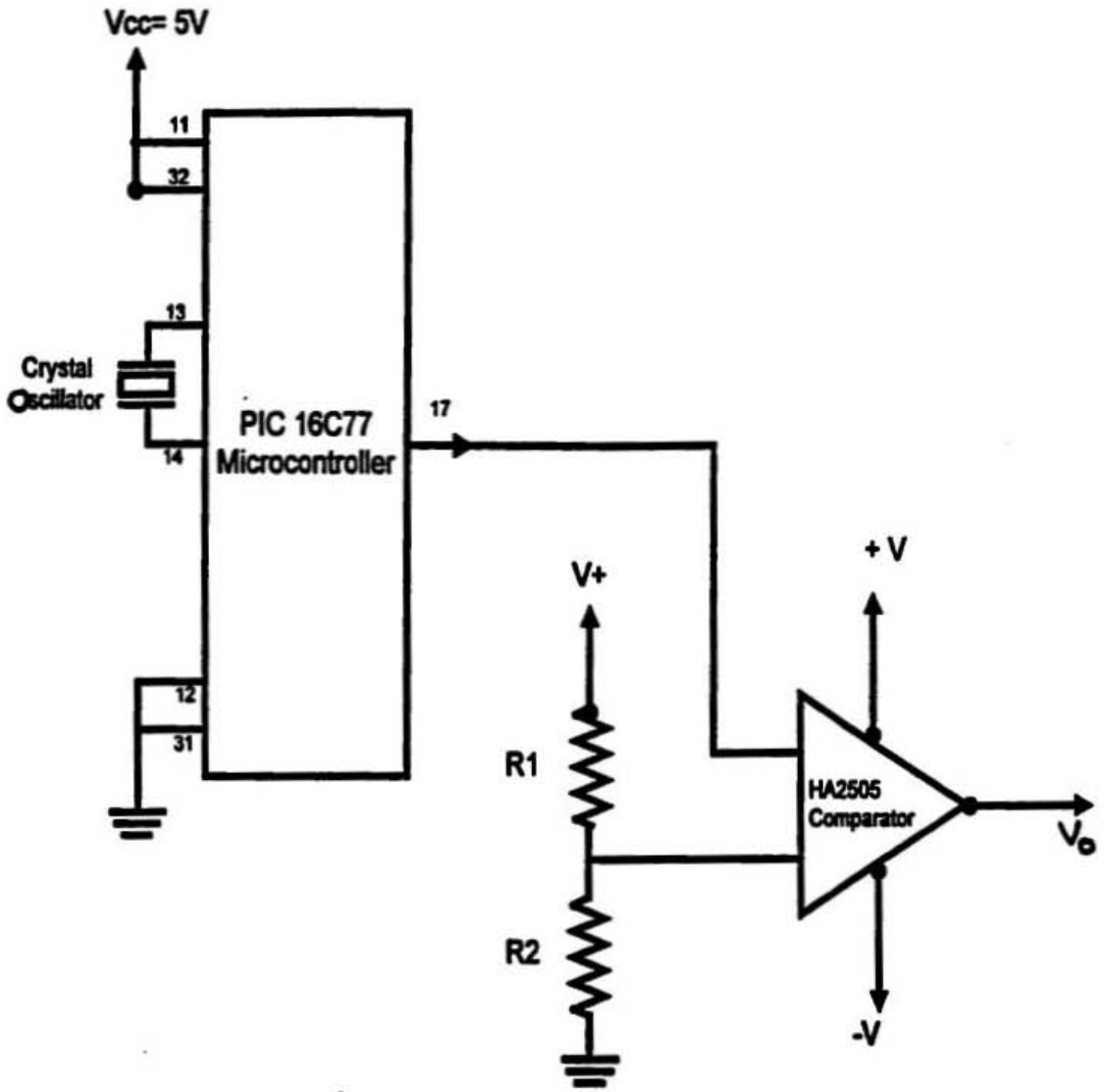

Figure 4.4: Circuit diagram for the implementation of the unified modulation scheme

the comparator was analyzed with the help of a low-frequency spectrum analyzer.

4.5.1 Issues related to the PIC implementation

- The switching frequency $f_s = 36 f_r$. As explained earlier, this was chosen such that the values of $\cos(\omega_r t)$ at 10 degree intervals could be stored in a look-up table. This saves computation time and makes it easy for the PIC to evaluate the amplitude of modulating signal and hence the pulse width for the next cycle, at that switching instant.

- The computational resources of the PIC are effectively used by employing the concept of pipelining. At the beginning of a switching cycle, the PIC computes the pulse width required for that cycle and this value is loaded into the PWM counter. Normally, the PIC would remain idle for the remaining of the switching cycle and would start to compute the modulating signal again, at the beginning of the next cycle. In this implementation, the normal idle time was used to compute the pulse width that would be required for the consecutive switching cycles.

- The clock frequency of the PIC was obtained from a crystal oscillator of 16 MHz.

4.6 Analysis of the experimental results

The output waveform and its corresponding frequency spectrum obtained for the experimental unified modulation scheme, for modulating frequencies $f_r = 30Hz$ and $f_r = 60Hz$ are shown in Fig. 4.5 and Fig. 4.6 respectively. The r.m.s. value of the

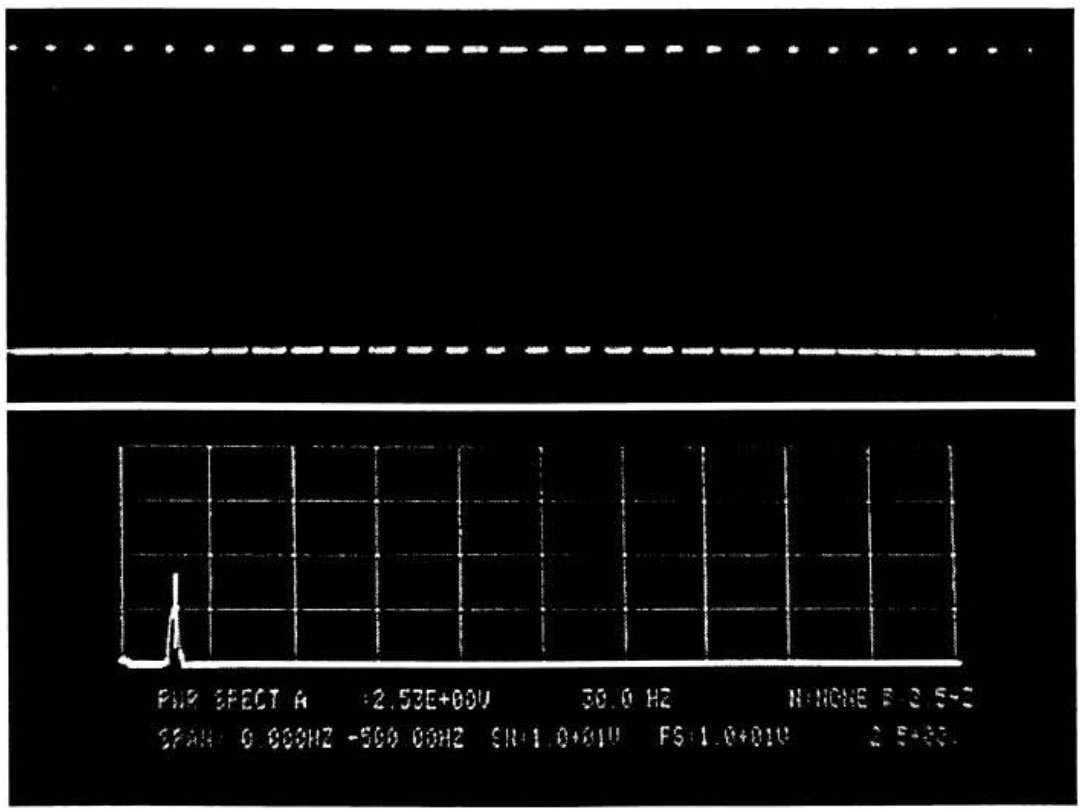

Figure 4.5: Experimental results of the unified modulation scheme at $f_r = 30Hz$
upper trace: modulator output voltage
lower trace: frequency spectrum of the modulator output

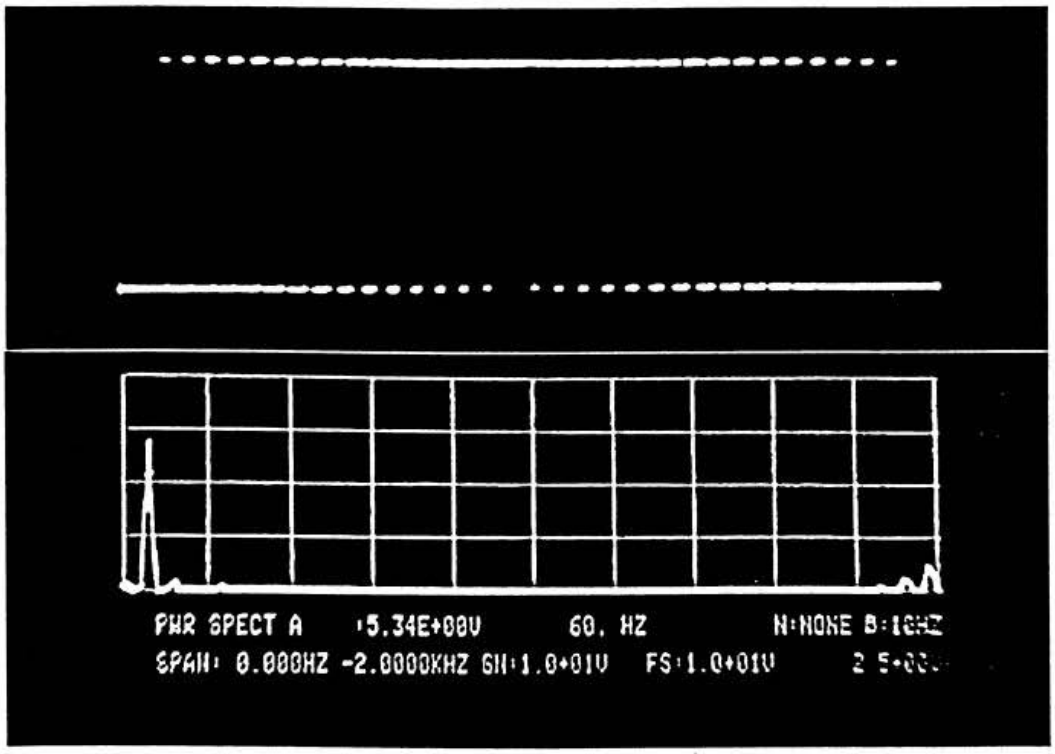

Figure 4.6: Experimental results of the unified modulation scheme at $f_r = 60Hz$
upper trace: modulator output voltage
lower trace:frequency spectrum of the modulator output

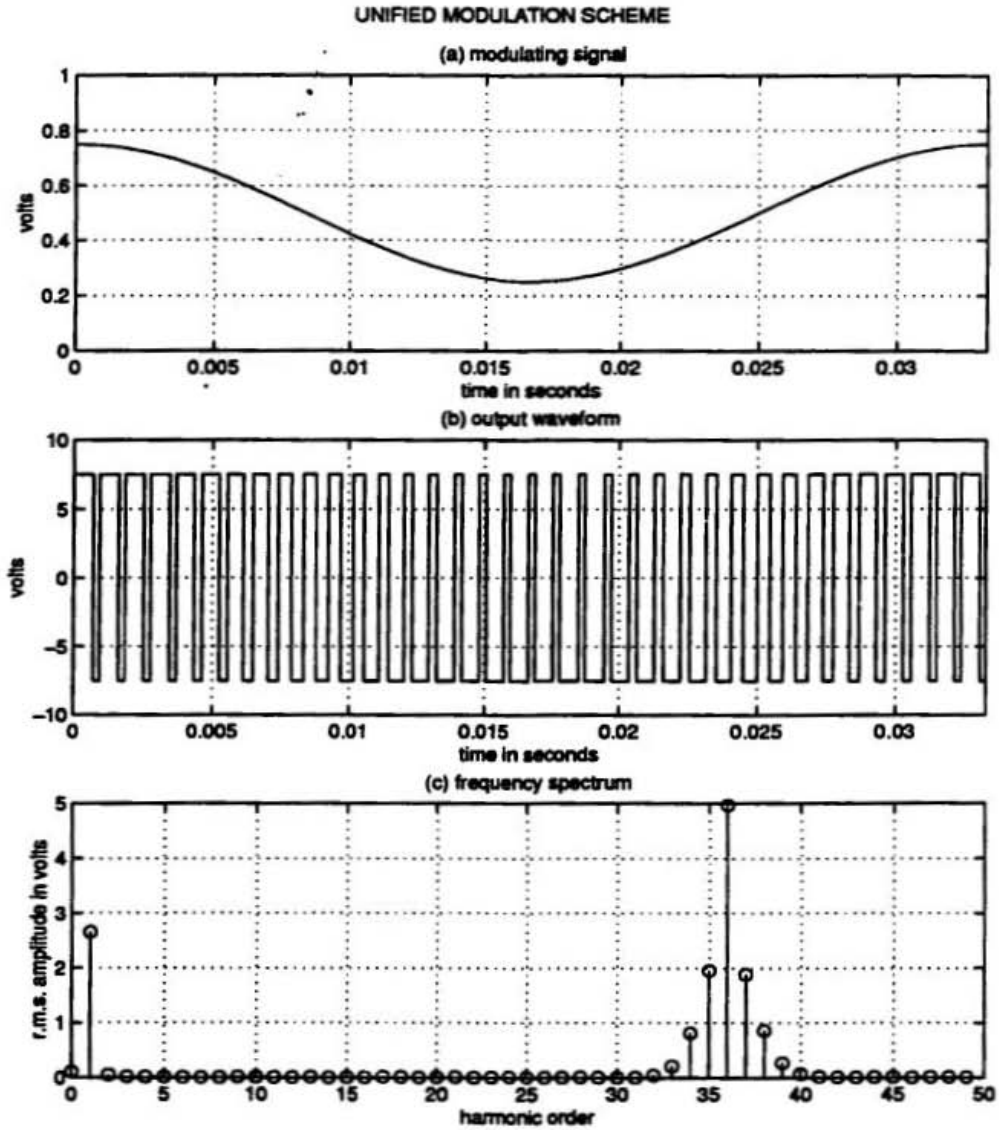

Figure 4.7: Simulation results of the unified modulation scheme at $f_r = 30Hz$.

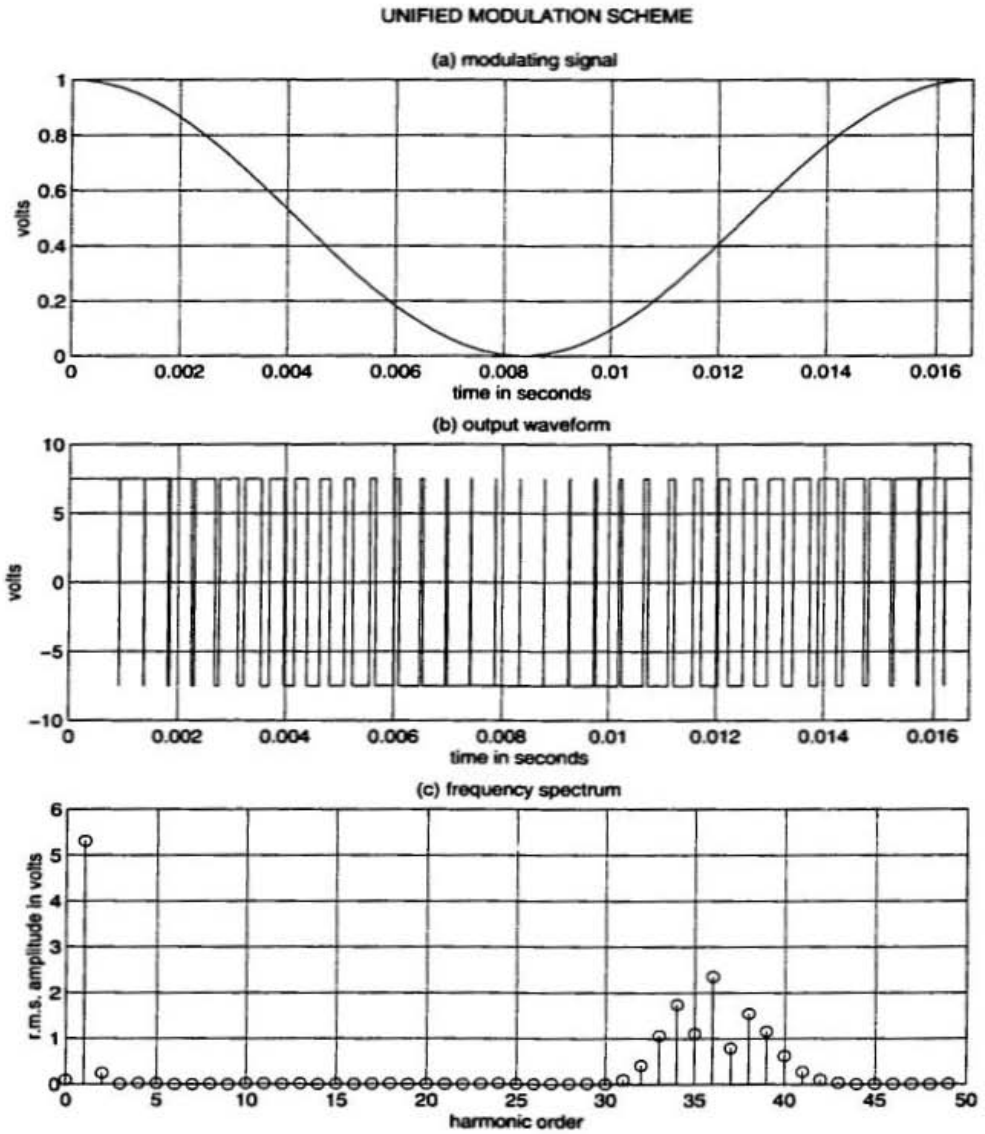

Figure 4.8: Simulation results of the unified modulation scheme at $f_r = 60Hz$.

fundamental component in both the cases, as shown in the results, is in agreement with the V/f characteristics specified in the design The simulation results obtained using MATLAB for the unified modulation scheme with the same design specifications are shown in Fig. 4.7 and Fig. 4.8 respectively.

The simulation results and the experimental results confirm the validity of the unified modulation scheme.

4.7 Summary

This chapter has outlined the experimental implementation of the unified modulation scheme. Digital implementation of the modulation scheme was carried out using the PIC microcontroller. The experimental results obtained were in perfect agreement with the simulation results obtained for the same design specifications. The experimental implementation confirms the feasibilty and ease of implementation of the unified modulation scheme.

Chapter 5

Variable frequency control of the induction motor

This chapter deals with the modeling of variable frequency induction motor drives which employ the unified modulation scheme and the delta modulation scheme. The drives are modeled using the SIMULINK software package. Simulation results for V/f control of the drives are discussed and the performance of the drives for the delta modulator and the unified modulator schemes are compared.

5.1 SIMULINK simulation of the induction motor drive

The induction motor drive has been implemented, using basic building blocks available in SIMULINK [33]. The motor drive consists of an induction motor model, obtained from the power system blockset, which is fed from a three-phase inverter. The inverter is controlled through the output pulses of the modulation scheme, i.e either the delta modulator or unified modulator. Since the output of the modulator is

similar in form to the output of the inverter, the inverter has been modeled as a gain block. The output pulses of the inverter are fed to the induction motor model. The drive was designed for open-loop speed control with the following set of specifications.

- Inverter supply voltage, $V_{dc} = 310V$
- Break frequency, $f_{rb} = 60Hz$
- Switching frequency $f_s = 40f_r$
- Duty-ratio modulation constant $K = 8.333 \exp -3s$

The motor ratings are given as follows

- Nominal power, $P_n = 2238VA$
- Line-line voltage, $V_{l-l} = 220V$
- Synchronous speed, $N_s = 1800rpm$
- Rated frequency, $f_{r(rated)} = 60Hz$

The ideal V/f characteristic corresponding to the given specifications is shown in Fig. 5.1. The SIMULINK model of the DMS inverter-fed induction motor drive is shown in Fig. 5.2 and the SIMULINK sub-system showing the implementation of the delta modulation scheme, which controls the inverter, is given in Fig. 5.3. Similarly, the SIMULINK model of the UMS inverter-fed induction motor drive is shown in

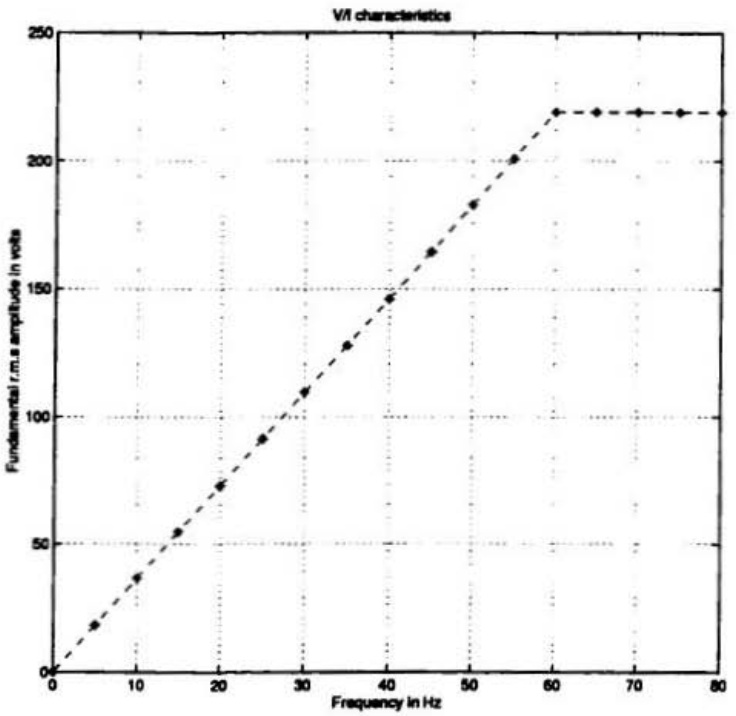

Figure 5.1: Ideal V/f characteristics for the inverter-fed induction motor drive

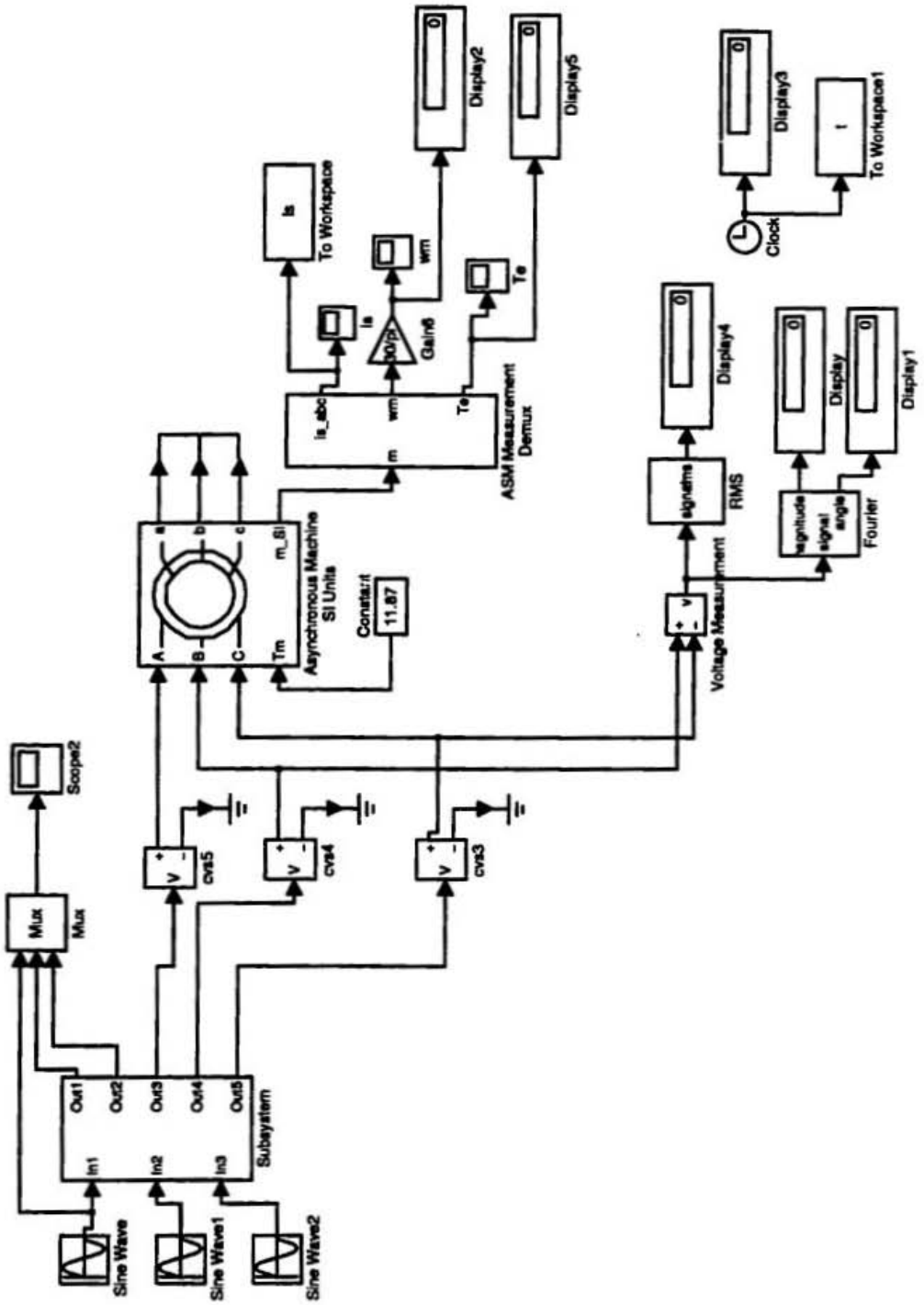

Figure 5.2: SIMULINK model of DMS inverter fed induction motor drive

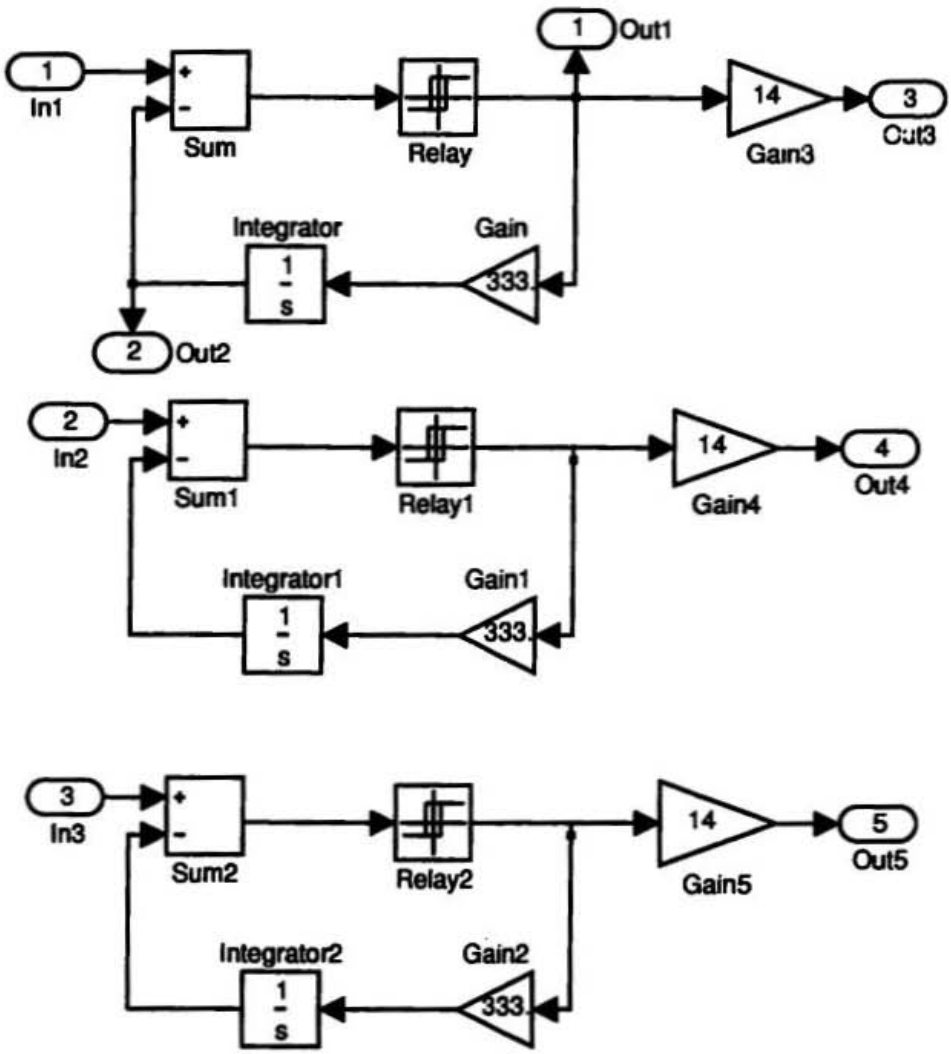

Figure 5.3: SIMULINK sub-system details of DM scheme

Fig. 5.4 and the SIMULINK sub-system showing the implementation of the unified modulation scheme, which controls the inverter, is given in Fig. 5.5.

5.2 Simulation results

Using the SIMULINK simulation results, the performance of the induction motor drive using V/f control for the delta modulation and the unified modulation schemes is discussed. The performance characteristics that are compared in this section are the stator current waveforms for constant speed operation, and sudden load change. The effects of the stator currents on the machine derating are also discussed.

5.2.1 Constant load torque case

The UMS inverter-fed and delta-modulated inverter-fed induction motor drive were simulated, under different operating frequencies (20Hz-60Hz), with a constant load torque i.e $T_L = 11.87Nm$. The stator current waveforms and frequency spectra were obtained for different operating frequencies. Fig. 5.6 to Fig. 5.11 show the stator current waveforms and the corresponding frequency spectra at operating frequencies $f_r = 20Hz, 30Hz$ and $55Hz$ for the DMS and UMS drives.

From the results, it is evident that the stator current waveform for the UMS drive shows significant attenuation of lower-order harmonics for higher operating frequencies. The dominant harmonics with negligible amplitude are seen clustered around the 25-th harmonic, as characterized by the unified modulation scheme. On the other

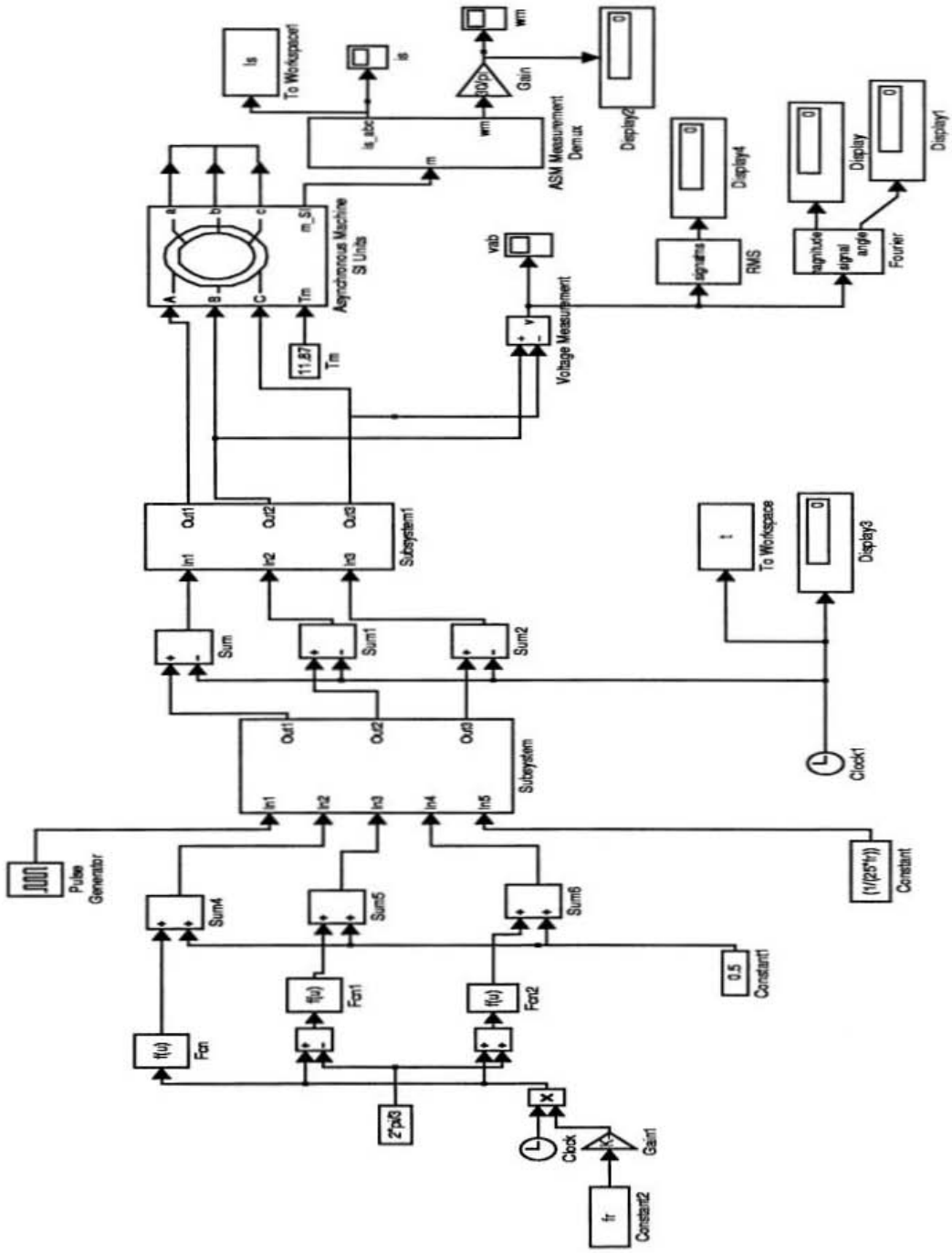

Figure 5.4: SIMULINK model of UMS inverter fed induction motor drive

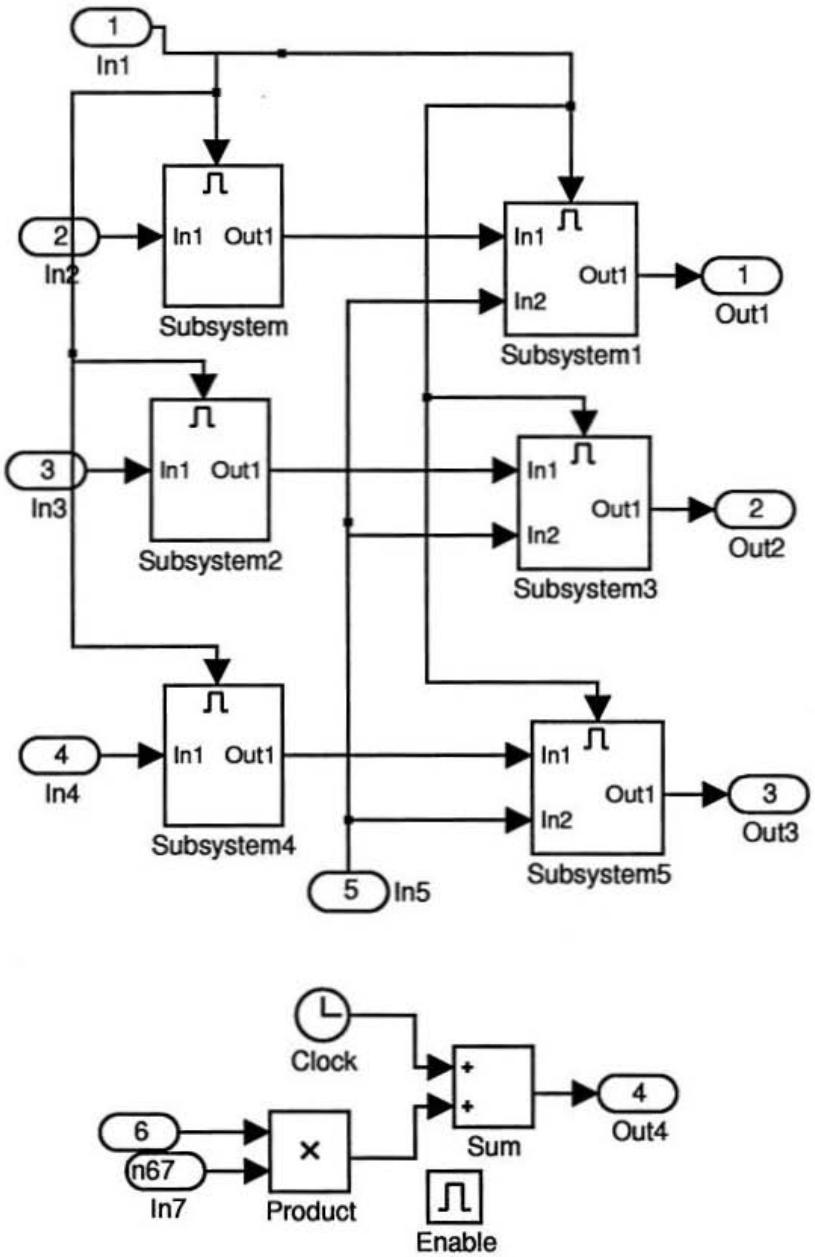

Figure 5.5: SIMULINK sub-system details of DM scheme

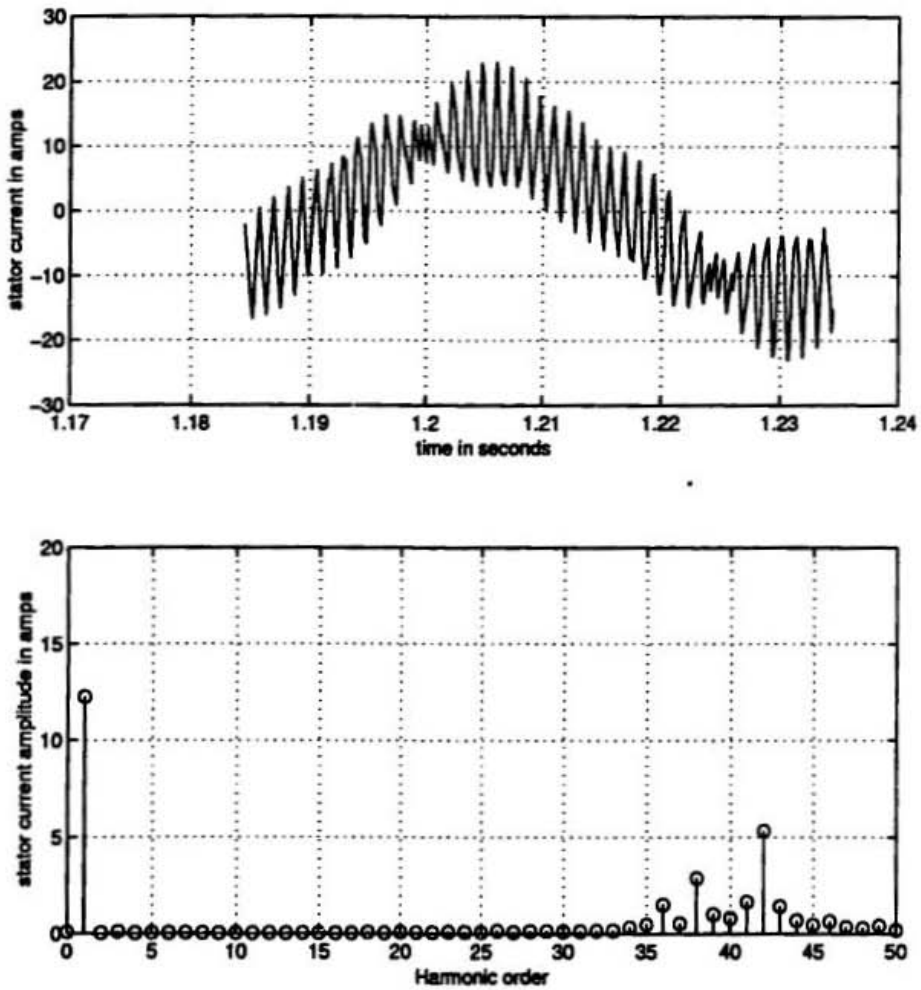

Figure 5.6: Stator current waveform (per phase) and its frequency spectrum obtained at $f_r = 20Hz$ for the DMS drive

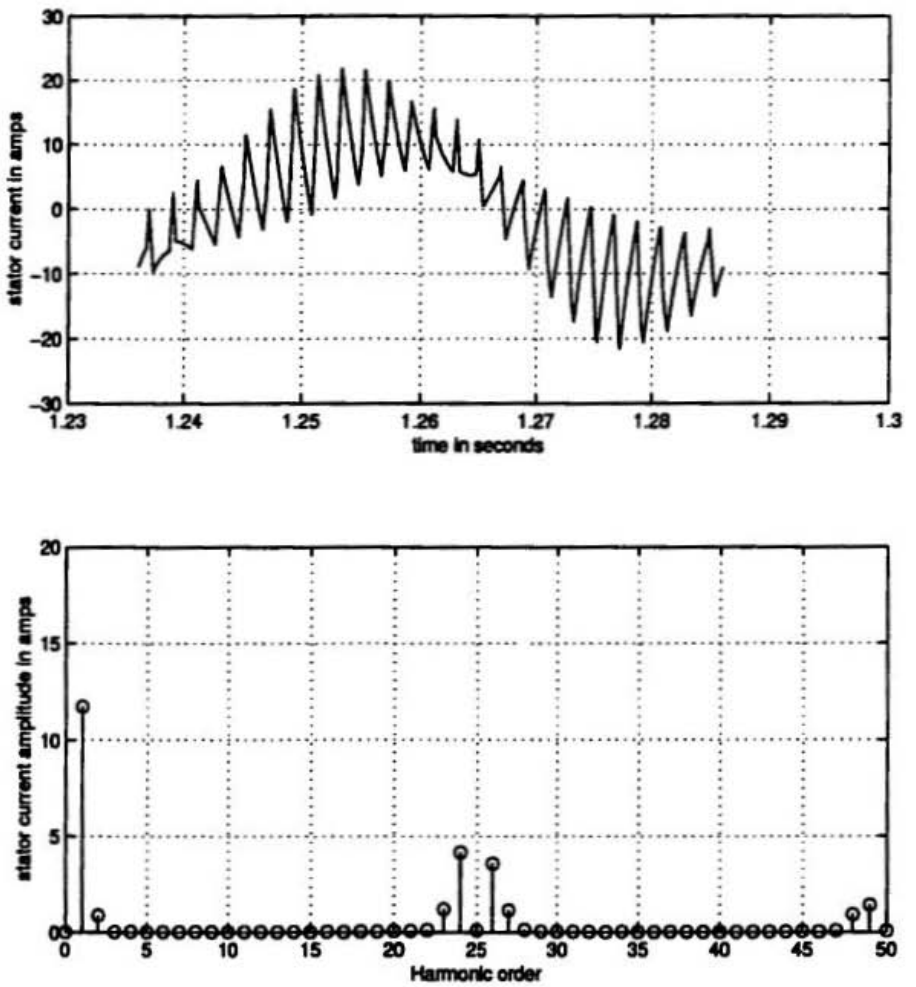

Figure 5.7: Stator current waveform (per phase) and its frequency spectrum obtained at $f_r = 20Hz$ for the UMS drive

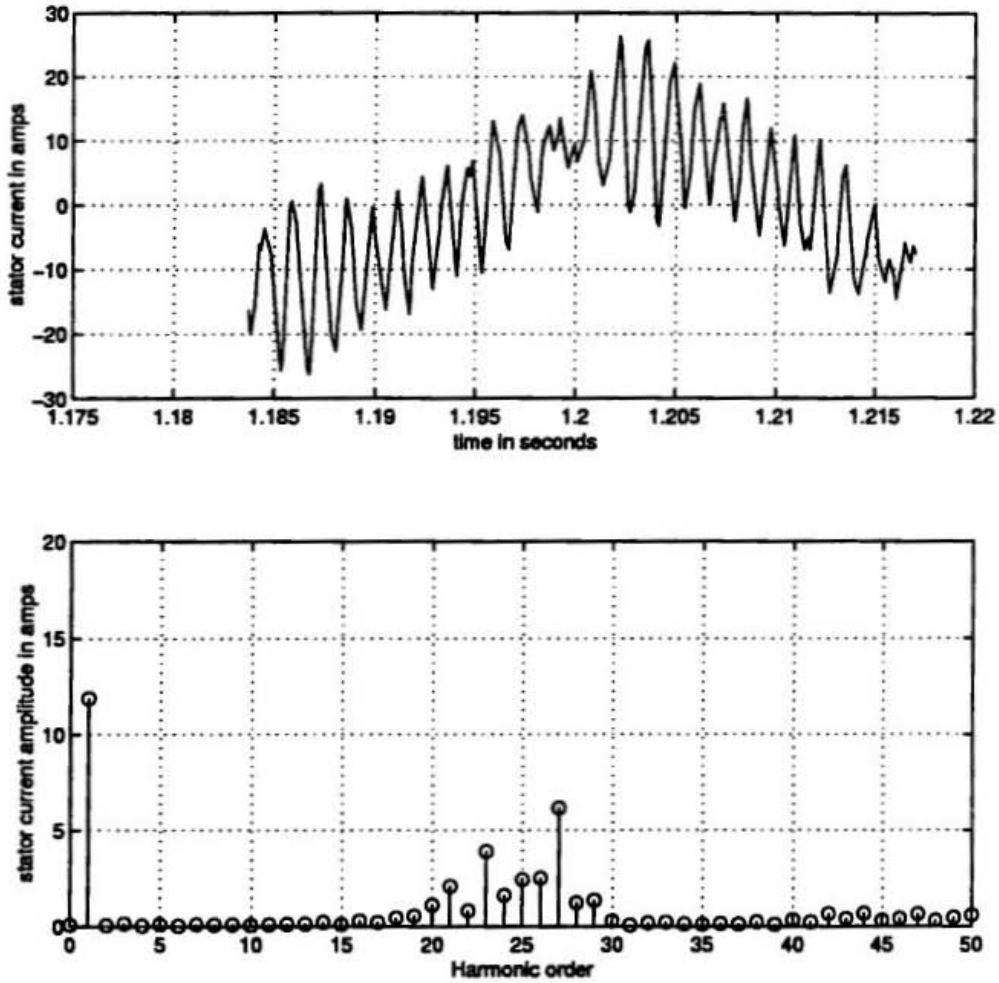

Figure 5.8: Stator current waveform (per phase) and its frequency spectrum obtained at $f_r = 30Hz$ for the DMS drive

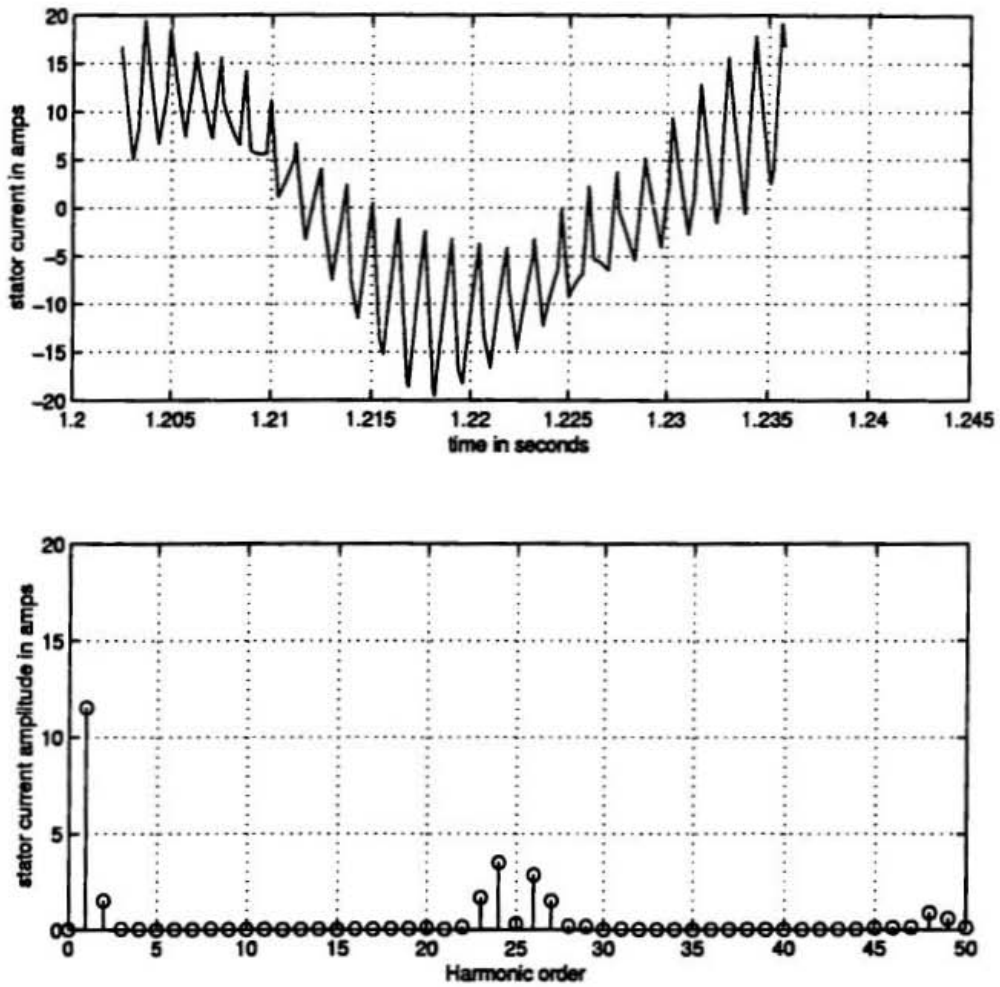

Figure 5.9: Stator current waveform (per phase) and its frequency spectrum obtained at $f_r = 30Hz$ for the UMS drive

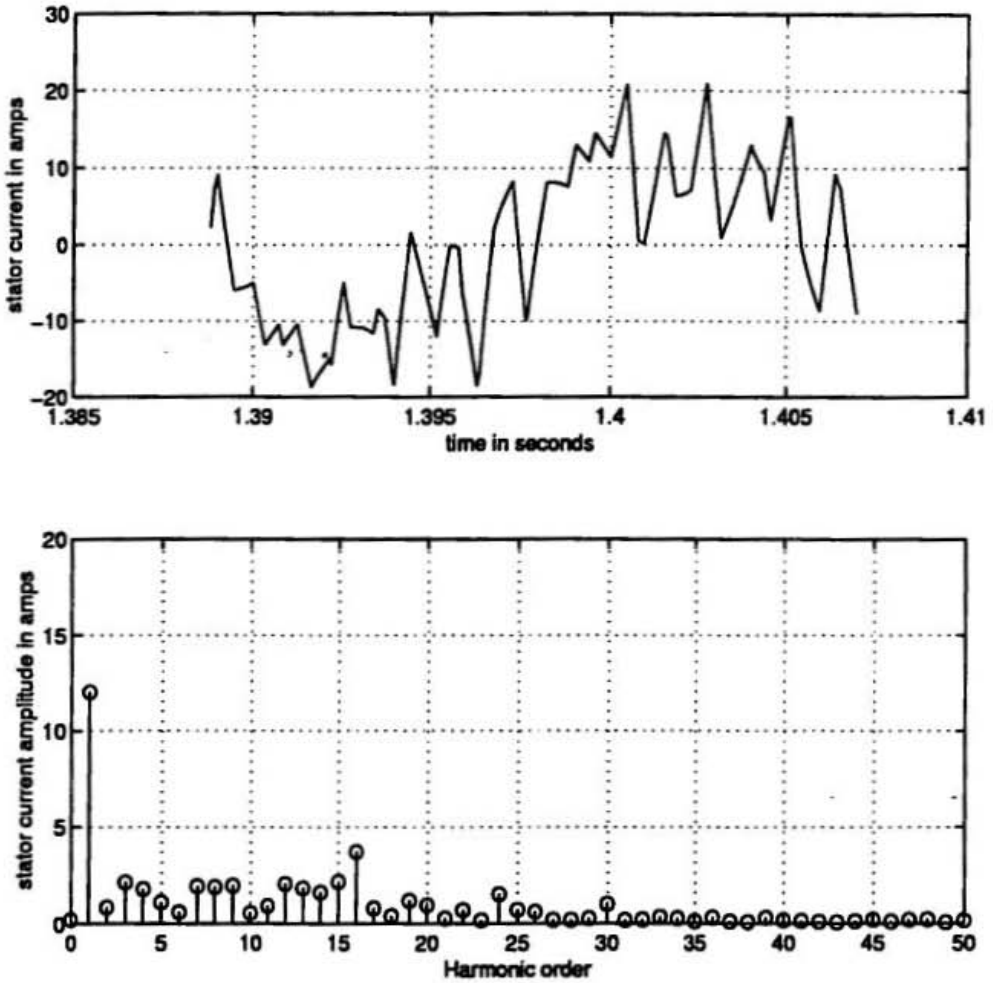

Figure 5.10: Stator current waveform (per phase) and its frequency spectrum obtained at $f_r = 55Hz$ for the DMS drive

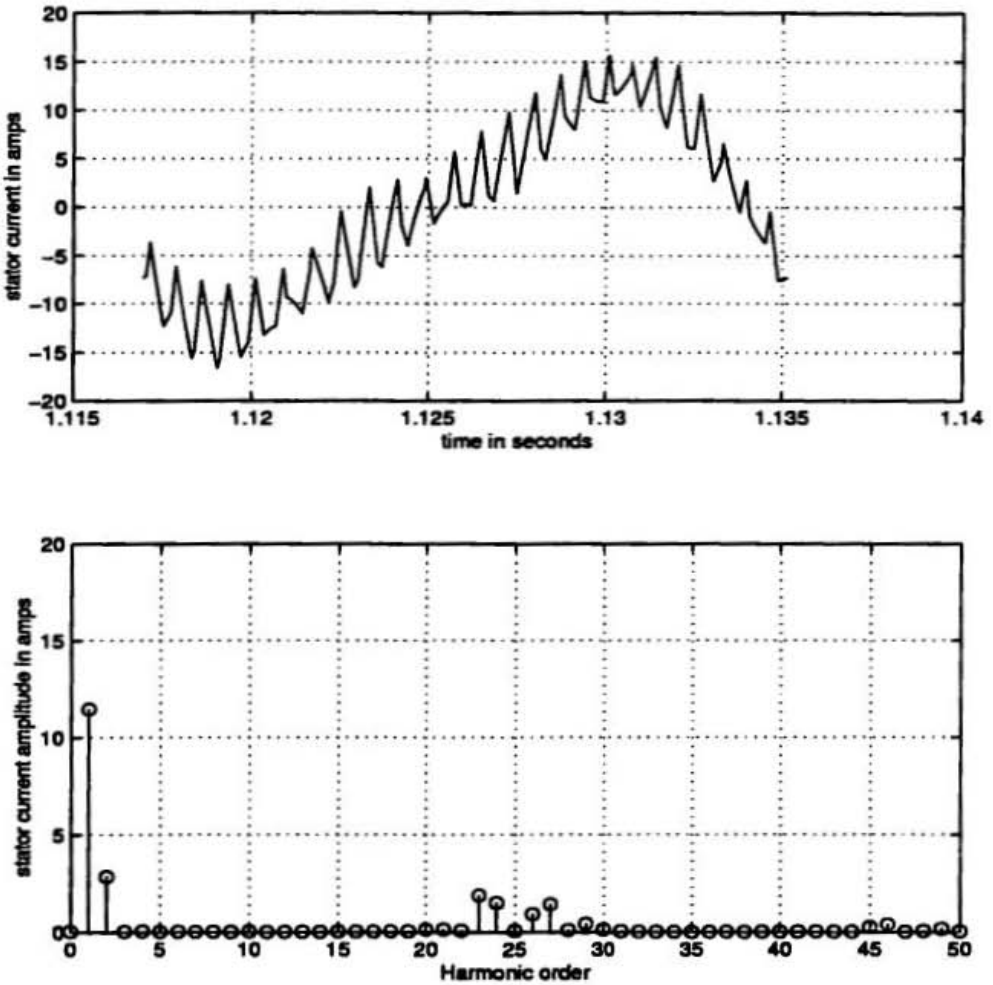

Figure 5.11: Stator current waveform (per phase) and its frequency spectrum obtained at $f_r = 55Hz$ for the UMS drive

hand, the results obtained for delta-modulated drive show that there are significant lower-order harmonics and an increased peak-to-peak ripple current. The effects of the harmonics are discussed in the subsequent section.

5.3 Effects of harmonics on induction motor drives

As shown in the simulation results, presented in the preceding section, the stator currents for both the modulation schemes contain harmonics. It is important to quantify the effects of these harmonics on the induction motor. In this section, the effects of the harmonics on machine derating is discussed and the machine derating resulting from the delta modulation and the unified modulation schemes is presented.

5.3.1 Harmonic losses, efficiency and machine de-rating

The per-phase k-th harmonic equivalent circuit for the k-th harmonic voltage and current can be derived from the fundamental equivalent circuit of the induction motor as shown in Fig. 5.12 The reactances are increased by a factor k. The stator and rotor resistances are also increased due to skin effect. The field wave due to the k-th harmonic rotates at a speed $k\omega_{ms}$, where ω_{ms} is the synchronous speed of the induction motor. The harmonic slip is given by [1]

$$s_k = \frac{k\omega_{ms} \mp \omega_m}{k\omega_{ms}} \tag{5.1}$$

where the negative sign is applicable to positive sequence harmonics and the positive sign to negative sequence harmonics. Except for very low fundamental frequencies,

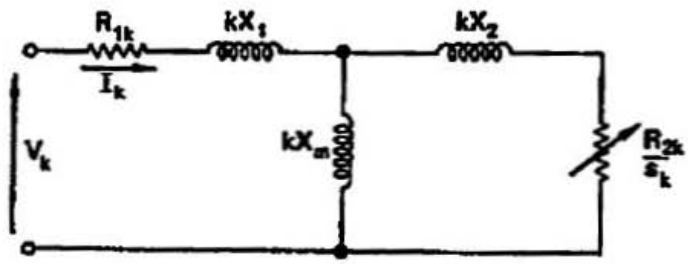

Figure 5.12: Per-phase k-th harmonic equivalent circuit of induction motor

the magnetizing reactance is much higher when compared to the rotor impedance in parallel with it. Neglecting the magnetizing reactance, the harmonic current in the stator, due to the k-th harmonic voltage is given by

$$I_{sk} = \frac{V_k}{\sqrt{(R_{sk} + \frac{R'_{rk}}{s_k})^2 + k^2(X_s + X'_r)^2}} \tag{5.2}$$

where I_{sk} is the k-th harmonic stator current

V_k is the k-th harmonic voltage at the stator

R_{sk} is the stator resistance accounting for the skin effect

X_s is the stator reactance

R'_{rk} is the rotor resistance referred to the stator after accounting the skin effect

X'_r is the rotor reactance referred to the stator

s_k is the harmonic rotor slip

Since the harmonic slip s_k is nearly unity at all motor speeds, the harmonic currents remain constant for all operating conditions. Only the fundamental stator current is determined by the motor loading and as a result, the relative harmonic content of the machine current is greater for light loads than for full-load. The harmonic currents do not contribute to the motor developed torque, but they produce additional copper and core losses in the machine.

The stator current harmonic establishes a time harmonic m.m.f in the air-gap, which rotates forward or backward at a multiple of the fundamental speed. The resultant air-gap m.m.f. at any point is due to the fundamental and the time harmonic m.m.f. waves. The increase in core loss due to the time harmonic fluxes is assumed negligible. But the end-leakage and skew-leakage fluxes, which normally contribute to the stray-load loss, cause appreciable core loss at harmonic frequencies.

The additional harmonic copper losses P_h in the machine are given by [1]

$$P_h = \sum_k I_{sk}^2 (R_{sk} + R'_{rk}). \tag{5.3}$$

These harmonic losses reduce the efficiency of the machine and also increase the thermal loading. Higher contents of lower-order harmonics reduce the efficiency and increase the thermal loading effect. This thermal loading effect causes de-rating of the machine, which implies that to avoid thermal overload and to prevent damage to the machine windings, the machine cannot be loaded to its rated load.

Operating frequency	% Derating in DMS drive	% Derating in UMS drive
$20Hz$	81.88%	86.29%
$30Hz$	65.87%	89.33%
$40Hz$	69.76%	91.62%
$55Hz$	74.12%	93.98%

Table 5.1: The percentage derating of inverter-fed induction motor for various operating frequencies using delta modulation and unified modulation schemes

The de-rating of the motor due to thermal loading has been calculated for the V/f control employing the delta modulation and unified modulation schemes. The following table shows the percentage derating at various frequencies.

5.3.2 Pulsating harmonic torques

The harmonic m.m.f. and air-gap flux waves produced due the harmonic currents are not stationary relative to each other. They rotate either forward or backward at a multiple of the fundamental frequency. The interaction between the fundamental air-gap flux and the harmonic rotor m.m.f. waves produces pulsating harmonic torques. These torque pulsations cause fluctuations in motor speed. At higher fundamental frequencies, the speed fluctuations are sufficiently low because of the motor inertia. But at low speeds, large fluctuations can be seen producing a jerky or stepped motion. The amplitude of these torque pulsations depend on the magnitude of the lower-order harmonics.

Thus, higher content of lower-order harmonics at the output of the inverter feeding an induction motor drive can reduce the efficiency, increase the thermal loading thereby causing machine de-rating, and cause speed fluctuations by way of pulsating

harmonic torques. This calls for an improved voltage quality at the inverter output.

5.4 Sudden change in load torque case

The drive models were simulated, for a sudden change in load torque for the DM and UM schemes, to study and compare the speed response in both the cases. At operating frequency $f_r = 45Hz$, the load torque was suddenly changed from 12Nm to 32Nm, at time $t = 1.5s$ after the steady state speed corresponding to the operating frequency has been attained. Fig. 5.13 and Fig. 5.14 show the respective stator current waveforms and the speed response obtained for the UMS drive. The stator current waveform and the speed response obtained from the simulation of the delta-modulated drive are shown in Fig. 5.15 and Fig. 5.16 respectively.

The results obtained from the simulation of the induction motor drive for both modulation schemes for a sudden change in load torque indicate that the speed response characteristic is identical in both the cases. However, there is a smooth transition in the stator current waveform of the UMS drive when compared to the delta-modulated drive in response to the sudden change in load torque.

5.5 Summary

This chapter has discussed the SIMULINK-based model implementation of V/f control of induction motor for the unified modulation and delta-modulation schemes. The models were simulated for a constant load condition and a sudden change in

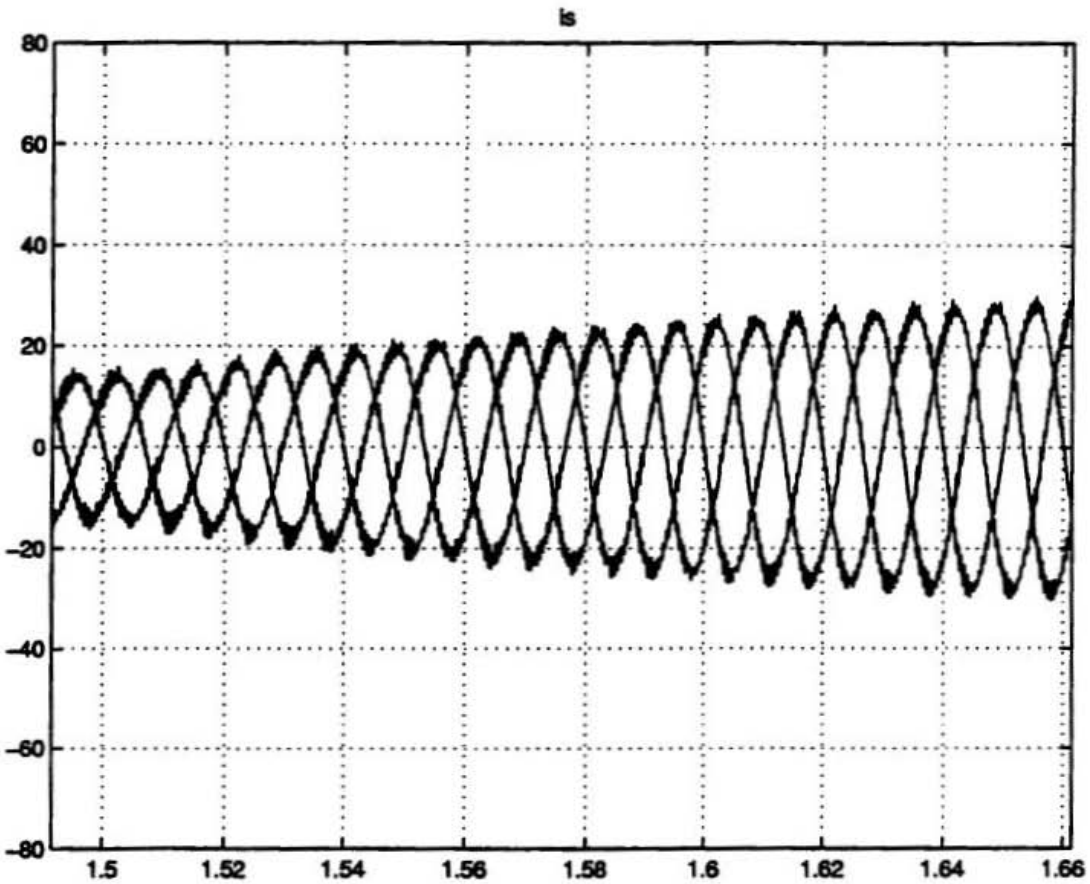

Figure 5.13: Stator current in amps Vs. time, for a sudden change in load torque, for the unified modulation scheme drive at $f_r = 45Hz$

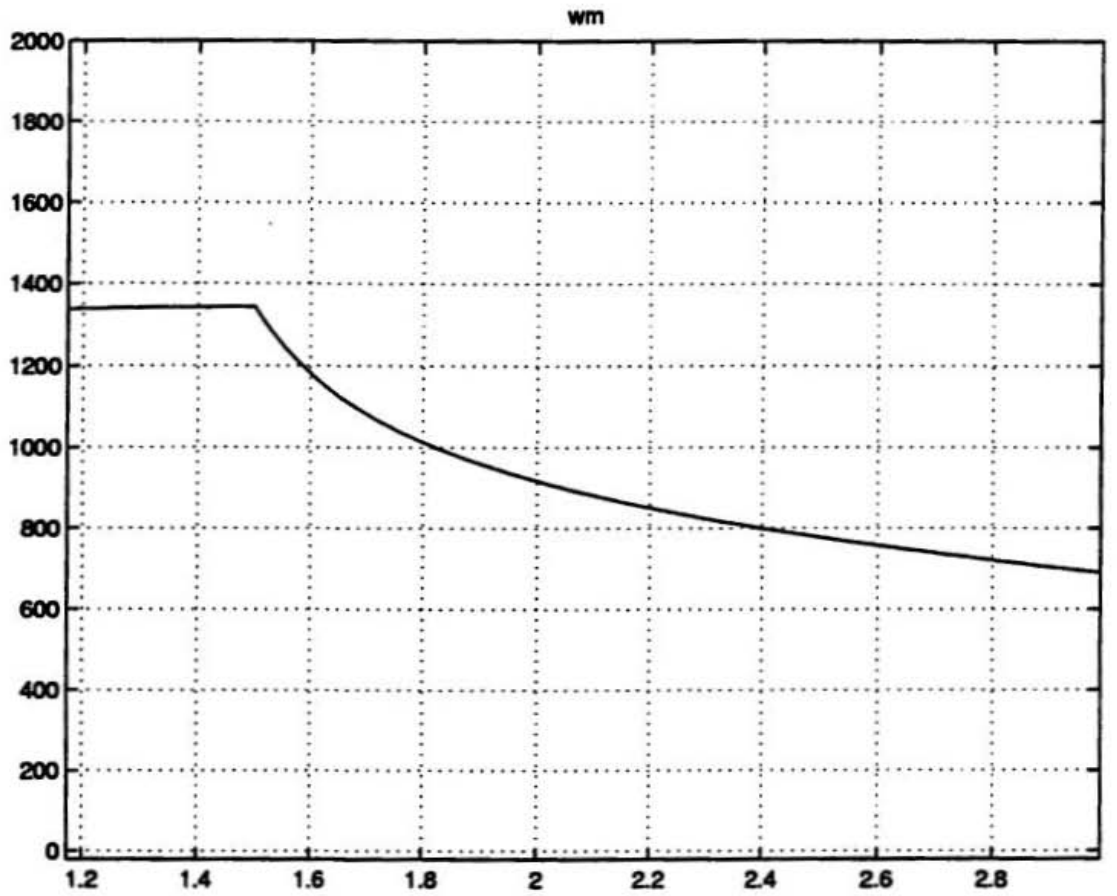

Figure 5.14: Speed response in rpm Vs. time, for a sudden change in load torque, for the unified modulation scheme drive at $f_r = 45Hz$

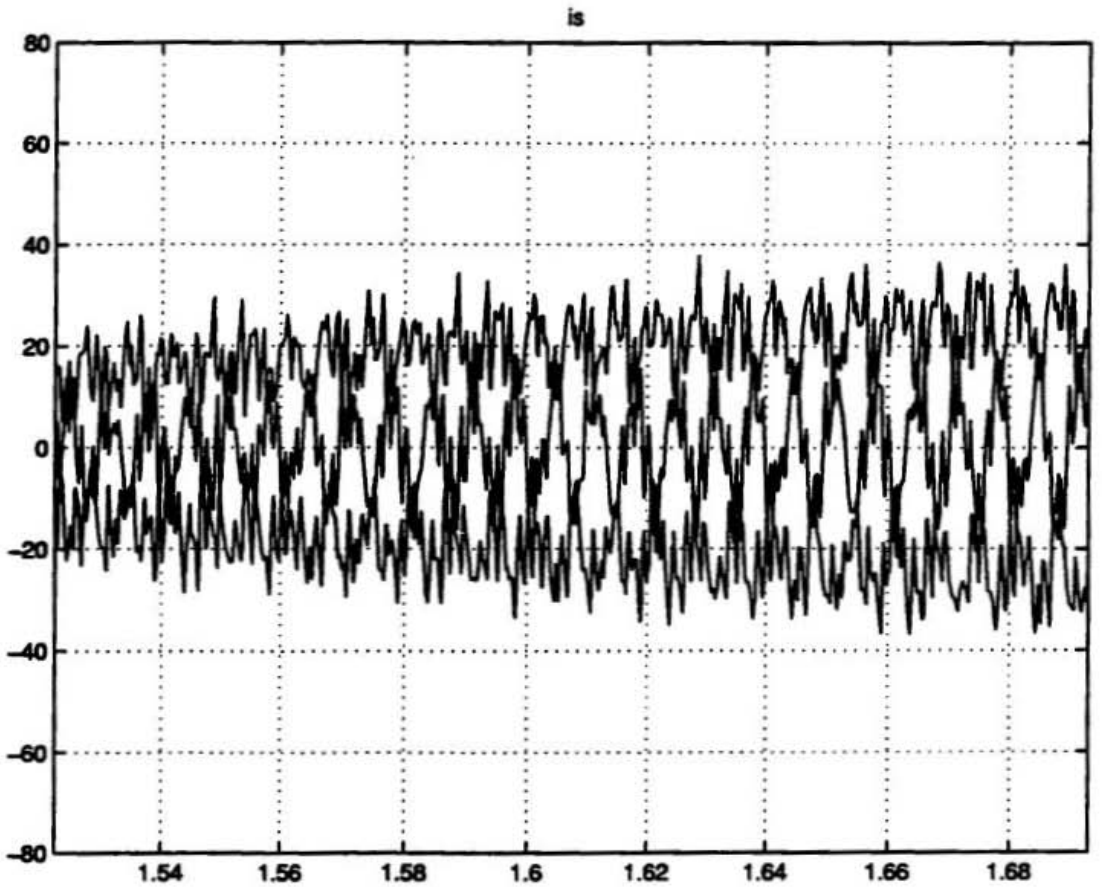

Figure 5.15: Stator current in amps Vs. time, for a sudden change in load torque, at $f_r = 45Hz$ for the delta-modulated drive

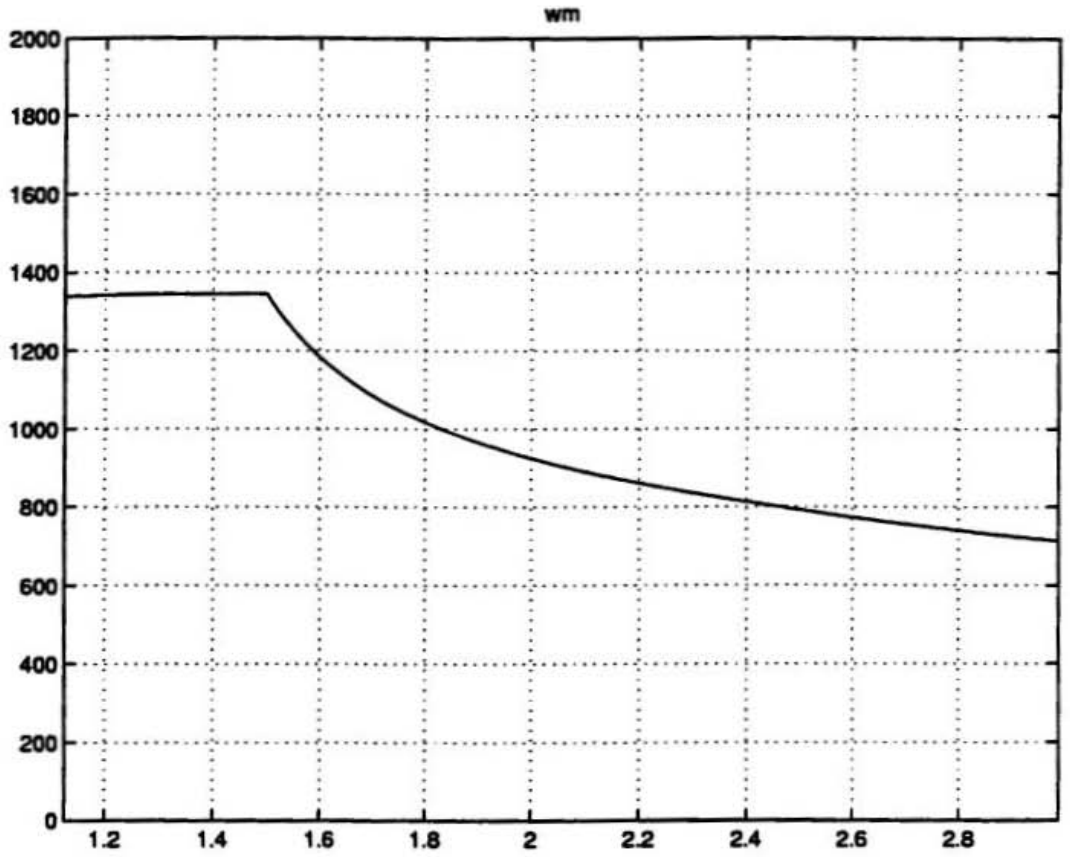

Figure 5.16: Speed response in rpm Vs. time, for a sudden change in load torque, at $f_r = 45Hz$ for the delta-modulated drive

load torque condition. The simulation results obtained for the constant load condition indicate that the UMS drive offers a better performance at higher operating frequencies in terms of efficiency and machine de-rating. The speed response curves obtained for the sudden change in load torque condition indicate an identical performance for both the modulation schemes.

Chapter 6

Modified unified modulation scheme

The implementation of the unified modulation scheme requires the generation of a cosinusoidal reference signal with a 0.5V dc offset. The modulator output is then obtained by sampling the reference signal at a fixed frequency. In order to simplify the implementation and still maintain the inherent features of the unified modulation scheme, the modulation process is modified by using the modulation procedure of the SPWM scheme. This chapter describes the development of a modified unified modulation scheme.

6.1 Development of the modified UM scheme

The reference or modulating signal is given by equation

$$\eta = 0.5 + K f_r \cos(\omega_r t). \tag{6.1}$$

The dc component of the modulating signal can be dropped from the equation 6.1. The effect of the dc offset can be taken into account by modifying the amplitude of

the cosinusoidal component. The modulating signal can therefore be represented as

$$v_r'(t) = K' f_r \cos(\omega_r t), \tag{6.2}$$

where K' is the slope of the V/f characteristic and is known as the modulation constant. Without the loss of generality, the modulating signal can be expressed as

$$v_r'(t) = K' f_r \sin(\omega_r t). \tag{6.3}$$

In the ideal case, the value of K' is chosen such that the amplitude modulation index M_a, which is a ratio of the modulating signal amplitude to the carrier signal amplitude, becomes unity, at the break frequency f_{rb} of the V/f curve. A triangular wave carrier signal whose switching frequency is always an integral multiple of the modulating frequency i.e $f_s = pf_r$, under different operating conditions, can be used to generate the modulated output signal similar to the case of the conventional sine PWM. Thus the modified UM scheme has a modulating signal of the form given in equation 6.3 and a switching frequency which will always be an integral multiple of the reference frequency. Thus the modified UM scheme is expected to exhibit the same characteristic features as the UM scheme. The following design example is used to obtain the characteristic features of the modified UM scheme.

Design specifications:

$V_{dc} = 12V$ (DC supply voltage)

$f_{rb} = 60Hz$ (Break frequency)

$f_s = 40 f_r$ (Switching frequency)

$K' = 0.2$ (Modified sine-PWM constant)

The value of K' is chosen 0.2 such that at the break frequency $f_{rb} = 60Hz$, the amplitude modulation index M_a becomes unity. The V/f characteristics pertaining to the above design specifications is shown in Fig. 6.1.

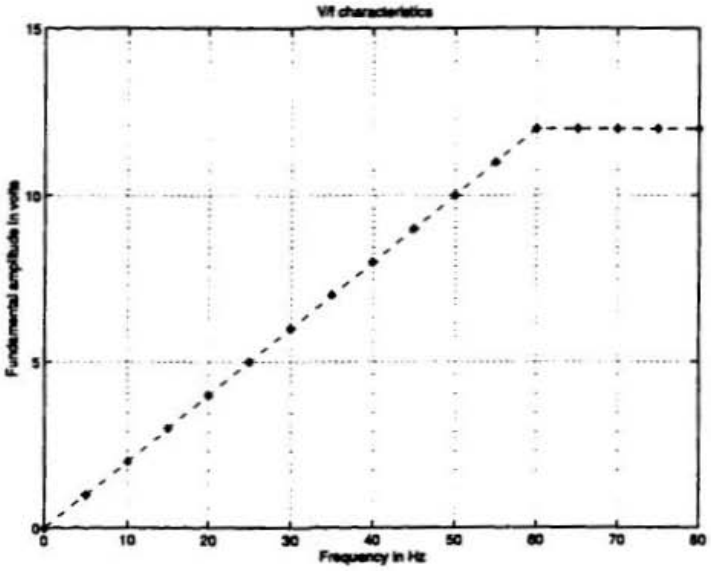

Figure 6.1: V/f design characteristics for modified UM scheme

The modified UM scheme with the mentioned design specifications was simulated in MATLAB. The modulating signal, the output of the modified UM scheme and the frequency spectrum of the output for operating frequencies $f_r = 30Hz$ and $f_r = 60Hz$ are shown in Fig. 6.2 and Fig. 6.3 respectively. From the results of the MATLAB simulation, the validity of the modulation scheme for V/f control can be ascertained.

Also, it can be seen from the frequency spectrum of the output that the order of the dominant harmonics are dependent on the switching frequency, which is an integral multiple of the modulating frequency.

The characteristic features of the modified UM scheme can be outlined as follows:

- The modulating signal, $v_r(t) = K' f_r \sin(\omega_r t)$, is naturally sampled by means of a high frequency carrier signal of peak amplitudes $+V_c$ and $-V_c$ and the cross-over points determine the pulse widths of the modulator output.

- The switching frequency f_s is always an integral multiple of the reference frequency i.e. $f_s = pf_r$ where p is a constant. Although the switching frequency changes with the change in modulating signal frequency, there is no frequency modulation. In this regard, it is similar to the conventional sine-PWM scheme. Similar to the unified modulation technique, the number of commutations per cycle of the modulating signal is dependent on p and is fixed.

- The amplitude modulation index M_a is given by

$$M_a = \frac{K' f_r}{V_c}, \tag{6.4}$$

and it controls the amplitude of the fundamental component at the output.

$$Vo1 = M_a V_{dc}. \tag{6.5}$$

Ideally the value of the amplitude modulation index can vary from 0 to 1. The constant K' is known as the modified UM constant and the value of K' decides

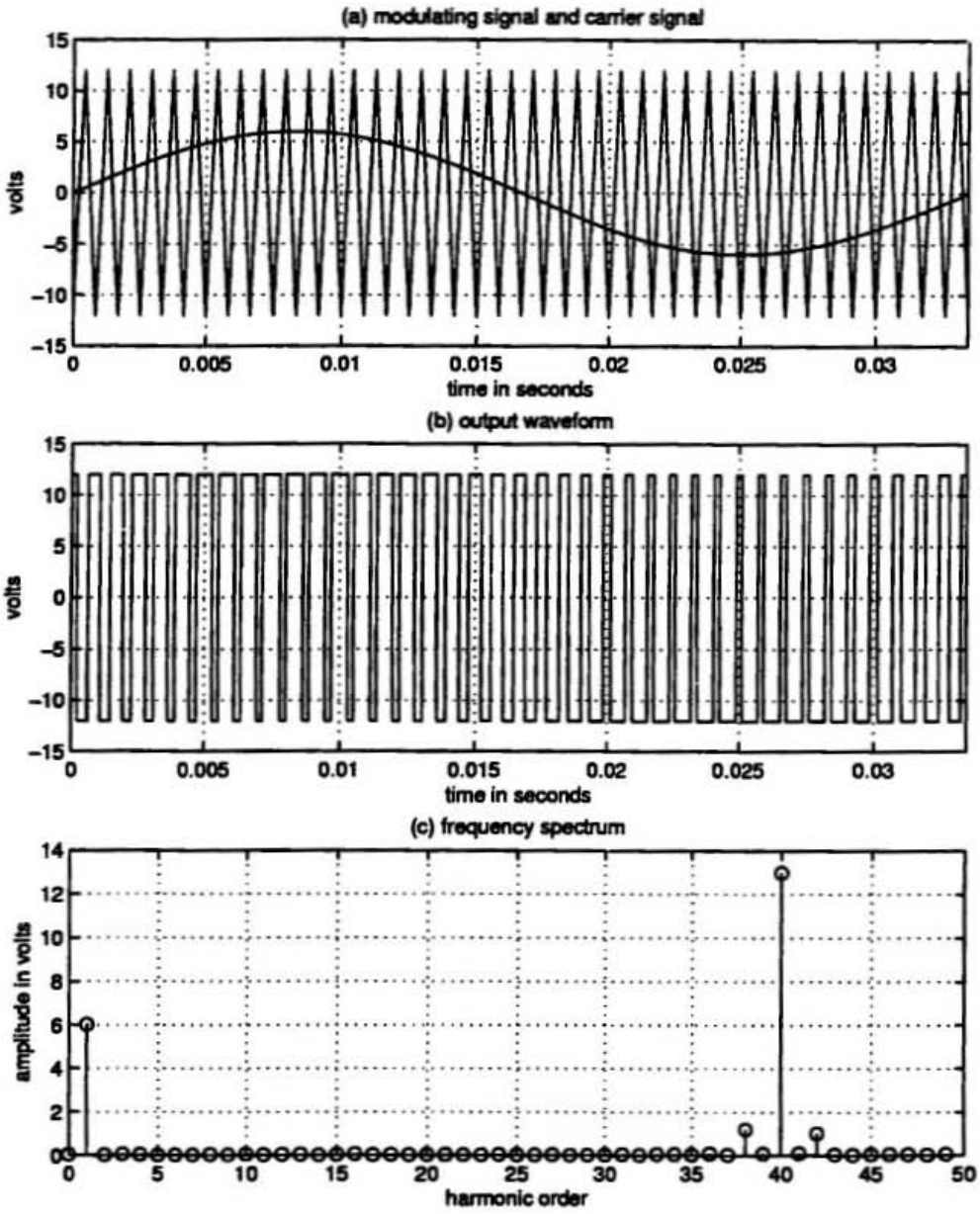

Figure 6.2: Waveforms of modified UM scheme for $f_r = 30Hz, f_{rb} = 60Hz$ and $K' = 0.2Vs$

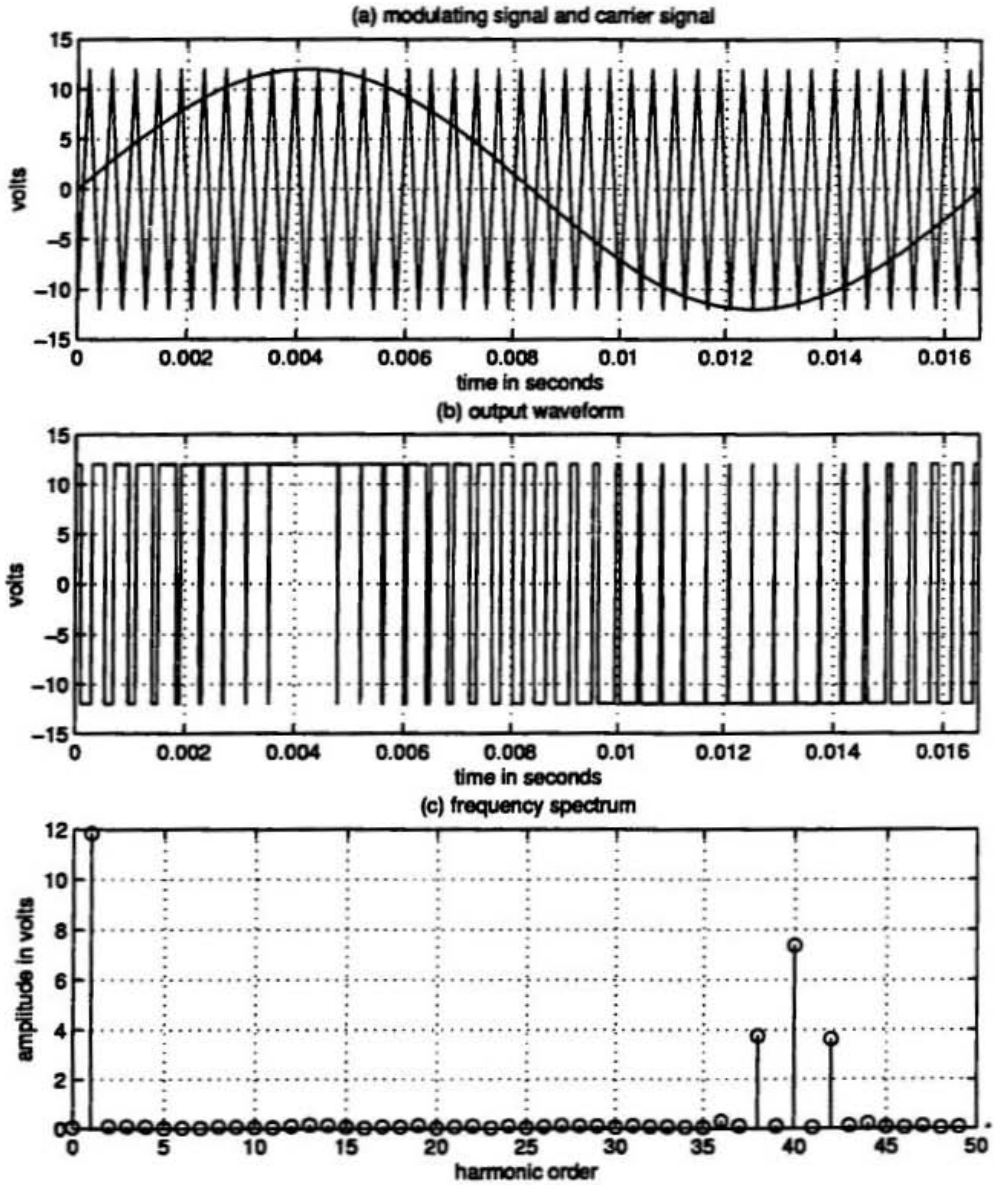

Figure 6.3: Waveforms of modified UM scheme for $f_r = 60Hz, f_{rb} = 60Hz$ and $K' = 0.2Vs$

the slope of the V/f characteristic. It is chosen such that for a particular break frequency f_{rb} on that V/f characteristic, the product $K'f_{rb}$ is set to V_c and for all values of $f_r > f_{rb}$, the value of $K'f_r$ is maintained at V_c in order to achieve the constant volts mode . But in the case of practical applications, the value of $K'f_r$ ranges between $(K'f_r)_{min}$ and $(K'f_r)_{max}$. $(K'f_r)_{min}$ is chosen to be greater than zero, in order to accommodate the low-voltage boost required at the low frequency operation of the induction motor. $(K'f_r)_{max}$ is chosen to be less than V_c, so as to prevent overmodulation, to avoid any commutation failure and to avoid any infringement on the minimum and maximum pulse width criteria for suitable inverter operation.

- The ratio of the carrier frequency to the modulating frequency is termed as the carrier ratio p. The distribution of undesired harmonics depends on the carrier ratio. For large carrier ratios, the modified UM inverter delivers a high-quality output voltage waveform in which the dominant harmonics are at the higher order, clustered around the carrier frequency and its harmonics. Thus the carrier ratio is crucial in determining the order of the dominant harmonics in the voltage output of the modified UM inverter. Since the carrier ratio remains constant at all frequencies of the modulating signal, it is easy to predict the position of the harmonics and thereby estimate derating due to harmonic losses in the motor.

6.2 Summary

This chapter detailed a method of improving the unified modulation scheme, based on the idea of the conventional sine-PWM technique. The simulation results of the modified UM scheme show that this scheme offers the same performance characteristics as that of the unified modulation scheme and is easy to implement.

Chapter 7

Conclusions and scope for future work

The principal aim of this thesis was to analyze the existing modulation schemes for V/f control of inverter-fed induction motors and propose an improved modulation technique, which could combine the advantages of the existing schemes and at the same time eliminate their disadvantages.

7.1 Summary of the research work

A concise summary of this thesis work is given below:

- The existing control schemes, such as sine-PWM and delta modulation, for V/f control of medium-performance inverter-fed induction motor drives have been reviewed.

- The advantages of the sine-PWM such as the absence of frequency modulation and harmonic attenuation at low frequencies, and limitations such as lack of

inherent V/f feature and unpredictable lower-order harmonics at higher frequencies, have been discussed.

- Similarly, the advantages of the delta modulation technique such as inherent V/f feature and harmonic attenuation at low frequencies, and the limitations such as presence of frequency modulation, generation of sub-harmonics and dominant lower-order harmonics at higher frequencies, substantiate the need for an improved modulation technique.

- The goals of the proposed scheme, called the unified modulation scheme, have been derived from the limitations of the existing schemes. The goals are inherent V/f control, severe lower-order harmonic attenuation at all operating frequencies and absence of frequency modulation.

- The core idea for the unified modulation scheme has been derived from the duty-ratio modulation characteristic of the delta-modulation technique and from the absence of frequency modulation of the sine-PWM technique.

- The main features of the unified modulation scheme are summarized as follows:

    1. The modulating signal is of the form,$\eta = 0.5 + Kf_r\cos(\omega_r t)$, which characterizes the duty-ratio modulation of the output pulses.

    2. The switching frequency is always a constant integral multiple of the reference or modulating frequency i.e. $f_s = pf_r$.

3. The dominant harmonics occur in and around the multiples of the switching frequency. Hence the choice of p determines the occurrence of dominant harmonics.

- For a common V/f characteristic, all the different modulation schemes have been designed and simulated using MATLAB programs.
- All the modulation schemes offer better harmonic attenuation at lower frequencies. But the unified modulation scheme offers consistent harmonic attenuation for all operating frequencies, unlike sine-PWM and delta modulation schemes where the harmonic attenuation fades with the increase in operating frequency.
- For unified modulation, sub-harmonics are insignificant or non-existent since the ratio of the switching frequency to the modulating frequency is always a integer constant.
- Experimental implementation of the unified modulation scheme has been carried out for a specified V/f characteristic using the PIC16C77 microcontroller. The PWM output of the microcontroller has been fed to a comparator to generate bipolar pulses. The results of the digital implementation prove the validity of the unified modulation scheme.
- SIMULINK model implementation of inverter-fed induction motor drives using unified modulation scheme and delta modulation scheme have been achieved.

The harmonic spectrum of the input current to the motor, obtained through simulation of the model, indicates an improved performance in the case of the unified modulation scheme in terms of better harmonic attenuation and hence reduced copper losses, reduced derating of the motor.

- Finally, a modified unified modulation technique has been presented. The modified UM scheme offers the same performance characteristics as that of the unified modulation scheme, such as inherent V/f feature and improved harmonic attenuation.

7.2 Contributions of this thesis

This thesis work has contributed towards developing an improved modulation technique for V/f control of inverter-fed induction motors. The advantages of the proposed unified modulation scheme are presented below:

- Inherent V/f control
- Severe attenuation of lower-order harmonics at all operating frequencies
- Increased efficiency and reduced derating of the inverter-fed induction motor drive
- Simple and feasible digital implementation

7.3 Scope for future work

Here are a few recommendations for future work based on the unified modulation scheme

- Experimental verification of open-loop speed control for an UMS inverter-fed induction motor drive
- Under varying load conditions, a pre-programmed open-loop V/f drive cannot maintain constant air-gap flux because the stator drop is a function of the stator current. Investigation of a flexible V/f drive (closed-loop) based on current loop is recommended.
- Experimental work to determine an optimum carrier ratio p for the switching frequency of the unified modulation scheme can be carried out. Higher carrier ratio causes increased switching losses while a lower carrier ratio might cause poor harmonic attenuation.

Bibliography

[1] G. K. Dubey, *Power semiconductor controlled drives.* Prentice-Hall Inc., 1989.

[2] J. Vithayathil, *Power Electronics - Principles and applications.* McGraw-Hill Inc., 1989.

[3] P. Vas, *Vector Control of AC machines.* Oxford Science Publications, 1990.

[4] F.Blaschke, "The Principle of Field-orientation as applied to the new TRANSVECTOR closed loop control system for Rotating field machines ," *Siemens review*, vol. 34, pp. 217–220, May 1972.

[5] A.Nabae, K.Otsuka, H.Uchins and R.Kurosawa , "An approach to Flux control of Induction motors with variable frequency power supply," in *IEEE / IAS Annual Meet Conference Record*, pp. 890–896, 1978.

[6] R.Gabriel, W.Leonhard and C.Nordby, "Field-oriented control of a standard AC motor using microprocessors," *IEEE Trans. Ind. Appl.*, vol. IA-16, pp. 186–192, Mar/Apr 1980.

[7] D.A.Paice, "Induction motor speed control by stator voltage control," *IEEE Trans. Power App. and Syst.*, vol. PAS-87, pp. 585–590, Feb 1968.

[8] T.A.Lipo, "The analysis of Induction motors with voltage control by symmetrically triggered thyristors," *IEEE Trans. Power App. and Syst.*, vol. PAS-90, pp. 515–525, Mar/Apr 1971.

[9] P.C.Krause , "A constant frequency Induction motor speed control," in *Proceedings of National Electronics Conference*, vol. 20, pp. 361–365, 1964.

[10] P.C.Sen, *Principles of Electric Machines and Power Electronics*. John Wiley and Sons,Inc., 1989.

[11] J.M.D.Murphy and F.G.Turnbull, *Power Electronic control of AC motors*. Pergamon Press, 1988.

[12] P.C.Sen and K.H.Ma, "Constant torque operation of Induction motors using Chopper in the rotor circuit," *IEEE Trans. Ind. Appl.*, vol. IA-14, pp. 408–414, 1978.

[13] G.K.Dubey, S.K.Pillai and P.P.Reddy, "Analysis and design of a doubly-fed chopper for speed control of Induction motor - Part I and II," *IEEE Trans. IECI.*, vol. 22, pp. 522–538, Nov 1975.

[14] A.Lavi and R.J.Polge, "Induction motor speed control with static inverter in the rotor," *IEEE Trans. Power App. and Syst.*, vol. PAS-85, pp. 76–84, Jan 1966.

[15] W.Shepherd and J.Stanway, "Slip power recovery in an Induction motor by the use of a thyristor inverter," *IEEE Trans. Ind. Gen. Appl.*, vol. IGA-5, pp. 74–82, Jan/Feb 1969.

[16] M.S.Erlicki, "Inverter rotor drive of an Induction motor," *IEEE Trans. Power App. and Syst.*, vol. PAS-84, pp. 1011–1016, Nov 1965.

[17] H.Kazuno, "A wide range speed control of an Induction motor with static Scherbius and Krmer systems," *Elec. Eng. in Jpn.*, vol. 89, no. 2, pp. 10–19, 1969.

[18] J.M.D.Murphy, *Thyristor control of AC motors.* Pergamon Press, 1973.

[19] B.K.Bose, *Power Electronics and Drives.* Prentice-Hall Inc., 1986.

[20] H.Patel and R.G.Hoft, "Generalized Technique of Harmonic Elimination and Voltage Control in Thyristor Inverters: part-I Harmonic Elimination ," *IEEE Trans. Ind. Appl.*, vol. IA-9, pp. 310–317, May/July 1973.

[21] P.N.Enjeti, P.D.Ziogas and J.F.Lindsay, "Programmed PWM technique to eliminate harmonics: a critical evaluation ," *IEEE Trans. Ind. Appl.*, vol. IA-26, pp. 302–316, March/April 1990.

[22] P.D.Ziogas, "The Delta Modulation Technique in Static PWM Inverters," *IEEE Trans. Ind. Appl.*, vol. IA-17, pp. 199–204, March/April 1981.

[23] R.Steele, *Delta Modulation Systems.* John Wiley & Sons, 1975.

[24] M.A.Rahman, J.E.Quaicoe and M.A.Choudhury , "Performance Analysis of Delta-Modulated PWM Inverters," *IEEE Trans. on Power Electronics.*, vol. PE-2, pp. 227–233, July 1987.

[25] Naser Abdel-Rahim, "Single phase delta-modulated inverter for ups applications," Master's thesis, Memorial university of Newfoundland, Feb 1989.

[26] S.R.Bowes and B.M.Bird, "Novel approach to the analysis and synthesis of modulation processes in power converters," in *IEEE Proceedings.*, vol. 122, pp. 1279–1285, 1975.

[27] M.A.Rahman, J.E.Quaicoe and M.A.Choudhury , "An Optimum Delta Modulation Strategy for Inverter Operation," in *IEEE Power Electronics Specialists Conference Record*, pp. 410–416, Vancouver - 1986.

[28] T.C.Green, J.C.Salmon and B.W.Williams, "Investigation of Delta Modulation Spectra and of Sub-Harmonic Elimination Techniques," in *IEEE Power Electronics Specialists Conference Record.*, pp. 1279–1285, Kyoto,Japan-1988.

[29] C.F.Christiansen, C.H.Rivetta and M.I.Valla, "A Synchronization technique for Static Delta-Modulated PWM Inverters ," *IEEE Trans. Ind. Electr.*, vol. IE-35, pp. 502–507, November 1988.

[30] Naser Abdel-Rahim and J.E.Quaicoe, "A Single Phase Delta-Modulated Inverter for UPS Applications," *IEEE Trans. Ind. Electr.*, vol. 40, pp. 347–354, June 1993.

[31] Technical Reference Manual, *MATLAB - The Language of Technical Computing. Ver.2.0.* The MathWorks Inc., 1997.

[32] Technical Reference Manual, *PIC16C7X Data sheet.* Microchip Technology Inc., 1998.

[33] Technical Reference Manual, *SIMULINK - Dynamic System Simulation for MATLAB. Ver.2.0.* The MathWorks Inc., 1997.